Journal of Biological Regulators & Homeostatic Agents

Vol 26, no. 2 (S2), April - June 2012

CONTENTS

EDITORIAL

A NOVEL BIOTECHNOLOGY PRODUCT FOR THE DEGRADATION OF BIOFILM-ASSOCIATED POLYSACCHARIDES PRODUCED BY *STREPTOCOCCUS MUTANS*

G. DI BONAVENTURA[1], M. URIANI[2], A. FABBRI[2], V. FLATI[4], S. MARTINOTTI[1], A. POMPILIO[1], A. GAMBI[1], R. ORRU[1], I. ROBUFFO[3], E. TONIATO [3*]

[1]Department of Biomedical Sciences, "G. d'Annunzio" University of Chieti-Pescara, Chieti, Italy.
[2]ABR Consulting S.r.l., Rome, Italy.
[3]Department of Oral Sciences, Nano- and Biotechnologies, "G. d'Annunzio" University of Chieti-Pescara, Chieti, Italy.
[4]Department of Clinical and Biotechnological Sciences, University of L'Aquila, Italy

In this study we evaluated the activity of ABR preparation, a first-in-class agent obtained through fermentation process by genetically unmodified *Bacillus* spp., in breaking down polysaccharide produced by *Streptococcus mutans*, primary coloniser of tooth surface and abundant in dental biofilms. Our results showed that ABR preparation is able in degrading sugars formed by *S. mutans*, both in broth culture and onto teeth surface. Its activity is not influenced by the presence of saliva, commercial mouthwashes or oral disinfectants. ABR preparation has the potential to remove preformed plaque and counteract its development, thus offering conservative control of gingival and periodontal disease.

Dental plaque is the paradigmatic example of biofilm, a sessile microbial community embedded within an self-produced extracellular matrix mainly formed by long chain polysaccharides (1).

Plaque-related diseases are probably the most common bacterial diseases occurring in man. The diseases process involves acidogenic plaque bacteria, including *Streptococcus mutans* (2, 3). This microorganism is one of the early colonizers of the oral cavity and it is a common member of the healthy dental biofilm (4, 5). However, under certain circumstances it can increase in number, initiating demineralization, which eventually leads to tooth decay. A well-characterized, clinically relevant factor in caries development is the ability of *S. mutans* to metabolize sucrose, whose fermentation is necessary for intracellular polysaccharide synthesis and, more importantly, for production of highly adhesive extracellular ones, mostly glucans (3, 6, 7). These polysaccharides promote *S. mutans* adhesion to the tooth surface, and contribute to the establishment of the extracellular polysaccharide matrix, which provides bulk and structural integrity for dental biofilms (8-10).

The need for removing the bacterial plaque to prevent the onset of tooth decay has been addressed in different ways, by means of non-specific mechanical and chemical removal or by antiseptic agents aimed to interfere with bacterial growth (11-13). However, none of the current available approaches offer a satisfactory solution. Particularly, the bactericidal substances contained in commercial mouthwashes (i.e., chlorexidine) despite being effective, have relevant side effects such as taste changes, tooth staining, numbness and, last but not least, the alteration of the normal flora thus increasing the risks of superinfections. Thus, further studies aimed to individuate novel approaches in the control of plaque-related diseases are warranted (11, 13).

In the present study we assessed the effectiveness of "ABR preparation" – a first-in-class agent obtained from fermentative activity of genetically unmodified *Bacillus spp* in the presence of both starch and cellulose - in degrading the polysaccharidic chain produced by *S. mutans*, both in culture broth and onto teeth surface. The effect of

Key-words: Streptococcus mutans; biofilm; dental plaque; reducing sugar activity.

* *Corresponding Author:*
Ospedale Clinicizzato "SS Annunziata",
Patologia Clinica, Via dei Vestini,
66100 Chieti, Italy.
Phone +39 0871-358668; Fax +39 0871-358568.
E-mail: e.toniato@unich.it.

0393-974X (2012)

the presence of saliva, commercial mouthwashes and oral disinfectants on sugar reduction activity of ABR preparation was also evaluated.

MATERIALS AND METHODS

Production process for ABR preparation. The production process we standardized to obtain a pilot batch of ABR preparation, was carried out on 1 liter-scale and consisted of 2 steps: fermentation and purification. i) Fermentation. Fermentation was performed in a medium consisting of: *Saccharomyces cerevisiae* (as block of brewer's yeast) 25 g; NaCl 5 g; soluble starch 0.5 g; microcrystalline cellulose 0.5 g; distilled water q.s. to 1000 ml. A single colony of *Bacillus clausii* ATCC 700160 reference strain was inoculated into 150 ml of fermentation medium without starch and cellulose, and incubated for 18 h at 37°C under stirring until reaching a bacterial concentration of about $3x10^8$ CFU/ml. Fifty milliliters of preinoculum were then added to 1 liter of fermentation medium and fermentation was carried out for 36-48 h under dynamic incubation (200 ± 10 rpm) at 37 ± 0.5°C, until reaching the end of logarithmic phase of growth (corresponding to a concentration of about $4x10^9$ CFU/ml). pH was then adjusted to a value of 9.0 ± 0.05, then the separation of the bacterial pellet from the growth broth was carried out by centrifugation (9.000 x g, 4°C, 20 min). The growth broth was then submitted to the purification process. ii) Purification. The extraction and the purification steps consisted of an ultrafiltration step using 0.2 µ Sartocon slice polyethersulfone cartridges or equivalent, having a surface of 0.1 m^2. The centrifuged culture broth, obtained from the above stated fermentation, was submitted to tangential filtration using cartridges having a molecular cut-off limit of 2 kDa with a total surface of about 0.2 m^2. A Watson-Marlow pump (model 520U) was employed at a flow of about 3.5 L/min, using a suitable support, adjusting the pressure to about 2-2.5 x 10^5 Pa. The filtration was prolonged until a recovery of 90 % of the initial volume in the permeate fraction. The process data are reported in Table 1. The activity observed with 3 different *Bacillus* strains (*B. clausii, B. cereus,* and *B. subtilis*), with or without starch and cellulose, is shown in Table 2.

Activity assay. The ability in reducing sugars (activity assay) was evaluated on the polysaccharide produced by *S. mutans* ATCC 33402 reference strain grown in the presence of sucrose (14, 15). Briefly, bacteria were grown in Brain Hearth Infusion (BHI) broth at 37 °C, 200 rpm, for 24 h. Five-hundreds microliters were then inoculated in BHI broth containing sucrose 40 g/L and incubated at 37 °C, 200 rpm, for 24 h. Cultures were then centrifuged, and the pellet was washed thrice with water, then suspended in water and used as the substrate for activity tests. The substrate was checked for the presence of polysaccharides by acid hydrolysis, and this solution was injected into an HPLC system under the following conditions: column Carbohydrates Ca - 6.5 x 300 mm, flow 0.5 ml/min, buffer water for HPLC, 90°C, using a refractive index as detector. A typical positive chromatogram is shown in Figure 1.

The substrate, as prepared, was used for all activity assays tests, through determination of reducing sugars using DNS (3,5-dinitrosalicylic acid) assay (16). Briefly, 0.5 ml of the ABR preparation (corresponding to about 400 µg) were challenged with the substrate at 37 °C for 30 minutes. The sample was then added to an equal volume of DNS reagent and heated for 3 minutes at 100°C. After cooling in ice, the absorbance at 540 nm was read. The activity was evaluated against a calibration curve constructed in the range 0.25 - 1.5 micromoles of glucose.

Activity of ABR preparation. The activity of ABR preparation was evaluated:

i) comparatively to that exhibited by five commercial mouthwashes (Product 1: containing essential oils of mint, thyme, eucalyptus and birch, sodium fluoride, alcohol; Product 2: containing sodium fluoride, cetylpyridinium; Product 3: containing sodium fluoride, and cetylpyridinium; Product 4: containing 0.12% chlorhexidine; and Product 5: containing aminefluoride). All products were tested at doses recommended by manufacturers.

ii) in the presence of four commonly used oral disinfectants: chlorexidine, cetylpirydinium, essential oils, and fluoride.

iii) in the presence of saliva. Saliva samples were taken from 8 women and 8 men (age: 18-50 years). Particularly, the female samples were taken in premenstrual and menstrual phases, and also in advanced state of pregnancy.

Activity test onto teeth surface. Sterilized teeth were exposed to *S. mutans* broth culture for 48 h to allow biofilm formation. Teeth were then collected and dried in a oven at 35°C for 30 min, then individually stained by Red-Cote dye (GUM Red-Cote Sunstar Americas). Color excess was then removed by washing with water, teeth were exposed to ABR preparation for 5 or 10 minutes at 35°C. The test was carried out in comparison with placebo (not treated with ABR) prepared in the same way as the sample.

Antibacterial assays. The antimicrobial activity of ABR preparation was evaluated against ATCC reference strains, representative for species commonly found in the oral cavity (*Staphylococcus aureus* ATCC 6538, *Streptococcus mutans* ATCC 33402, *Escherichia coli* ATCC 8739, *Pseudomonas aeruginosa* ATCC 9027, *Aspergillus niger* ATCC 16404), comparatively to that exhibited by five commercial mouthwashes described above. Briefly, each strain was grown in Triptycase Soy Broth under dynamic conditions (200 rpm), at 37°C for 18 h, resulting in a bacterial density of about 10^8 CFU/ml. The activity of each product was evaluated by challenging 20 ml of mouthwash, corresponding to a single dose, with 1 ml of standardized inoculums for the time indicated on the product's packaging. Bacterial suspensions then underwent to serial dilutions for colony counts on TSA.

Statistical analysis. All assays were performed in triplicate and repeated in at least two different occasions. Differences between means were assessed by unpaired-t test by using GraphPad Prism software (version 4.0; GraphPad Software Inc.). p values of < 0.05 were considered as statistically significant.

RESULTS

ABR preparation exhibits reducing sugars activity. The activity of ABR in reducing sugars was evaluated

Table 1. *Controlling process data. Activity is referred to the determination of reducing sugars following incubation with substrate at 37°C for 30 min.*

Sample	Volume (ml)	Proteins (mg/ml)	Activity (units)	Yield (%)
Fermented	1000	0.87	1214	100
Bulk	900	0.76	1056	87

Table 2. *Activity in reducing sugars observed in the absence or the presence of starch and cellulose. Results are expressed as micromoles of reducing sugar.*

Strain	Classic fermentation (Starch-/Cellulose-)	Starch+	Cellulose+	Starch+ /Cellulose+
B. clausii	0	0	0	0.345
B. cereus	0	0	0	0.298
B. subtilis	0	0	0	0.324

comparatively to 5 commercial mouthwash products. Contrarily to commercial products, ABR preparation exhibited activity on polysaccharide produced by *S. mutans* (mean ± SD: 0.295 ± 0.007 micromoles/ml).

ABR preparation's activity is not affected by oral disinfectants. Activity in reducing sugars, assessed by the DNS assay, was also tested in the presence of four commonly used oral disinfectants. Our results showed that the activity of ABR preparation was not significantly affected in the presence of disinfectants tested (Figure 2). These results posed rationale for using of the ABR preparation in combination with other active ingredients already known, thus adding at the capabilities of biofilm disintegration also antibacterial activity.Saliva does not interfere with ABR preparation's reducing sugar activity. In order to evaluate the effectiveness of the product in conditions simulating those observed in the oral cavity, parallel activity tests were performed in the presence of saliva. Our results showed that, in all cases examined, the presence of saliva did not significantly affect the activity of ABR preparation (Figure 3). Samples consisting of saliva only did not show effects on polysaccharide produced by *S. mutans*.

ABR preparation is effective in detaching S. mutans biofilm on teeth surface. The activity of ABR preparation was assessed on the polysaccharides formed onto the surface of extracted teeth. Figure 4 show results obtained after 5 and 10 minutes of exposure to ABR at 37°C using two different teeth.

ABR preparation does not possess antimicrobial activity. The antimicrobial activity of ABR preparation was assessed comparatively to five commercial mouthwashes, and results are shown in Figure 5. ABR preparation did not exhibit antibacterial and antifungal activity. On the contrary, exposure to commercial mouthwashes provoked a reduction in microbial viability of at least 70%, except for Product 3 against *S. aureus* ATCC 6538 strain (50%). Product 5 showed the highest activity against *A. niger* ATCC 16404 strain.

DISCUSSION

In the present study, we evaluated the effectiveness of a biotechnologically derived product, namely "ABR preparation" in degrading polymers formed by *S. mutans*. Our results showed that ABR preparation is able to break down the polysaccharide produced by *S. mutans*, and consequently to significantly remove microbial biofilm formed onto teeth surface. This activity was not affected by the presence of saliva, oral mouthwashes or disinfectants.

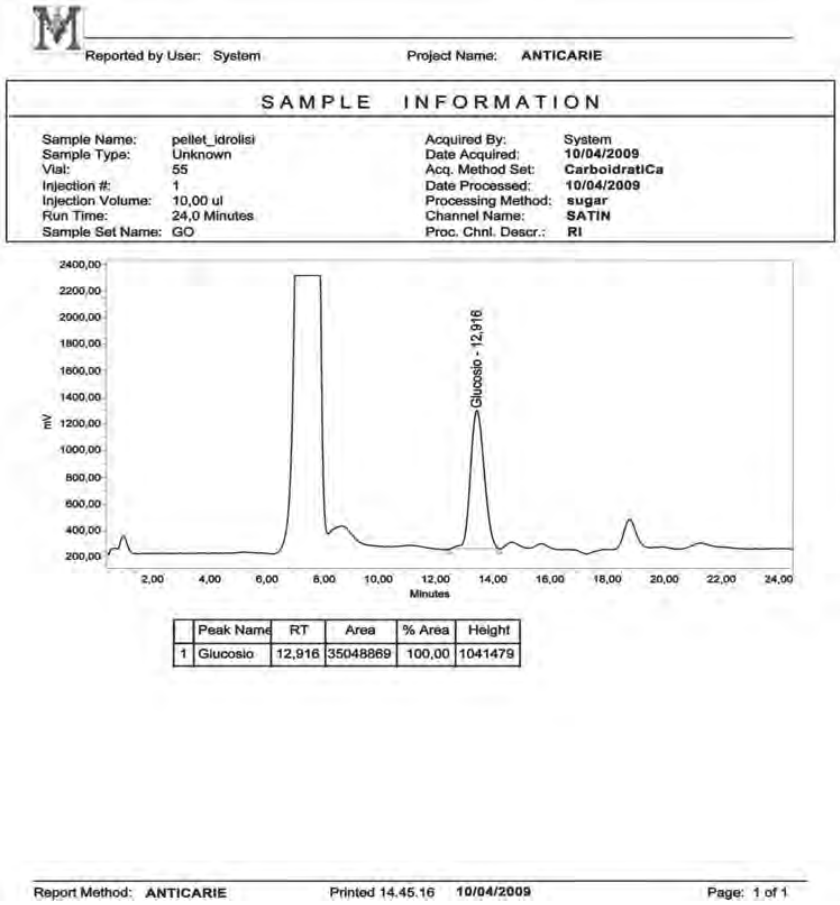

Fig. 1. *Evaluation of the presence of polysaccharides in the substrate used for the activity assay: typical positive HPLC-chromatogram.*

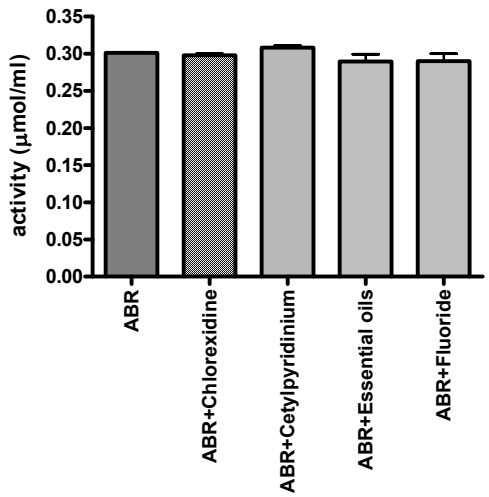

Fig. 2. *Activity in reducing sugars, as assessed by the DNS test, of the ABR preparation in the absence or the presence of 4 commonly used disinfectants of the oral cavity (Chlorexidine, Cetylpyridinium, Essential oils, and Fluoride). Results are expressed as means + SDs.*

ABR preparation doesn't contain proteins and doesn't show a typical enzymatic activity; furthermore, it does not exhibit activity changes in a range of pH between 4.0 and 8.0. The activity shown against *S. mutans* polysaccharide does not depend on the type of *Bacillus* strain used or on the fermentation medium. It was observed that the addition to the culture medium of only one of the two components between soluble starch (i.e., rice starch, corn starch, potato starch) or cellulose (i.e., microcrystalline cellulose, methyl cellulose, carboxymethyl cellulose, and ethyl cellulose), does not allow to obtain active preparations. On the contrary, this activity was observed with the concomitant addition of starch and cellulose, probably because is induced the production of one or more compounds that otherwise would not be produced. Thus, the disruptive activity cannot probably be ascribed to substances already known in the state-of-the-art.

Commercial mouthwashes are commonly used, because of their antimicrobial activity, as an adjunct to

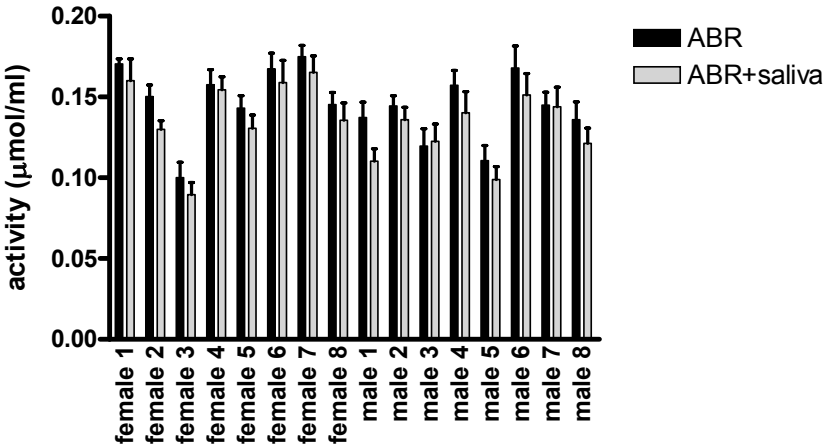

Fig.3. *Effect of the presence of saliva on the activity of ABR preparation in reducing sugars, both in female and male subjects. Results are means ± SDs.*

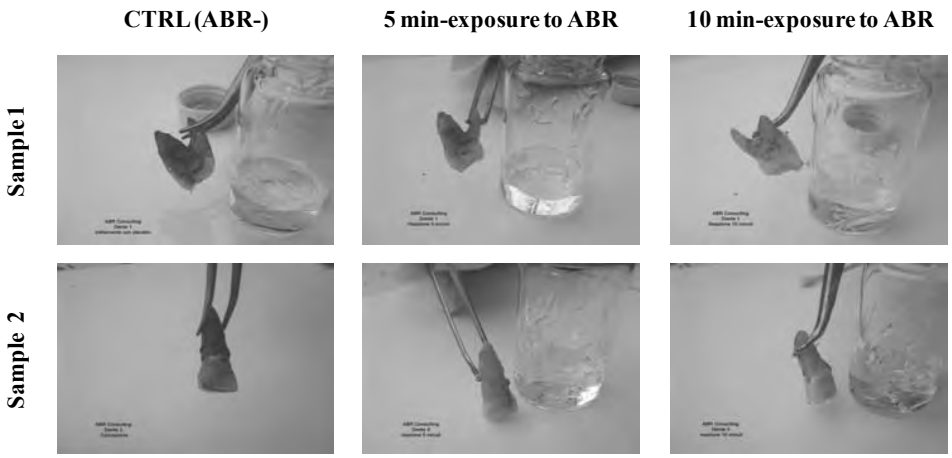

Fig. 4. *Effect of exposure to ABR preparation on 48h-biofilm formed by S. mutans onto dental surface. Assay was performed using two teeth (sample 1, sample 2). Biofilm was exposed to ABR preparation ("ABR") for 5 or 10 min. The presence of biofilm formed on tooth surface was shown by staining with Red-Cote dye.*

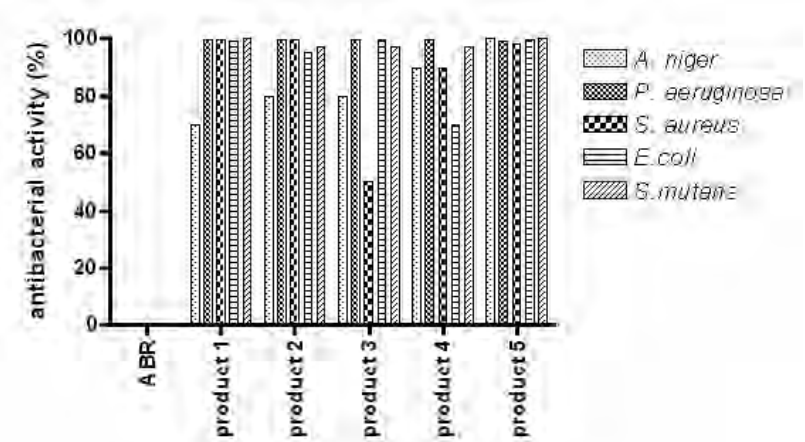

Fig. 5. *Antibacterial activity exhibited by ABR preparation and five commercial mouthwashes against bacterial and fungal species commonly found in the oral cavity. Antibacterial activity was expressed as percentage of reduction in bacterial viability, compared to the initial inoculum (100% viability). (Product 1: containing essential oils of mint, thyme, eucalyptus and birch, sodium fluoride, alcohol; Product 2: containing sodium fluoride, cetylpyridinium; Product 3: containing sodium fluoride, and cetylpyridinium; Product 4: containing 0.12% chlorhexidine; Product 5: containing amine fluoride).*

daily oral hygiene or as a mono-therapy in the prevention of plaque accumulation and gingival inflammation (17-23). Our results confirmed that most commercially available mouthwashes were able to significantly decrease viability, up to 90%, of bacterial and fungal species commonly found in the oral cavity. However, an indiscriminate bacterial eradication from the oral cavity is not *per se* a solution to the phenomenon because the perturbation of oral microbiota may have adverse effects, such as the risk of superinfections. In this regard, our results showed that ABR preparation, contrarily to commercial oral disinfectants, showed no antibacterial and antifungal activity, suggesting that its use can therefore be considered safe in that the oral flora is not perturbed.

In conclusion, taken together our results posed rationale for using of ABR preparation in combination with commonly used oral mouthwashes/disinfectants, thus adding the ability, not shown by mouthwashes, to remove preformed plaque and counteract its development, thus offering conservative control of gingival and periodontal disease.

Indeed, the therapeutic potential that ABR preparation may be much more high, due to several reasons: i) it could be administrated by different formulations, optimal for treatment of biofilm-associated diseases (mouthwash or toothpaste for dental plaque treatment; gel, for treatment of chronic infected wounds; and spray or inhalation powder for treatment of cystic fibrosis-associated respiratory infections); ii) its production is relatively simple and unexpensive; iii) it is produced alcohol free and, with suitable excipients, may be used in the pediatric patients; and, finally iv) it may also be used to prevent bacterial adhesion to medical devices (dental implants, catheters, etc.). Further studies are warranted to better define the real therapeutic significance of ABR preparation.

ACKNOWLEDGEMENTS

U.M. and F.A. are Managing Directors of ABR Consulting S.r.l., Ascoli Piceno, Italy.

REFERENCES

1. Marsh PD, Moter A, Devine DA. Dental plaque biofilms: communities, conflict and control. Periodontol 2000 2011;55(1):16-35.
2. Allaker RP, Hardie JM. Oral infections. In Topley and Wilson's microbiology and microbial infections (9th ed.), vol. 3, Arnold, London, 1998; p. 373–90.
3. Kuramitsu HK, Wang BY. Virulence properties of cariogenic bacteria. BMC Oral Health 2006;6 (Suppl 1):S11.
4. Kuramitsu HK, Wang BY. The whole is greater than the sum of its parts: dental plaque bacterial interactions can affect the virulence properties of cariogenic *Streptococcus mutans*. Am J Dent 2011;24(3):153-4.
5. Nicolas GG, Lavoie MC. *Streptococcus mutans* and oral streptococci in dental plaque. Can J Microbiol 2011;57(1):1-20.
6. Paes Leme AF, Koo H, Bellato CM, Bedi G, Cury JA. The role of sucrose in cariogenic dental biofilm formation – new insight. J Dent Res 2006;85:878–887.
7. Tanzer JM, Freedman ML, Fitzgerald RJ. Virulence of mutants defective in glucosyltransferase, dextran-mediated aggregation, or dextranase activity. In: Molecular basis of oral microbial adhesion. Mergenhagen SE, Rosan B, ed. Washington, DC: American Society of Microbiology, 1985: 204–211.
8. Bowen WH. Do we need to be concerned about dental caries in the coming millennium? J Am Dent Assoc 2002;133:1405–07.
9. Tenuta LM, Ricomini Filho AP, Del Bel Cury AA, Cury JA. Effect of sucrose on the selection of mutans streptococci and lactobacilli in dental biofilm formed *in situ*. Caries Res 2006;40(6):546-9.
10. Duarte S, Klein MI, Aires CP, Cury JA, Bowen WH, Koo H. Influences of starch and sucrose on *Streptococcus mutans* biofilms. Oral Microbiol Immunol 2008;23(3):206-12.
11. Allaker RP, Douglas CW. Novel anti-microbial therapies for dental plaque-related diseases. Int J Antimicrob Agents 2009;33(1):8-13.
12. Cense AW, Peeters EA, Gottenbos B, Baaijens FP, Nuijs AM, van Dongen ME. Mechanical properties and failure of *Streptococcus mutans* biofilms, studied using a microindentation device. J Microbiol Methods 2006;67(3):463-72.
13. Islam B, Khan SN, Khan AU. Dental caries: from infection to prevention. Med Sci Monit 2007;13(11):RA196-203.
14. Kreth J, Zhu L, Merritt J, Shi W, Qi F. Role of sucrose in the fitness of *Streptococcus mutans*. Oral Microbiol Immunol 2008;23(3):213-9.
15. Duarte S, Klein MI, Aires CP, Cury JA, Bowen WH, Koo H. Influences of starch and sucrose on *Streptococcus mutans* biofilms. Oral Microbiol Immunol 2008;23(3):206-12.
16. Harwood CR, Cutting SM. Molecular Biological Methods for *Bacillus*. John Wiley & Sons, 199; p. 380-383.
17. Pires JR, Rossa Junior C, Pizzolitto AC. *In vitro* antimicrobial efficiency of a mouthwash containing triclosan/gantrez and sodium bicarbonate. Braz Oral Res 2007;21(4):342-7.
18. van der Mei HC, Engels E, de Vries J, Busscher HJ. Effects of amine fluoride on biofilm growth and salivary pellicles.

Caries Res 2008;42(1):19-27.

19. Dolińska E, Stokowska W. Short time effect of Elmex and Listerine mouthrinses on plaque in 12-year-old children. Adv Med Sci 2006;51(Suppl 1):73-6.
20. Albert-Kiszely A, Pjetursson BE, Salvi GE, Witt J, Hamilton A, Persson GR, Lang NP. Comparison of the effects of cetylpyridinium chloride with an essential oil mouth rinse on dental plaque and gingivitis - a six-month randomized controlled clinical trial. J Clin Periodontol 2007;34(8):658-67.
21. Modesto A, Drake DR. Multiple exposures to chlorhexidine and xylitol: adhesion and biofilm formation by *Streptococcus mutans*. Curr Microbiol 2006;52(6):418-23.
22. Fine DH, Markowitz K, Furgang D, Goldsmith D, Charles CH, Lisante TA, Lynch MC. Effect of an essential oil-containing antimicrobial mouthrinse on specific plaque bacteria *in vivo*. J Clin Periodontol 2007;34(8):652-7.
23. Witt J, Ramji N, Gibb R, Dunavent J, Flood J, Barnes J. Antibacterial and antiplaque effects of a novel, alcohol-free oral rinse with cetylpyridinium chloride. J Contemp Dent Pract 2005;6(1):1-9.

MICROBIOLOGIC EVALUATION OF CREVICULAR FLUID IN PATIENTS TREATED WITH PLATFORM SWITCHING AND TRADITIONAL IMPLANTS

A. MANNI[1], E. SPALLETTA[2], M. ARENA[2], P. CATTANI[3], S. MARCHETTA[3], R. CELLETTI[2]

[1]Dental School, Catholic University of Rome, Rome, Italy
[2]Dental School, University of Chieti-Pescara, Italy
[3]Microbiology Institute Catholic University of Rome, Rome, Italy Università cattolica del sacro Cuore Roma

Background: The purpose of this study was to compare the microbiota around natural teeth and dental implants with different restorative platforms. Attention was focused on whether the microbiological environment could change according to the implant platform used i.e. traditional or Platform Switching implants. As the latter show less signs of bone resorption, a correlation with the presence of certain periodontal bacteria was suggested. Methods: Seven partially edentulous patients with dental implants, either traditional or Platform Switching, were included in this study. All the implants were in function at least for 1 year. Gingival crevicular fluid samples were obtained before any periodontal probing from natural teeth and different implant platforms and assayed using DNA extraction and PCR sequences in order to determine quality and quantity of microbiota. Statistical analysis included chi square test were used to establish differences in the microbiological distribution between the two implant platforms. Results: There were not statistical differences neither regarding the distribution of microbiota around natural teeth and implants nor between the two implant platforms. The presence of *B.forsythus* was revealed in the majority of the samples (from 90% to 100%) while *A.actinomycetemcomitans* was rarely found (from 0% o 25%). As for the other periodontal microbiota, their presence or absence showed a variation according to different sites or patients, without a predictable pattern. Conclusions: It was not possible to find a link between the colonization of certain types of bacteria and the reduction of bone loss which occurs around Platform Switching implants. Therefore the preservation of bone crest is only due to biomechanical aspects, which are related to the reposition of the implant-abutment interface away from the outer edge of the implant platform and from the bone.

Several studies have demonstrated that more than 500 species of bacteria are likely to colonize the oral cavity and in each patient 150 or more species have been characterized. It has been found that the microbiota associated with stable implants is predominantly composed by Gram-positive cocci with very low counts of spirochetes and motile rods resembling the microbiota of healthy teeth among partially and fully edentulous patients.(1) in contrast, implants affected with perimucositis tend to harbour microbiota with higher levels of Gram-negative bacteria including *Fusobacterium* spp. and low proportions of Gram-positive microorganisms. Fusobacterium spp and P.gingivalis have been implicated as important pathogens in peri-implant disease (2-3) and have also been isolated from natural teeth with destructive periodontal disease (4-5). It is possible that these organisms interact with periodontal tissues in the same way periodontopathic bacteria do in destructive periodontal disease (6) and, therefore, may have a role in the pathogenesis of peri-implant lesions. In addition, non-indigenous oral microorganisms have been found in samples taken from sites showing signs of peri-implantitis. *Enterobacteriaceae* species, *Candida albicans*, and *Staphylococcus* species were identified on 72% of 18 failing implants.(7) These potential pathogenic microorganisms were also present subgingivally at neighbouring and non-neighbouring teeth, thus demonstrating their transmission from residual pockets around teeth to implants in partially edentulous patients. (8-9) This is responsible for microbial colonization of the implants and infection of the peri-implant tissues, resulting in peri-mucositis, bone loss and implant failure. The purpose of this study was to compare the microbiota

Key words: implants, Platform Switching, microbiota, crevicular fluid.

Corresponding author:
Renato Celletti, Professor of Periodontology I, University G.d'Annunzio, via dei Vestini,66100 Chieti, Italy; email: celletti@unich.it; phone number: +39 0871 3554062.

0393-974X (2012)

around natural teeth and dental implants with different restorative platforms. Attention was focused on whether the microbiological environment could change according to the implant platform used i.e. traditional or Platform Switching implants. As the latter show less signs of bone resorption, a correlation with the presence of certain periodontal bacteria was suggested.

METHODS

Seven partially edentulous patients with dental implants, either traditional or Platform Switching, were included in this study. All the implants were in function at least for 1 year. In each patient the conditions of natural teeth and the two implant platforms were considered. All the patients underwent a regular periodontal therapy of maintenance (scaling-root planing) before being involved in the study. Those patients who were taking such medication (systemic antibiotics, corticosteroids and non-steroidal anti-inflammatory drugs) were excluded from this study, in order not to alter the composition of crevicular fluid. In the same way, patients affected by aggressive periodontitis and pregnant women were not taken into consideration.

Gingival(CGF) and peri-implant(PICF) crevicular fluid samples were obtained before any periodontal probing, so as not to alter the nature of the CGF/PICF. The site to be sampled was isolated with cotton rolls, a saliva ejector was used and supragingival plaque was gently removed. After the site was dried in air with an air syringe, CGF was collected with paper strips, which were inserted into the gingival crevice until mild resistance was felt and then allowed to remain for 2 minutes. Strips visually contamined with saliva or blood were discarded. Two paper strips were inserted into each peri-implant vestibular crevice and two were used to collect CGF from natural teeth. All the samples were then immediately put into sterile boxes and sent to the Microbiological Institute of Catholic University of Rome, where they were stored at 4°C and assayed. All the paper strips were stored separately site by site, in order to avoid any possible contamination from each other.

DNA extraction

All the strips were assayed within 48 hours from sampling. Each clinical sample was subjected to DNA extraction, after being suspended in a saline solution and stored at 4°C before being used. The amount of samples was centrifugated at 14000rpm for 15' at 4°C in order to separate the cellular elements from the liquid phase of the solution where they were stored. Pellet cells were resuspended in 300µl of solution (50 mM Tris, 10 mM EDTA and 10% SDS) containing lysozyme (5mg/ml). The role of this enzyme is to break down bacterial cell walls thus improving nucleid acid extraction efficiency. The solution was then kept for 1 hour at 37°C, the temperature needed by the enzyme to be active. Proteinase K (200µg/ml) was added to damage bacterial cell walls and ,after 1 hour of incubation at 65°C, DNA was separated using a solution of phenol and chloroform/isoamilic acid (CIA). Total DNA was precipitated by chilled ethanol and kept at -20°C overnight. After being centrifuged at 14000rpm at 4°C for 40', the pellet was washed with chilled 70% ethanol and centrifuged again at 14000rpm at 4°C for 10' and resuspended in 50µl of distilled water.

Polymerase chain reaction

The polymerase chain reaction (PCR) is a technique to amplify a single or few copies of a piece of DNA across several orders of magnitude, generating millions or more copies of a particular DNA sequence. Primers (short DNA fragments) containing sequences complementary to the target region along with a DNA polymerase are key components to enable selective and repeated amplification. As PCR progresses, the DNA generated is itself used as a template for replication, setting in motion a chain reaction in which the DNA template is exponentially amplified. This process allows the DNA quantity to double every time the cycle is repeated, following the scientific relationship $y=2^n$ (y=amount of final product, n=number of amplification cycles). This reaction is thus highly specific (because of the complementary bases) and extremely sensible (for the number of amplifications). The whole process can be divided into three different steps for every single cycle of amplification, based on temperature changes: denaturation, annealing and extension/elongation step. 10µl of extracted DNA were analyzed for each bacterial type, while the primer of gene 16S rRNA was used. 30 pmol of each primer, deoxynucleotide triphosphates (dNTPs) (200µM), 1,5 mM of $MgCl_2$, 10mM of Tris-HCl (pH 8), 50 mM of KCl and 2,5 U of Hot Start DNA-polymerase enzyme (Qiagen S.p.a., Milan, Italy) were added to each sample to get a final volume of 50µl.

PCR is carried out with cycles that have three temperature steps:

1) Denaturation : this step is the first regular cycling event and consists of heating the reaction to 94-98°C for 20-30 seconds, after an initialization step where the enzyme is heated at 95°C for 15'. Denaturation causes melting of DNA template and primers by disrupting the hydrogen bonds between complementary bases of the DNA strands, yielding single strands of DNA. 45 cycles of denaturation (at 94°C for 30'') are repeated.

2) Annealing: the reaction temperature is lowered to 30-65°C allowing annealing of the primers to the single-

stranded DNA template. Stable DNA-DNA hydrogen bonds are only formed when the primer sequence very closes matches the template sequence. The polymerase binds to the primer-template hybrid and begins DNA synthesis.

3) Extension-elongation step: commonly a temperature of 72°C (variable from 65°C to 72°C) is used with the Hot-Start DNA-polymerase. At this step the enzyme synthesizes a new DNA strand complementary to the DNA template strand by adding deoxynucleotide triphosphates that are complementary to the template in 5' to 3' direction, condensing the 5'-phosphate group of the dNTPs with the 3'-hydroxyl group at the end of the nascent (extending) DNA strand. The extension time depends both on the DNA polymerase used and on the length of the DNA fragment to be amplified. At a temperature of 72°C the Hot-Start DNA-polymerase will polymerize 3550 bases per minute.

These three steps are generally repeated (45 cycles), leading to exponential amplification of the specific DNA fragment.

A basic PCR set up requires several components and reagents. These components include:

1) DNA template that contains the DNA region (target) to be amplified, accurately extracted and purified.

2) Two primers that are complementary to the 3'(three prime) ends of each of the sense and anti-sense strand of the DNA target.

3) Buffer solution, providing a suitable chemical environment for optimum activity and stability of the DNA polymerase (KCl, 50mM; Tris-HCl, 10mM, pH 8,3; $MgCl_2$, 1,5mM).

4) Deoxynucleotide triphosphates (dNTPs), the building blocks from which the DNA-polymerase synthesizes a new DNA strand (normally used at a concentration of 200mM).

5) The enzyme DNA-polymerase.

To check whether the PCR generated the anticipated DNA fragment, agarose gel electrophoresis was employed for size separation of the PCR products, which were then coloured with ethidium bromide and exposed to ultraviolet light (FluorS™ Multilmager, Bio-Rad), as shown in figure 1. The size of PCR products was determined by comparison with a DNA ladder (a molecular weight marker VIII, Roche Diagnostics S.p.a. Monza,MI), which contains DNA fragments of known size, run on the gel alongside the PCR products.

The dimensions of the amplified PCR products was as follows:

-Actinobacillusactinomycetemcomitans	443bp
-Porphyromonas gingivalis	404bp
-Prevotella intermedia	589bp
-Bacteroides forsythus	641bp
-Campylobacter rectus	598bp
-Treponema denticola	316bp

RESULTS

From the microbiological analysis of CGF and PICF samples, a different distribution of microbiota was revealed, following not a predictable pattern, even though some common features regarding the distribution of certain bacteria were noticed. The periodontal pathogens analyzed in this study were: *Actinobacillus actinomycetemcomitans*, *Porphyromonas gingivalis*, *Prevotella intermedia*, *Porphyromonas endodontalis*, *Campylobacter rectus*, *Campylobacter gracilis*,*Treponema denticola* and *Bacteroides forsythus*.

The microbiological results of each single patient were reported in tables I, II, III, IV, V, VI, VII:

In each table, the patient's surname is indicated in the first column, as well as the implants and natural teeth that were considered in the study (using the international FDI World Dental Federation two-digit notation). In the other columns instead, the precence or absence of the main periodontal pathogens is reported, indicating with **v** their presence while with **x** their absence. *Actinobacillus actinomycetemcomitans* was revealed to be absent in the majority of cases around Platform Switching and traditional implants and also around natural teeth. A different pattern of distribution was showed by *Bacteroides forshythus* that was almost always present. As for the other bacterial strains, their presence or absence seemed to undergo a variation according to different sites and patients. *Actinobacillus* has been associated more with localized aggressive periodontitis than generalized, while *Bacteroides forshythus* has been found in higher

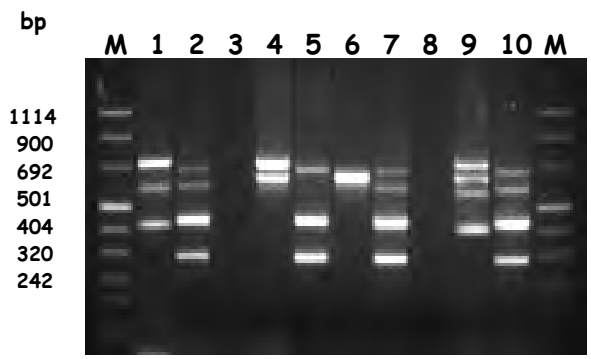

(base pieces=nucleotides)

Fig. 1.

Table I. *Distribution of microbiota in different sites in the patient G.*

G.	Aa	Pg	Pi	Pe	Cr	Cg	Td	Bf
Platform Switching 11	x	v	v	v	x	v	x	v
Platform Switching 21	x	x	v	v	x	v	x	v
Implant 23	x	x	x	v	v	v	x	v
Implant 26	x	v	v	v	v	v	x	v
Natural tooth 45	x	x	x	x	v	v	x	v

Table II. *Distribution of microbiota in different sites in the patient PA.*

PA.	Aa	Pg	Pi	Pe	Cr	Cg	Td	Bf
Implant 26	x	x	x	v	x	x	x	v
Implant 33	x	v	v	v	v	x	x	v
Implant 34	x	x	x	v	x	x	v	v
Implant 45	x	x	v	v	x	x	x	v
Implant 44	x	x	v	v	v	x	x	v
Natural tooth 25	x	v	v	v	x	x	x	v

Table III. *Distribution of microbiota in different sites in the patient S.*

S.	Aa	Pg	Pi	Pe	Cr	Cg	Td	Bf
Implant 33	x	x	v	v	v	x	v	v
Implant 34	x	x	v	v	v	x	v	v
Implant 36	x	v	x	v	v	x	v	v
Implant 37	x	v	v	x	v	x	v	x
Implant 13	x	v	x	v	x	x	v	v
Natural tooth 21	x	x	v	v	x	x	v	v

quantity in destructive periodontal disease rather than in gingivitis or in health status. The precence of this pathogens certainly leads to an increased probability of bone resorption, reduction of the attachment level and tooth loss. In tables VIII, IX, X the results are not showed for every single patient, but they are grouped according to different implant platforms and natural teeth (indicating with 0 the absence and with 1 the precence of the various periodontal bacteria).

The yellow line contains the percentage values regarding the precence of bacteria in the whole group examinated.

It is evident also from this tables that the percentage values of presence of each bacterial strain are very similar, thus reflecting a common distribution of the microbiota (significant differences were not reported between Platform Switching and traditional implants). In both cases the amount of certain bacteria is minimal (*Actinobacillus actinomycetemcomitans*), while other types seemed to find a proper environment for their

Table IV. *Distribution of microbiota in different sites in the patient C.*

C.	Aa	Pg	Pi	Pe	Cr	Cg	Td	Bf
Platform Switching 44	x	v	v	v	x	x	x	v
Platform Switching 45	x	x	x	v	v	x	x	v
Platform Switching 46	x	x	x	x	v	x	x	x
Platform Switching 36	x	v	v	v	v	x	x	v
Implant 34	x	v	v	v	x	x	x	v
Implant 35	x	x	x	x	x	x	x	v
Natural tooth 33	x	v	x	x	x	x	x	v
Dental root 11	x	x	v	v	v	x	x	v

Table V. *Distribution of microbiota in different sites in the patient B.*

B.	Aa	Pg	Pi	Pe	Cr	Cg	Td	Bf
Platform Switching 15	x	x	x	x	x	x	x	v
Natural tooth 13	x	x	x	v	v	x	v	v

Table VI. *Distribution of microbiota in different sites in the patient F.*

F.	Aa	Pg	Pi	Pe	Cr	Cg	Td	Bf
Implant 25	v	x	x	v	x	x	x	v
Natural tooth 23	v	x	v	v	x	x	x	v

Table VII. *Distribution of microbiota in different sites in the patient PB.*

PB.	Aa	Pg	Pi	Pe	Cr	Cg	Td	Bf
Platform Switching 16	x	v	x	v	v	v	v	v
Platform Switching 26	x	v	x	v	v	v	v	v
Platform Switching 27	x	x	x	v	v	v	v	v
Natural tooth 14	v	x	x	v	v	v	v	v

colonization (Bacteroides forshythus, Porphyromonas endodontalis).

The histogram shown in figure 2 compares the presence of bacteria in all the three groups that were taken into consideration:

No correlation between the presence of a certain bacterial strain and the implant platform used was found.

In order to achieve a more scientific evidence, statistical analysis including chi-square test were used to establish differences in the microbiological distribution between the two implant platforms. Chi-square is a statistical test commonly used to compare observed data with data we would expect to obtain according to a specific hypothesis. The chi-square test is always testing the null hypothesis, which states that there is no significant difference between the expected and observed result. The sampling distribution (if the null hypothesis is true) can be made to approximate a chi-square distribution as closely as desired by making the sample size large enough.

Table VIII. *Presence or absence of bacteria around Platform Switching implants.*

	Aa	Pg	Pi	Pe	Cr	Cg	Td	Bf
Platform Switching	0	0	0	0	0	0	0	1
Platform Switching	0	1	0	1	1	1	1	1
Platform Switching	0	1	0	1	1	1	1	1
Platform Switching	0	0	0	1	1	1	1	1
Platform Switching	0	1	1	1	0	0	0	1
Platform Switching	0	0	0	1	1	0	0	1
Platform Switching	0	0	0	0	1	0	0	0
Platform Switching	0	1	1	1	1	0	0	1
Platform Switching	0	1	1	1	0	1	0	1
Platform Switching	0	0	1	1	0	1	0	1
Total	0	5	4	8	6	5	3	9
	0	50	40	80	60	50	30	90

The results showed that there is not a statistical significant difference in the distribution of bacteria.

DISCUSSION

The aim of this study was to establish a correlation between the presence of certain bacterial strains and the use of different implant platforms, in order to find a microbiological answer to the preservation of bone crest that occurs around Platform Switching implants. There were no statistical significant differences between the implant platform used and the colonization of different types of bacteria; this means that the microbiological environment around Platform Switching implants is not populated by less pathogenic species as it was supposed to be. Therefore the preservation of bone crest is only due to biomechanical aspects, which are related to the reposition of the implant-abutment interface away from the outer edge of the implant platform and from the bone [10].

The advantages of using Platform Switching implants are summed up as follows:

-expanded platform
-primary stability
-more centred abutment; axial forces
-more preservation of bone height and soft tissues
-high aesthetic value

The microbiological composition of CGF and PICF around different implant platforms did not reveal such differences in this study, however it should be considered how there could be a variation of the microbiota whether there is a health status or the implant shows signs of peri-mucositis and peri-implantitis.

Table IX. *Presence or absence of bacteria around traditional implants.*

	Aa	Pg	Pi	Pe	Cr	Cg	Td	Bf
Implant	0	0	0	1	0	0	0	1
Implant	0	1	1	1	1	0	0	1
Implant	0	0	0	1	0	0	1	1
Implant	0	0	1	1	0	0	0	1
Implant	0	0	1	1	1	0	0	1
Implant	0	0	1	1	1	0	1	1
Implant	0	0	1	1	1	0	1	1
Implant	0	1	0	1	1	0	1	1
Implant	0	1	1	0	1	0	1	0
Implant	0	1	0	1	0	0	1	1
Implant	0	1	1	1	0	0	0	1
Implant	0	0	0	0	0	0	0	1
Implant	1	0	0	1	0	0	0	1
Implant	0	0	0	1	1	1	0	1
Implant	0	1	1	1	1	1	0	1
Total	1	6	8	13	8	2	6	14
	6,7	40,0	53,3	86,7	53,3	13,3	40,0	93,3

It has been demonstrated that implants showing signs of peri-implantitis reveal a subgingival microbiota similar to the microbiota around natural teeth with periodontal disease.[11] Patients with a past history of periodontal disease tend to have a high prevalence of anaerobic putative periodontal pathogens after 6 months exposure of implants to oral environment.[12] These findings established a possible association between periodontopathic bacteria and peri-implantitis. Moreover, a phenomenon called intraoral translocation plays a determinant role in the composition of subgingival microbiota.[13] Periodontopathic bacteria can be transferred from periodontal pockets to peri-implant niches by means of oral hygiene aids [14] and dental instruments,[15] thus increasing the risk of a peri-implant infection. The monitoring of the periodontal-peri-implant status in partially edentulous patients using microbiological parameters represents an approach for the long-term success of osseointegrated implants.[16-18]

CONCLUSIONS

In this study attention was mostly focused on the microbiological aspect, however further studies could be developed regarding, besides the presence of certain periodontal bacteria on the implant surfaces, their amount and the volume of crevicular fluid, which suddenly increases from healthy gingiva to gingivitis and periodontitis. A recent hypothesis suggests that when using the same diameter for implant and abutment, inflammation is extended only in a vertical plane, thus leading to an increased volume of crevicular fluid which tends to wash out all the inflammatory products. In this

Table X. *Presence or absence of bacteria around natural teeth.*

	Aa	Pg	Pi	Pe	Cr	Cg	Td	Bf
Natural tooth	0	0	0	1	1	0	1	1
Natural tooth	1	0	0	1	1	1	1	1
Natural tooth	0	1	1	1	0	0	0	1
Natural tooth	0	0	1	1	0	0	1	1
Natural tooth	0	1	0	0	0	0	0	1
Natural tooth	0	0	1	1	1	0	0	1
Natural tooth	1	0	1	1	0	0	0	1
Natural tooth	0	0	0	0	1	1	0	1
Total	2	2	4	6	4	2	3	8
	25,0	25,0	50,0	75,0	50,0	25,0	37,5	100,0

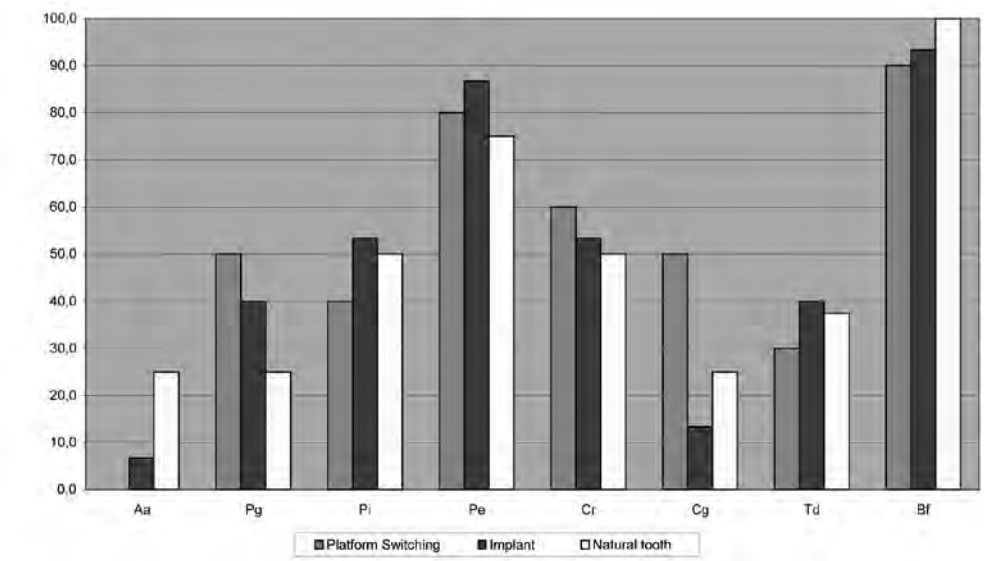

Fig. 2.

way inflammation results to be localized on the bone crest, determining an irritating action responsible for its resorption.

In conclusion, although no microbiological differences have been found between traditional and Platform Switching implants, the latter undoubtedly show great advantages due to less bone resorption around the implant shoulder, improving the whole biomechanical performance.

REFERENCES

1. Kohavi D, Greenberg R, Raviv E, Sela MN. Subgingival and supragingival microbial flora around healthy osseointegrated implants in partially edentulous patients. Int J Oral Maxillofac Implants 1994;9:673-678.
2. Mombelli A, Maxer M, Gaberthuel T, Grunder U, Lang NP. The microbiota of osseointegrated implants in patients with a history of periodontal disease. J Clin Periodontol 1995;22:124-130.
3. Shibli JA, Martins MC, Lotufo RF, Marcantonio E Jr. Microbiologic and radiographic analysis of ligature-induced peri-implantitis with different dental implant surfaces. Int J Oral Maxillofac Implants 2003;18:383-390.
4. Slots J. Subgingival microflora and periodontal disease. J Clin Periodontol 1979;6:351-357.
5. Rutar A, Lang N, Buser D, Burgin W, Mombelli A. Retrospective assessment of clinical and microbiological factors affecting peri-implant tissue conditions. Clin Oral Implant Res 2001;12:189-195.
6. Page RC, Kornman KS. The pathogenesis of human periodontitis: An introduction. Periodontol 2000 1997;14:9-11.
7. Alcoforado GAP, Rams TE, Feik D, Slots J. Microbial aspects of failing osseointegrated dental implants in humans. J Parodontologie 1990;10:11-18.
8. Leonhardt A, Adolfsson B, Lekholm U, Wikström M, Dahlen G. A longitudinal microbiological study on osseointegrated titanium implants in partially edentulous patients. Clin Oral Implant Res 1993;4:113-120.
9. Lee KH, Tanner ACR, Maiden MFJ, Weber HP. Pre- and post-implantation microbiota of the tongue, teeth, and newly placed implants. J Periodontol Clin 1999;26:822-832.
10. Lazzara RJ, Porter SS. Platform Switching: a new concept in implant dentistry for controlling postrestorative crestal bone levels. Int J Periodontics Restorative Dent 2006;26:9-17.
11. Ong ES, Newman HN, Wilson M, Bulman JS. The occurrence of periodontitis related microorganisms in relation to titanium implants. J Periodontol 1992;63:200-205.
12. Mombelli A, Maxer M, Gaberthuel T, Grunder U, Lang NP. The microbiota of osseointegrated implants in patients with a history of periodontal disease. J Clin Periodontol 1995;22:124-130.
13. Quirynen M, De Soete M, Dierickx K, van Steenberghe D. The intra-oral translocation of periodontopathogens jeopardizes the outcome of periodontal therapy. A review of the literature. J Clin Periodontol 2001;28:499-507.
14. Contreras A, Astudillo M, Daza LH, et al. Microbial toothbrush contamination in patients with periodontal disease (in Spanish). Revista Estomatologia 2002;10:4-14.
15. Haffaje AD, Socransky SS. Microbial etiological agents of destructive periodontal diseases. Periodontol 2000 1994;5:78-111.
16. Leonardt A, Gröndal K, Bergström C, Lekholm U. Long term follow up of osseointegrated titanium implants using clinical, radiographic and microbiological parameters. Clin Oral Implant Res 2002;13:127-132.
17. Di Stefano A, D'Aurizio E, Trubiani O, Grande R, Di Campli E, Di Giulio M, Di Bartolomeo S, Cellini L. Viscoelastic properties of Staphylococcus aureus and Staphylococcus epidermidis mono-microbial biofilms. Microbial Biotechnol 2009; 6:634-641.
18. Cellini L, Grande R, Di Campli E, Di Bartolomeo S, Di Giulio M, Traini T, Trubiani O. Characterization of an Helicobacter pylori environmental strain. J Appl Microbiol 2008; 3:761-769.

HISTOLOGICAL AND HISTOMORPHOMETRIC EVALUATION OF IMPLANT WITH NANOMETER SCALE AND OXIDIZED SURFACE. *IN VITRO* AND *IN VIVO* STUDY.

V. CORVINO, G. IEZZI, O. TRUBIANI, T. TRAINI, M. PIATTELLI

Dental School, University of Chieti-Pescara (Italy).

Background: The biological fixation of an implant to bone is influenced by numerous factors, including surface chemistry and surface topography. Various methods have been developed to create rough implant surfaces in order to improve the clinical performance of implants and to guarantee a stable mechanical bone-implant interface. Anodic oxidation is a dental implant surface modification technique that results in oxide layer growth up to a thickness of 1–10 micron. The purpose of this study was to evaluate the performance of the surface through the osteoblasts cells growth and the influence of oxidixed surface on BIC %, in the human posterior maxilla after 2 months of unloaded healing. Material and methods: In vitro commercially available primary human osteoblasts (NHOst) from both femur and tibia of different donor systems (Lonza Walkersville Inc, Walkersville, MD, USA) were grown in Osteoblast Growth Media (OBM) (Lonza). Osteogenic differentiation was induced for a period of 4 weeks by the OGM medium (OBM basal medium supplemented with 200nM of hydrocortisone-21-hemisuccinate and 7.5 mM of ®glycerophosphate). The viability of NHOst cells seeded test A and B was measured by the quantitative colorimetric MTT (3-[4,5-dimethyl-2-thiazolyl]-2,5-diphenyl-2Htetrazoliumbromide test) (Promega, Milan, Italy). One custom-made 2 x 10-mm site evaluation implant (SEI) with nanometer scale and oxidized surface (test) (Evo® Plan 1 Health s.r.l. - Amaro, UD, Italy), and one SEI with hydroxyapatite sandblasted surface (control) (Osseogrip® Plan 1 Health s.r.l. – Amaro, UD, Italy), were placed in the posterior maxilla of 15 patients. Patients received one of each type of SEI placed on controlateral side. Results: The proliferation rate studied by the MTT assay showed that during the incubation time, starting at 24 h, an increased proliferation rate was evident in Test B respect to Test A. After 2 months of unloaded healing BIC% was significantly higher in oxidized implants. BIC% mean values for the Osseogrip ® surface was 36,133 ±4,888 ER and 53,533 ± 5,180 ER for the Evo® surface(P = 0,028). Conclusion: These results seem to confirm that implant surface topography entails mechanical restrictions to the spread and locomotion of the cells involved in bone healing

In recent years numerous studies have been attempted to improve the osseointegration of titanium oral implants (1,2) and especially the early formation of a direct contact between implant and surrounding bone (3), in order to extend clinical indications like critical host tissues and concepts of immediate or early loading (4-6). The biological fixation of an implant to bone is influenced by numerous factors, including surface chemistry and surface topography (7-9). Earlier studies (10,11) suggested that implant surface topography was the only parameter that significantly affected bone-to-implant contact (BIC) and interface shear strength. These findings were later confirmed by studies with animals, which indicated that a certain degree of surface roughness favored BIC, as assessed by the removal torque test (12-17).

Histological evaluation and surface analysis of torque tested implants have demonstrated an increased affinity of osteoblasts, more rapid formation of direct bone contact to surfaces and higher resistance to shear forces for rough implant surfaces[16,18] in comparison with smoother surfaces (19-22). Various methods have been developed to create rough implant surfaces in order to improve the clinical performance of implants and to guarantee a stable mechanical bone-implant interface (23).

Modifications of the micro and macrogeometry of biomaterials alter the biomolecular and cellular responses in vitro, as well as the soft and bone tissue responses in vivo (24,25).

Key words: implant dentistry, oxidized surface, nano scale.

Corresponding author:
Prof. Piattelli Maurizio
Department of Medical, Oral and Biotechnological Sciences, "G. D'Annunzio" University of Chieti-Pescara, Via dei Vestini 31, 66100, Chieti, Italy.
E-mail: mpiattelli@unich.it

0393-974X (2012)

In fact, these surface's properties are crucial during the bone healing phase in the peri-implant region. After implantation, implant surfaces are in contact with body fluids and interact with a lot of proteins and different cell types. Cell adhesion is one of the initial stages for subsequent proliferation and differentiation of osteoblastic cells producing bone tissue. It has been shown that osteoblastic cell adhesion, growth and differentiation are related to surface energy and roughness (26,27).

Rough surfaces encourage the entrapment of fibrin protein, adhesion of osteogenic cells and mechanical stability of implants in host bone (28–30). Numerous surface modifications including turned, blasted, acid-etched, porous-sintered, oxidized, plasma-sprayed, hydroxyapatite coated surfaces, or a combination of these procedures have been developed and are currently used with the aim of enhancing clinical performance (31).

There is growing evidence that micrometer and nanometer scale topographies may be able to modify different aspects of cell behavior like cell adhesion, morphology, proliferation and differentiation, as well as the production of local factors and microenvironments (32–37). The variation in results obtained thus far may depend on the roughness amplitude and the method used to produce the surface topography and texture(36–40). Histology from animal experiments (41,42) demonstrated roughness not only provides better mechanical stability between the bone tissue and the implant surface, but also a configuration that retains blood clots properly and stimulates the bone healing process.

Anodic oxidation is a dental implant surface modification technique that results in oxide layer growth up to a thickness of 1–10 micron. This surface also features numerous pores of variable sizes (43,44). This process results in a growth of the native titanium oxide layer and a porous surface topography. It has been found that surface oxide properties of the titanium implant significantly influence bone tissue response and the observed strong bone reaction was speculated to depend on the formation of a bone-like apatite layer by $Na_2$0-Ti0_2 amorphous phase on the implant surface(45).The apatite formation was assumed to start with an ionic exchange of the alkali ions in the alkali titanate and the hydronium ion in simulated body fluid, thus treated substrates formed a dense and uniform bonelike apatite layer on their surfaces in simulated body fluid (sbf) with ion concentrations nearly equal to those of human blood plasma(46). The resultant surface structure changed gradually from the outermost apatite layer to the inner Titanium (Ti) and its alloys through a hydrated titanium and titanium oxide layers. This provides not only the strong bonding of the apatite layer to the substrates but also a uniform gradient of stress transfer from bone to the implants. The present chemical surface modification is therefore expected to allow the use the bioactive Ti and its alloys as artificial bones even under load-bearing conditions. Studies that evaluated implant surface topography showed that BIC reacts to it more strongly than mach it appears as if hydrophilic surfaces supported adhesion of various cell types whereas hydrophobic surfaces often inhibited the interaction between cells and artificial surfaces enclosed implants (21,48,49).

In the present study we have evaluated the performance of the surface through the osteoblasts cells growth and the influence of oxidixed surface on BIC % in the human posterior maxilla after 2 months of unloaded healing.

MATERIALS AND METHODS

In vitro study

Cells culture

Commercially available primary human osteoblasts(NHOst) from both femur and tibia of different donor systems (Lonza Walkersville Inc, Walkersville, MD, USA) were grown in Osteoblast Growth Media (OBM) (Lonza).

The phenotype of the cells was characterized by the expression levels of alkaline phosphatase (ALP), collagen type I, osteocalcin and CD44, and formation of mineralization nodules.

Cells in the developing adherent layer were used for the experiments described below, after removal with 0.1% trypsin solution, and cell growth was evaluated by the Trypan Blue exclusion test. Cells were periodically checked under a phase contrast light microscope and finally analysed by scanning electron microscopy (SEM) and processed for biochemical analyses. All experiments were carried out using cells at the second passage and repeated with two different cell lines with similar results.

MTT assay

The viability of NHOst cells seeded test A and Bwas measured by the quantitative colorimetric MTT (3-[4,5-dimethyl-2-thiazolyl]-2,5-diphenyl-2Htetrazoliumbromide test) (Promega, Milan, Italy). 5.000 cells/well were seeded into a 96-well culture plate with OBM medium, after 24 h of incubation at 37°C, 15 µl/well of MTT was added to culture medium, and cells were incubated for 3 hrs at 37°C). The supernatants were read at 650 nm wavelength using an ND-1000 NanoDropSpectrophotometer (NanoDrop Technologies, Rockland,DE, USA). The MTT assay was performed in four independent experiments, six replicate wells for each experimental point.

Scanning electron microscopy (SEM)

The samples were prefixed for 4 h at 4 °C in 2% glutaraldehyde in 0.05M phosphate buffer (pH7.4), postfixedin 1% OsO4, dehydrated in increasing ethanol concentrations and then critical point-dried. They were then mounted on aluminium stubs and gold-coated in an Emitech K550 (EmitechLtd. Ashford, UK) sputter-coater before imaging by means of a SEM (LEO435VpCambridge, UK).

Statistical analysis

For statistical analysis One Way ANOVA was used for the MTTassay. A *P*-value of <0.05 was considered statistically significant.

In vivo study

This randomized controlled double blind study evaluated 15 patients (mean age : 43.6 years) enrolled between October 2008 to June 2009, with partial or full edentulism, who had elected to receive dental implants to restore their lost dentitions. The protocol was approved by Ethics Committee of the University of Chieti-Pescara and all patients provided written informed consent. Exclusion criteria included pregnancy, nursing and any systemic condition that could affect bone healing. One custom-made 2 x 10-mm site evaluation implant (SEI) with nanometer scale and oxidized surface (test) (Evo® Plan 1 Health s.r.l. - Amaro, UD, Italy), and one SEI with hydroxyapatite sandblasted surface (control) (Osseogrip® Plan 1 Health s.r.l. – Amaro, UD, Italy), were placed in the posterior maxilla of 15 patients. Patients received one of each type of SEI placed on controlateral side. The microimplants were placed in the posterior region of the maxilla, always distal to the last conventional implant placed. The recipient sites of microimplants were prepared with a 1,8 mm diameter twist drill and inserted with screw driver. Microimplants were placed approximately 2 mm above the crestal bone margin. (Fig. 1) If the microimplants presented low primary stability, a second surgical site was prepared. Drilling procedures were made under profuse irrigation with sterile saline. The flaps were sutured with single interruped silk sutures (Assusilk®- Assut Medical Sàrl, Pully-Lausanne-Switzerland) submerging the microimplants. After placement of the SEIs, panoramic radiographs were obtained (Fig. 2). Amoxicillin (Augmentin® 1 g - GlaxoSmithKline S.p.A.- Verona-Italy) was given two times per day for five days to prevent postoperative infection. For postoperative plaque control subjects were prescribed 0,2 % chlorhexidine (Corsodyl® - GlaxoSmithKline Consumer Healthcare S.p.A.– Baranzate di Bollate- Milan-Italy) rinses three times per day for 14 days. The sutures were removed after a week. The protocol for this study involved unloaded healing for all of the implants. All SEIs were retrieved after healing time of 2 months using a 4,1 mm internal diameter trephine with irrigation (FIG.3) and specimens were fixed by immediate immersion in 4% neutral formalin. A guide was mounted on the SEIs to estabilish the orientation of the trephine along the long axis of the implant. They were evaluated by light microscopy for histomorphometric analysis of the bone-implant contact (BIC). The hystomorphometric data for each specimen were recorded as percentage and means for the control and test groups ± standard error.

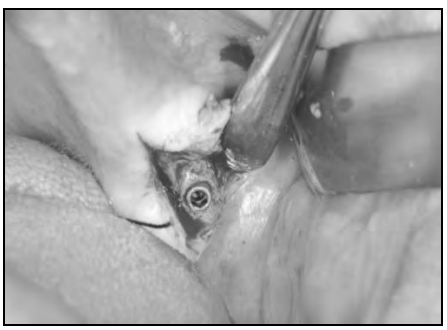

Fig. 1 *SEI placement in the posterior maxilla*

Specimen Processing and Histometric Analyses

The biopsies were processed (Precise 1 Automated System®, Assing, Rome, Italy) to obtain thin ground sections as previously described.[49] The specimens were dehydrated in an ascending series of alcohol rinses and embedded in glycol

methacrylate resin (Technovit® 7200 VLC, Kulzer, Wehrheim, Germany). After polymerization, the specimens were sectioned lengthwise along the larger axis of the implant, using a high-precision diamond disk, to about 150 µm, and ground down to about 30 µm. Two to three slides were obtained from each implant along the long axis. The slides were stained with basic fuchsin and toluidine blue. BIC% was defined as the amount of mineralized bone in direct contact with the implant surface. The measurements were made throughout the entire extent of the microimplant. These evaluations were performed using a light microscope (Laborlux S®, Leitz, Wetzlar, Germany) connected to a high-resolution video camera (3CCD®, JVC KY-F55B, Milan, Italy) and interfaced to a monitor and personal computer. This optical system was associated with a digitizing pad (Matrix Vision GmbH, Milan, Italy) and a histometry software package

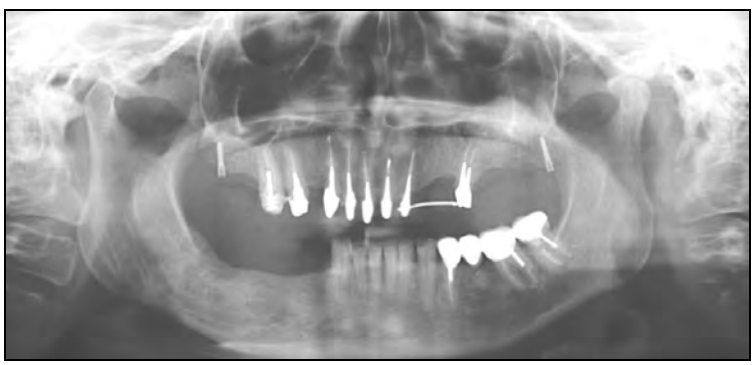

Fig. 2 *Radiograph taken after SEI placement*

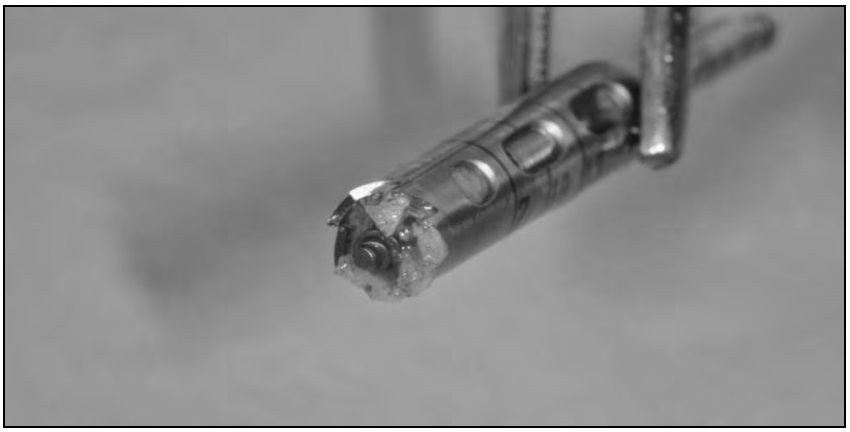

Fig. 3 *Trephine and core sample*

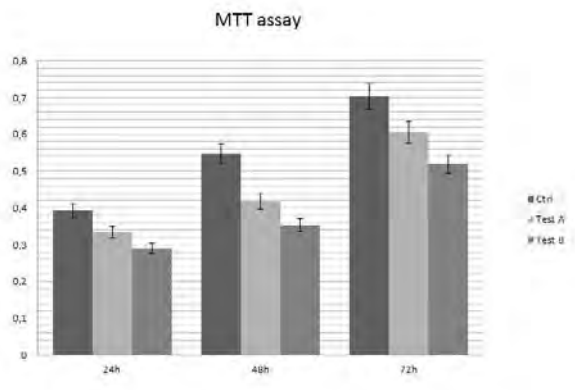

Fig. 4. *Cell growth evaluated by MTT assay*

with image-capture functionalities (Image-Pro Plus® 4.5, Media Cybernetics, Immagini & Computer Snc, Milan, Italy). The Mean and standard error of histometric variables were calculated for each implant, then for each group. Paired t-test was used to compare the surface topography. The significance test was 2-tailed and conducted at a 5% level of significance.

In vitro results

In the present study, normal human primary osteoblasts from Clonetics (Lonza) tested by the company for alkaline phosphatase (ALP), type I collagen, osteocalcin, CD44 and von Kossa mineralized nodules were used. [50]

The proliferation rate studied by the MTT assay showed that during the incubation time, starting at 24 h, an increased proliferation rate was evident in Test B respect to Test A (FIG. 4).

Scanning electron microscopy helped to clarify the behavior of cells in contact with the titanium implant surfaces.

In Figure 5, section A1 and A2, we observed the geometric surface of test A; the sample analysis allowed to distinguish in the implant macrodesigns the profile of the coils that cover the surface.

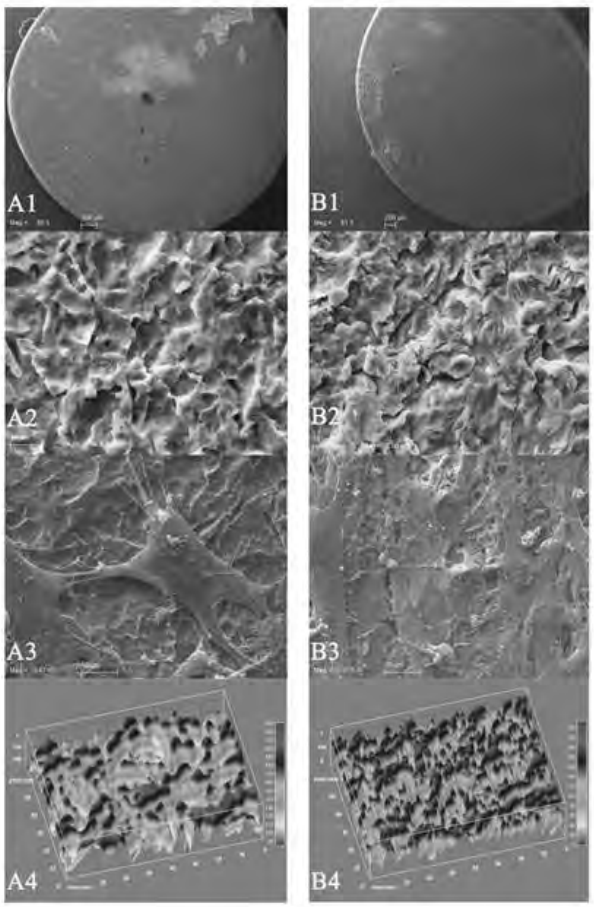

Fig. 5. *Morphological analysis carried out at scanning electron microscopy*

The Test B showed a nanostructured surface with more homogeneous roughness than in test A, moreover peaks and valleys arrangement demonstrated a more regular shape (Fig 5, section B1 and B2).

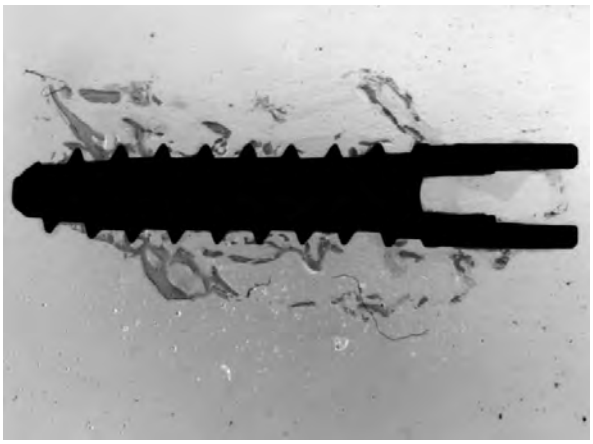

Fig. 6 *Undecalcified section from the control group. Toluidine blue-acid fuchsine staining. (12 X)*

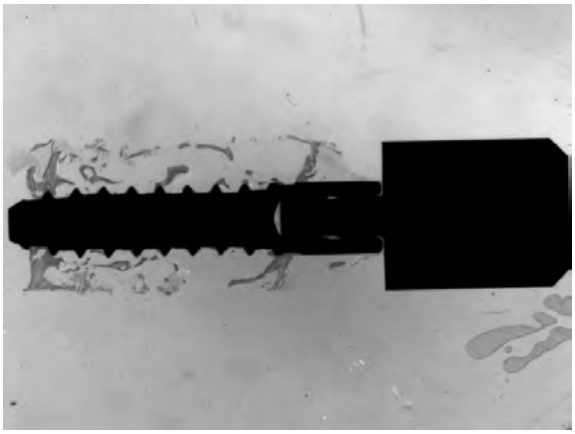

Fig. 9 *Undecalcified section from the test group. Toluidine blue-acid fuchsine staining (12 X)*

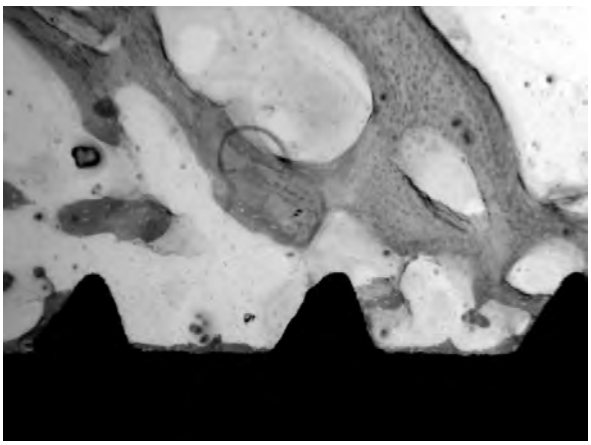

Fig. 7. *Newly formed bone was related only to some area of the implant surface. (40 X)*

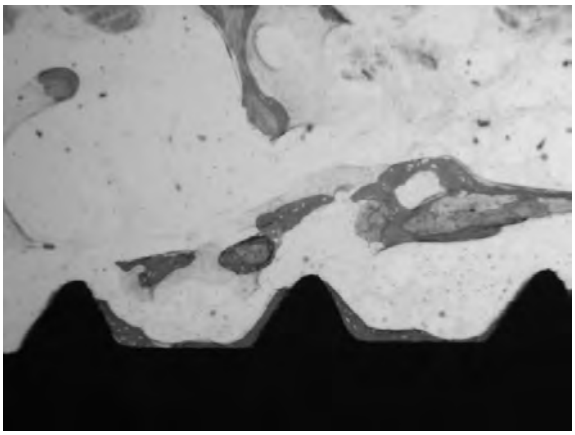

Fig 10 *Newly formed bone appeared to cover mostly of the implant surface (40X)*

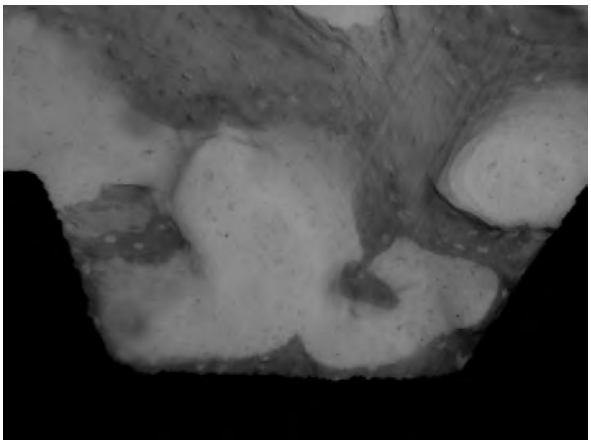

Fig 8 *In the bottom of the threads osteoblasts involved in the deposition of osteoid matrix not yet mineralized were observed (100 X)*

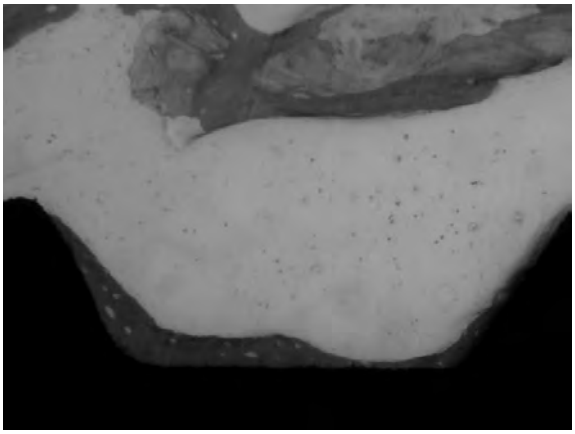

Fig. 11. *The new bone appeared to be spread over the implant surface showing an high grade of osteoconductivity. (100 X)*

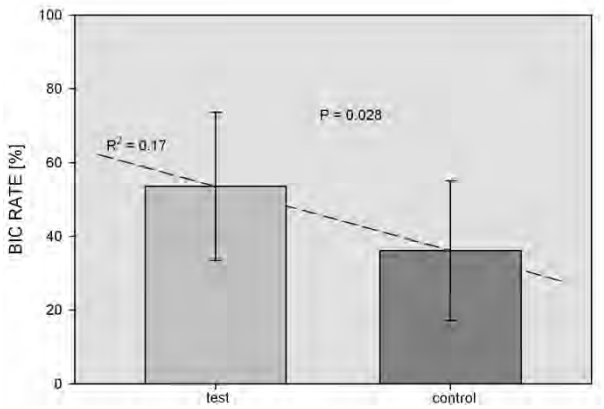

Fig. 12 *4 BIC rate of either test and control groups. The difference was statistically significant (P < .05). The linear regression showed a significant tendency of the BIC to increase in function of the type of the implant surface. (t = 2,457 with 14 degrees of freedom. (P = 0,028) 95 percent confidence interval for difference of means: 2,213 to 32,587 Power of performed test with alpha = 0,050: 0,547)*

The analysis of the profile in section D and D1confirmed respectively the previous observations.

In section B and B1 no signs of biomaterial degradation were observed at the conclusion of the treatment.

Photomicrographs of primary cultures of NHOstcells showed a specific cell morphology: in fact the cells showed a morphologically homogeneous fibroblast-like appearance with a stellate shape and long cytoplasmic processes.(Fig 5, section C).

The ultrastructural analysis of the test B evidenced many cells attached to the surface, and a marked interaction between cells and implant was evident. The osteoblasts established through extending cytoplasmic processes and filopodia contact zone, which enabled the anchorage to surface and between them (Fig 5, section C1).

Histological and Histometric Results

Overall, the bone surrounding the microimplants was healthy.

The specimens showed the presence of remodeling activity in the bone immediately adjacent to the microimplant.

At low magnification (12x), in all control sections considered the implant appeared surrounded by trabecular bone with marrow spaces (Fig. 6).

Some parts of the implant surface were completely surrounded by a thin layer of newly formed bone tissue (Fig. 7), while others portions were only partially in contact with bone and more with bone marrow.

At high magnification (100x), in some portions, particularly in the bottom of the threads osteoblasts involved in the deposition of osteoid matrix not yet mineralized were observed (Fig.8)

At low magnification (12 x) in all test sections considered the implant was surronded by trabecular bone with large marrow space. (Fig. 9)

At higher magnification (40 x) large marrow space were observed with the presence of some very thin trabecular bone. (Fig.10) A thin layer of bone trabeculae was interposed between the old bone and the implant.

The existing bone was in close contact with the implant surface, osteoblasts were observed still active, involved in the deposition of osteoid matrix. (Fig.11)

None of the microimplants with oxidized surface showed superficial debris or particle inclusions in the surrounding tissue close to the bone area.

BIC% was significantly higher in oxidized implants. BIC% mean values for the Osseogrip ® surface was 36,133 ±4,888 ER and 53,533 ± 5,180 ER for the oxidized surface(P = 0,028). (Fig.12)

DISCUSSION

In vitro cell culture provides an ideal tool to investigate specific different biomaterial scaffolds, and the current study assessed the cellular response to Test A and Test B. A plating efficiency assay verified that after 24 h the cells were adherent to the scaffold previously incubated overnight with OBM medium. During the first contact between cells and the examined surfaces no significant difficulty in the adhesiveness process was observed, confirming the biocompatibility of the three-dimensional implant examined. Considering the different geometry surfaces our results prove that a higher performance of the Test B respect to Test A, indicating the key role that acquire the nano-topographic profile.

In this study oxidized surface implants were histologically evaluated after removal from the human maxilla and compared with Osseogrip® implants after 2 months of healing.

The findings demonstrated that micro-implants with oxidized surfaces, subjected to an unloaded healing period of 2 months showed a higher bone-implant contact percentage (53,533 ± 5,180) than the BIC% for Osseogrip® implants surfaces (36,133 ±4,888).

These results seem to confirm that implant surface topography entails mechanical restrictions to the spread and locomotion of the cells involved in bone healing(51,52).

This healing starts immediately after implant insertion, with the formation of blood clots in the periimplant gap(53–56) and surface roughness is an important factor in this process.

When a biomaterial is implanted into a body, its surface is immediately covered with blood and serum proteins.

Materials that adsorb more attachment proteins can provide more sites for osteoblast precursor bonding to the implant, which then lead to faster bone in-growth and implant stabilization.

The implant surface topography properties, as well as the specific properties of individual proteins, determine

the organization of the adsorbed protein layer. Conversely, these events are affected by physicochemical interaction between the molecules and cells in the surrounding area(57).

More recently, studies have shown that implant surface topography itself can affect not only the osteoblast gene expression but also cell differentiation into osteoblasts (58,59).

The prerequisite for an implant with bioactive coating to be clinically used is its stability. Easy peeling off the layer from the substrate results in decrease in bonding strength of the implant to the host tissue. In addition, the layer may be accidentally scratched during operation, or dissolved after implantation by contacting with surrounding body fluids.

When a positive voltage is applied to a Ti electrode placed in an electrolyte, an anodizing process occurs and a porous TiO_2 layer is produced on the Ti surface. The porous and rough surface provides stronger bonding strength with the coating on it than a smooth surface. Additionally, electron beam evaporation with ion beam bombardments is one of the important techniques to produce high quality film, in which a film is deposited on a substrate while being simultaneously bombarded with ion beam. The reason for formation of strong adherent films provided by this method is that the interface between substrate and film is mixed by ion bombarding.

Besides the coating-to-substrate bond strength, the chemistry and crystallinity of coating could be the key factors affecting the stability of the coating. Coatings deposited by electron beam evaporation usually contain hydroxyapatite (HA), tricalcium phosphate (TCP), tetracalcium phosphate (TTCP), calcium oxide (CaO) and amorphous calcium phosphate (ACP) even the evaporant used was highly crystalline HA because of the extreme heat flame. Although other impurities except for ACP have a crystalline structure, all of these components are more soluble in physiological fluids than crystalline HA (59,60).

CONCLUSION

Within the limits of the present study, the histological data in humans confirmed that surface topography has an important influence on early bone tissue response under unloaded conditions.

Clinically, the anodized specimens showed more visible attached bone compared with the Osseogrip surfaces.The anodizing process presents newly-formed bone with early stages of remodeling in close contact with the implant surface.The anodized surface enhanced BIC and bone density in the thread area mainly in the maxilla (type IV bone). However, the surface implant topography did not affect the bone in a 500 μm wide zone lateral to the implant surface.In a histological evaluation of bone response between oxidized and turned titanium micro-implants in human jawbone, the author placed one test (oxidized surface, TiUnites, Branemark System) micro-implant and one control (turned surface, Mark IIIs, Branemark System) micro-implant, in totally 20 patients during implant surgery (21) .After a mean healing time of 6.6 months in the maxilla and 3.5 months in the mandible, the microimplants and the surrounding tissue were removed with a trephine bur. It was found that surface roughness and enlargement were greater for the oxidized implants than for the turned implants. Histomorphometric evaluation demonstrated significantly higher bone-to-implant contact for the oxidized implants, both in the maxilla and in the mandible. Ivanoff (21) concluded that there was a significantly higher bone response for anodic-oxidized titanium implants than for implants with turned surface, and the findings may depend on one or more differences of the surfaces: (1) the thicker oxide layer, (2) increased surface roughness, (3) differences in surface morphology in terms of porosity and (4) change in crystal structure. Zhu also reported that the cells on micron- and submicron-scale structures were observed to enter the pores and attach to the substrate by filopodia, and he attributed this phenomenon to pores acting as positive attachment sites for the filopodia(62). Hydrophilicity is also an important factor for cells adhesion to the substrates (63). The osteoblastic cells bind to the proteins at the implant surface via their integrin receptors. The addition of calcium ions to the surface changes the free surface energy and creates active sites with positive charge. Positively charged surfaces are favourable binding sites for extracellular matrix proteins as well as for phosphate ions (64). In-vitro experiments have shown that a calcium-containing surface absorbs more proteins compared to a surface with phosphate ions. Both calcium and phosphate ions may function as binding sites for proteins, but calcium ions play a more important role in osteoblast adhesion (65). The dissolution of calcium ions, which most likely takes place, may have an effect on surrounding cells. Calcium ions mediate cell–cell conjunction and communication (66) and may therefore contribute to increased cell activity and adhesion. Most of the studies demonstrated an advantage for the possibly bioactive surfaces in comparison with controls with respect to cell and bone response. Whether or not a chemical bond exists remains unproven.

REFERENCES

1. Davies JE. Mechanisms of endosseous integration. Int J Prosthodont 1998;11:391–401.
2. Berglundh T, Abrahamsson I, Lang NP, Lindhe J. De novo

alveolar bone formation adjacent to endosseous implants. Clin Oral Impl Res 2003;14:251–62

3. Wennerberg A, Albrektsson T . Suggested guidelines for the topographic evaluation of implant surfaces. Int J Oral Maxillofac Implants 2000;15:331-344
4. Jaffin RA, Berman CL. The excessive loss of Branemark fixtures in type IV bone: a 5-year analysis. J Periodontol. 1991 Jan;62(1):2-4.
5. Schoen PJ, Reintsema H, Raghoebar GM, Vissink A, Roodenburg JL. The use of implant retained mandibular prostheses in the oral rehabilitation of head and neck cancer patients. A review and rationale for treatment planning. Oral Oncol.2004 Oct;40(9):862-71.
6. Ostman PO, Hellman M, Sennerby L. Immediate occlusal loading of implants in the partially edentate mandible: a prospective 1-year radiographic and 4-year clinical study. Int J Oral Maxillofac Implants. 2008 Mar-Apr;23(2):315-22.
7. Albrektsson T, Wennerberg A. Oral implant surfaces. Part 2. Review focusing on clinical knowledge of different surfaces. Int J Prosthodont 2004;17:544–64.
8. Esposito M, Coulthard P, Thomsen P, Worthington HV. The role of implant surface modifications, shape and material on the success of osseointegrated dental implants. A Cochrane systematic review. Eur J Prosthodont Restor Dent 2005;13:15–31.
9. Puleo DA, Thomas MV. Implant surfaces. Dent Clin N Am 2006;50:323–38.
10. Thomas K, Cook SD. Relationship between surface characteristics and the degree of bone-implant integration. J Biomed Mater Res 1992;26:831– 833.
11. Albrektsson T, Bra¨nemark PI, Hansson HA, Lindstrom J. Osseointegrated titanium implants. Acta Orthop Scand 1981;52: 155–170.
12. Gotfredsen K, Hjorting-Hansen E, Jensen JS, Holmen A. Histomorphometric and removal torque analysis for TiO2-blasted titanium implants. Clin Oral Implants Res 1992;3:77– 84.
13. Gotfredsen K, Wennerberg A, Johansson C, Skovgaard LT, Hjorting-Hansen E. Anchorage of TiO2-blasted, HA-coated, and machined implants: An experimental study in rabbits. J Biomed Mater Res 1995;29:1223–1231.
14. Buser D, Schenk RK, Steinemann S, Fiorellini JP, Fox CH, Stich H. Influence of surface characteristics on bone integration of titanium implants. A histomorphometric study in miniature pigs. J Biomed Mater Res 1991;25:889 –902.
15. Buser D, Nydegger T, Hirt HP, Cochran DL, Nolte LP. Removal torques values of titanium implants in the maxilla of miniature pigs. Int J Oral Maxillofac Implants 1998;13:611– 619.
16. Wennerberg A, Albrektsson T, Andersson B, Kroll JJ. A histomorphometrical and removal torque study of screw-shaped titanium implants with three different surface topographies. Clin Oral Implants Res 1995;6:24 –30.
17. Wennerberg A, Albrektsson T, Johanson CB, Andersson B. Experimental study of turned and grit blasted screw-shaped implants with special emphasis on effects of blasting material and surface topography. Biomaterials 1996;17:15–22.
18. Li D, Ferguson SJ, Beutler T, et al. Biomechanical comparison of sandblasted and acid-etched and the machined and acid-etched titanium surface for dental implants. J Biomed Mater Res 2002; 60:325–332.
19. Brunette DM. Principles of cell behaviour on titanium surfaces and their application to implanted devices. In: Brunette DM, Tengval P, Textor M, Thomsen P, eds. Titanium in medicine. Berlin, Germany: Springer, 2001:485–512.
20. Wennerberg A, Albrektsson T, Lausmaa J. Torque and histomorphometric evaluation of c.p. titanium screws blasted with 25- and 75-microns-sized particles of Al2O3. J Biomed Mater Res 1996; 30:251–260.
21. Ivanoff CJ,Widmark G, Johansson C,Wennerberg A. Histologic evaluation of bone response to oxidized and turned titanium micro-implants in human jawbone. Int J OralMaxillofac Implants 2003; 18:341–348.
22. Ivanoff CJ, Hallgren C, Widmark G, Sennerby L, Wennerberg A. Histologic evaluation of the bone integration of TiO(2) blasted and turned titanium microimplants in humans. Clin Oral Implants Res 2001; 12:128–134.
23. Le Guehennec L, Soueidan A, Layrolle P, Amouriq Y. Surface treatments of titanium dental implants for rapid osseointegration. Dent Mater 2007;23:844–54.
24. Brunette DM, Chehroudi B. The effects of the surface topography of micromachined titanium substrata on cell behavior in vitro and in vivo. J Biomech Eng 1999; 121:49–57.
25. Kieswetter K, Schwartz Z, Dean DD, Boyan BD. The role of implant surface characteristics in the healing of bone. Crit Rev Oral Biol Med 1996; 7:329–345.
26. Cooper LF, Masuda T, Yliheikkila PK, Felton DA. Generalizations regarding the process and phenomenon of osseointegration. Part II. In vitro studies. Int J Oral Maxillofac Impl 1998;13:163–74.
27. Anselme K. Osteoblast adhesion on biomaterials. Biomaterials 2000;21:667–81.
28. Lauer G, Wiedmann-Al-Ahmad M, Otten JE, Hu¨bner

U, Schmelzeisen R, Schilli W. The titanium surface texture effects adherence and growth of human gingival keratinocytes and human maxillar osteoblast- like cells in vitro. Biomaterials 2001;22:2799–809.

29. Mustafa K, Wennerberg A, Wroblewski J, Hultenby K, Lopez BS, Arvidson K. Determining optimal surface roughness of TiO2 blasted titanium implant material for attachment, proliferation and differentiation of cells derived from human mandibular alveolar bone. Clin Oral Impl Res 2001;12:515–25.
30. Ellingsen JE, Johansson CB, Wennerberg A, Holme´n A. Improved retention and bone-to implant contact with fluoride-modified titanium implants. Int J Oral Maxillofac Impl 2004;19:659–66.
31. Binon PP. Implants and components: entering the new millennium. International Journal of Oral and Maxillofacial Implants 2000;15(1):76–94.).
32. Lohmann CH, Tandy EM, Sylvia VL, Hell-Vocke AK, Cochran DL, Dean DD, Boyan BD,Schwartz Z. Response of normal female human osteoblasts (NHOst) to 17beta-estradiol is modulated by implant surface morphology. J Biomed Mater Res. 2002 Nov;62(2):204-13.
33. Boyan BD, Lossdörfer S, Wang L, Zhao G, Lohmann CH, Cochran DL, Schwartz Z. Osteoblasts generate an osteogenic microenvironment when grown on surfaces with rough microtopographies. Eur Cell Mater. 2003 Oct 24;6:22-7.
34. Mante M, Daniels B, Golden E, Diefenderfer D, Reilly G, Leboy PS. Attachment of human marrow stromal cells to titanium surfaces. J Oral Implantol. 2003;29(2):66-72.
35. Lossdörfer S, Schwartz Z, Wang L, Lohmann CH, Turner JD, Wieland M, Cochran DL, Boyan BD. Microrough implant surface topographies increase osteogenesis by reducing osteoclast formation and activity. J Biomed Mater Res A. 2004 Sep 1;70(3):361-9.
36. Zinger O, Anselme K, Denzer A, Habersetzer P, Wieland M, Jeanfils J, Hardouin P, Landolt D. Time-dependent morphology and adhesion of osteoblastic cells ontitanium model surfaces featuring scale-resolved topography. Biomaterials. 2004 Jun;25(14):2695-711.
37. Lüthen F, Lange R, Becker P, Rychly J, Beck U, Nebe JG. The influence of surface roughness of titanium on beta1- and beta3-integrin adhesion and the organization of fibronectin in human osteoblastic cells. Biomaterials. 2005 May;26(15):2423-40.
38. Buser D, Nydegger T, Oxland T, Cochran DL, Schenk RK, Hirt HP, Snétivy D, Nolte LP. Interface shear strength of titanium implants with a sandblasted and acid-etched surface: a biomechanical study in the maxilla of miniature pigs. J Biomed Mater Res. 1999 May;45(2):75-83.
39. Anselme K, Bigerelle M, Noel B, Dufresne E, Judas D, Iost A, Hardouin P. Qualitative and quantitative study of human osteoblast adhesion on materials with various surface roughnesses. J Biomed Mater Res. 2000 Feb;49(2):155-166.
40. Zinger O, Zhao G, Schwartz Z, Simpson J, Wieland M, Landolt D, Boyan B. Differential regulation of osteoblasts by substrate microstructural features. Biomaterials. 2005 May;26(14):1837-47.
41. Larsson C, Thomsen P, Lausmaa J, Rodahl M, Kasemo B, Ericson LE. Bone response to surface modified titanium implants: studies on electropolished implants with different oxide thicknesses and morphology. Biomaterials 1994; 15:1062–1074.
42. Sul YT, Johansson CB, Jeong Y, Wennerberg A, Albrektsson T. Resonance frequency and removal torque analysis of implants with turned and anodized surface oxides. Clin Oral Implants Res 2002; 13:252–259
43. Hall J, Lausmaa J. Properties of a new porous oxide surface on titanium implants. Appl Osseointegr Res 2000;1:5– 8.
44. Sul YT. The significance of the surface properties of oxidized titanium to the bone response: Special emphasis on potential biochemical bonding of titanium implants. Biomaterials 2003; 24:3893–3907.
45. Kokubo T. Recent progress in bioactive materials. The Hague, Netherlands: The North Sea Biomaterials, 1998.
46. Kim HM, Miyaji F, Kokubo T, Nakamura T. Preparation of bioactive Ti and its alloy via simple chemical surface treatment. J Biomed Mater Res 1996; 32:409-417.
47. Huang YH, Xiropaidis AV, Sorensen RG, Albandar JM, Hall J, Wikesjo¨ UME. Bone formation at titanium porous oxide (TiUnite®) oral implants in type IV bone. Clin Oral Implants Res 2005;16:105–111.
48. Jungner M, Lundqvist P, Lundgren S. Oxidized titanium implants (Nobel Biocare® TiUnite™) compared with turned titanium implants (Nobel Biocare® markIII™) with the respect to implant failure in a group of consecutive patients treated with early functional loading and two-stage protocol. Clin Oral Implants Res 2005;16:308 –312.
49. Piattelli A, Scarano A, Quaranta M. High-precisio, cost-effective system for producing thin sections of oral tissues containing dental implants. Biomaterials 1997;18:577–579.
50. Trubiani O, Fulle S, Traini T, Paludi M, la Rovere R, Orciani M, Caputi S, Piattelli A. Functional assay, expression of growth factors and proteins modulating bone-arrangement in human osteoblasts seeded on an anorganic bovine bone biomaterial. Eur Cell Mater. 2010 Jul 21;20:72-83.

51. Den Braber ET, De Ruijter JE, Smits HTJ, Ginsel LA, Von Recum AF, Jansen JA. Effect of parallel surface microgrooves and surface energy on cell growth. J Biomed Mater Res 1995;29:511–518.
52. Lumbikanonda N, Sammons R. Bone cell attachment to dental implants of different surface characteristics. Int J Oral Maxillofac Implants 2001; 16:627– 636.
53. D'Hoedt B. The influence of implant materials and material surfaces on blood clotting: A scanning electron microscopy study. In: van Sttenberghe D, Albrektsson T, Bra¨nemark PI, Henry PJ, Holt R, Linden C, editors. Tissue integration in oral and maxillofacial reconstruction. Proceedings of an International Congress. Current Clinical Practice Series 1985;29:46– 50.
54. Meyer A, Baier R, Natiella J, Meenagha M. Investigation of tissue/implant interactions during the first two hours of implantation. J Oral Implantol 1988;14:363–379.
55. Zechner W, Tangl S, Fu¨rst G, Tepper G, Thams U, Mailath G, Watzek G. Osseous healing characteristics of three different implant types. A histological and histomorphometric study in mini-pigs. Clin Oral Implant Res 2003;14:150 –157.
56. Wen X, Wang X, Zhang N. Microrough surface of metallic biomaterials: A review. Biomed Mater Eng 1996;6:173–189.
57. Yan WQ, Nakamura T, Kobayashi M, Kim HM, Miyaji F, Kokubo T. Bonding of chemically treated titanium implants to bone. J Biomed Mater Res 1997;37:267–275.
58. Schneirder GB, Zaharias R, Seabold D, Keller J, Stanford C. Differentiation of preosteoblasts is affected by implant surface microtopographies. J Biomed Mater Res A 2004;64:462– 468.
59. Schneider GB, Perinpanayagam H, Clegg M, Zaharias R, Seabold D, Keller J, Stanford C. Implant surface roughness affect osteoblast gene expression. J Dent Res 2003;82:372–376.
60. Chou L, Marek B, Wagner WR. Effects of hydroxylapatite coating crystallinity on biosolubility, cell attachment efficiency and proliferation in vitro. Biomaterials 1999;20:977-985.
61. Zhang QY, Chen JY, Feng JM, Cao Y, Deng CL, Zhang XD. Dissolution and mineralization behaviors of HA coatings. Biomaterials 2003;24: 4741-4748.
62. Zhu XL, Chen J, Scheideler L, Reichl R, Geis-Gerstorfer J. Effects of topography and composition of titanium surface oxides on osteoblast responses. Biomaterials 2004;25:4087–4113.
63. Bhattarai SR, Bhattarai N, Viswanathamurthi P, Yi HK, Hwang PH, Kim HY. Hydrophilic nanofibrous structure of polylactide—Fabrication and cell affinity. J Biomed Mater Res Part A 2006;78:247–257.
64. Hanawa T, Kon M, Doi H, Ukai H, Murakami K, Hamanaka H, Asaoka K. Amount of hydroxyl radical on calciumion-implanted titanium and point of zero charge of constituent oxide of the surfacemodified layer. J Mater Sci 1998: 9: 89-92.
65. Feng B, Weng J, Yang BC, Qu SX, Zhang XD. Characterization of titanium surfaces with calcium and phosphate and osteoblast adhesion. Biomaterials 2004:25: 3421–3428.
66. Anselme K. Osteoblast adhesion on biomaterials. Biomaterials 2000: 21: 667– 681.

EFFECTS OF BISPHOSPHONATES IN ORTHODONTIC THERAPY:SYSTEMATIC REVIEW

D. RODOLFINO[A], M. SACCUCCI[B], A. FILIPPAKOS[A], R. GERXHANI[A], G. LOPEZ[A], F. FELICE[A], C. D'ARCANGELO[C]

[a]*Department of Medical, Oral Sciences and Biotechnology - Orthodontic School - University "G. d'Annunzio" Chieti - Pescara - Italy*
[b]*Oral and maxillofacial Department, Sapienza University of Rome*
[c]*Department of Medical, Oral Sciences and Biotechnology - Restorative Dentistry - University "G. d'Annunzio" Chieti - Pescara - Italy*

Background: Currently, the use of oral and systemic bisphosphonates, in the form of anti-osteoporosis medications or as a part of a chemotherapeutic regimen for several malignant diseases, is increasing dramatically in a large group of orthodontic patients. Animal studies have reported adverse dental effects from bisphosphonates, including decreased tooth movement, impaired bone healing, and osteonecrosis in the mandible and the maxilla. Objective: The objective of this paper was to analyze the effects of bisphosphonates on orthodontic therapy in humans. Strategy: The literature was systematically reviewed using PubMed, LILACS and OvidMedline up to December 31, 2011. Handsearching included several dental journals. Study selection: All RCT's, controlled trials and case reports-series about the effects of bisphosphonates on orthodontic therapy were analyzed and selected independently by two different researchers based on previously established inclusion and exclusion criteria. The main search terms were: bisphosphonates, orthodontic treatment and tooth movement. Results: The search strategy yielded 136 titles/abstracts: 134 from PubMed and 2 from LILIACS; no articles from OvidMedline, Chocrane Library and manual search. Eighty three records were screened, after removal of duplicates. After applying the inclusion/exclusion criteria, 135 papers were removed: 43 studies on animals, 4 French and Portuguese articles, 17 reviews and letters, 18 unrelated to orthodontic therapy or to the topic of this review. Conclusions: Further studies are required to assess possible adverse effects of bisphosphonate on orthodontic treatment in humans.

Recently, the issue of bisphosphonate (BP) treatment and its impact on dentistry, especially orthodontics, has become a topic of concern (1).

Bisphosphonates, stable analogues of naturally occurring pyrophosphate-containing compounds, are potent bone resorption inhibitors. The BP pharmacological site of action is in the osteoclast, where enzyme inhibition causes a decrease proteins responsible for cytoskeletal integrity and intracellular signaling. There is some evidence that this drug group might also inhibit osteoclast precursors and osteoblast communication with osteoclasts (2).

Consequently, bisphosphonates have been widely and successfully used in a variety of bone diseases associated with excessive osteoclast activity, including osteoporosis, Paget's disease, and fibrous dysplasia. Another clinical application of bisphosphonates is for metastatic and osteolytic bone disease. Bisphosphonates are now established as an effective therapeutic intervention for bone metastases of breast, lung, and prostate cancers (3).

Because bisphosphonates work by inhibiting bone resorption by osteoclasts, they can have side

effects in dental treatment, including inhibited tooth movement, impaired bone healing, and induced osteonecrosis in the maxilla and the mandible (4). There are numerous references in the literature to the use of bisphosphonates in dental practice; however, the results are often obtained in animal experimental studies with a short follow-up period and used drugs with very different antiresorptive

pawers (5). As yet, there have been no reports of orthodontic-related problems associated with

Key words: biposphonates, orthodontic therapy.

Corresponding Author:
Camillo D'Arcangelo,
Dept. Medical Oral Sciences and Biotechnology,
University "G. d'Annunzio" Chieti, Italy
tel.+39-085-4549652
e-mail: cdarcang@unich.it

0393-974X (2012)

bisphosphonate treatment (1). Increasing our knowledge on bisphosphonates is critical because these drugs have the potential to impede orthodontic treatment and increase morbidity to the maxilla and mandible. The main purpose of this systematic review was to analyze the available scientific evidence about the effect of bisphosphonate application in orthodontic therapy.

MATERIALS AND METHODS

Search strategy

The search strategy was conducted according to the Cochrane Collaboration guidelines (6).

Development of a comprehensive search strategy was a crucial aspect of undertaking this review

to ensure the identification of all randomized controlled trials, controlled trials, case reports-series, available on Cochrane Library, LILACS, PubMed and OvidMedline, published up to December 31, 2011. Handsearching included several dental journals.

The key MeSH (Medical Subject Headings) terms used were: ''diphosphonates'' or ''bisphosphonates'' combined with ''orthodontics'', ''orthodontic treatment'' or ''tooth movement''.

Selection criteria

Inclusion criteria were:

Study design: randomized controlled trials, controlled trials, case reports-series

Human samples

Systemic or topical administration of bisphosphonate.

Description of administration dose and regimen.

Description of direction and magnitude of the force.

English language.

We excluded review articles, opinion articles, letters, and articles that did not correspond to the objectives of this review.

Data gathering and analysis

The initial selection of articles was based on title and abstract, with a review of the complete article whenever there was any doubt as to whether to include it or not. Two reviewers (M.D. and D. R.), independently applied the inclusion and exclusion criteria to every article, with good concordance being shown (kappa index, 0.8).

Data were independently extracted by each reviewer, with intraexaminer conflicts being resolved by discussing the article in question until consensus was reached.

The methodological quality of the selected paper was assessed (5). The following characteristics were considered: sample size, previous estimation of sample size, validity of measuring methods, appropriate statistics, method error analysis, blinding of measurements, and losses of subjects to the study. Quality was classified as low, medium and high.

RESULTS

The search strategy yielded 136 titles/abstracts: 134 from PubMed and 2 from LILIACS; no articles from OvidMedline, Chocrane Library and manual search. Eighty three records were screened, after removal of duplicates.

After applying the inclusion/exclusion criteria, 135 papers were removed: 43 studies on animals, 4 French and Portuguese articles, 17 reviews and letters, 18 unrelated to orthodontic therapy or to the topic of this review. The remaining article was then read in full (Table I) (Fig. 1).

Analysis quality

The only article included in this review was considered to have low methodological quality (Table II). The quality defects were: inadequate size of study sample; inappropriate measurement methods and statistic; absence of method error analysis and absence of blinding in measurements.

DISCUSSION

Millions of peri- and postmenopausal women are currently taking oral bisphosphonates at the recommendation of their physicians for the prevention of skeletal events related to osteoporosis.

Tens of thousands of patients are also receiving bisphosphonate therapy as part of their chemotherapeutic regimens for the treatment of malignant diseases. As we continue to treat an aging population, it is incumbent upon orthodontists to be acutely aware of the potential impact of this class of drugs on our patients (7). This systematic review applied a strict protocol and a well defined search strategy to analyze the effect of bisphosphonate application in orthodontic therapy.

Of the different designs of clinical studies, the randomized controlled trial is recognized as providing the best scientific evidence (8).

Because of the lack of RTCs, the research strategy was extended to all controlled trials and case reports-series. After applying our inclusion and exclusion criteria, only one article, a report of 2 orthodontic patients using bisphosphonates, was finally selected (Table I) (1). When the methodological quality assessment was applied, this publication was considered to have low methodological quality. Because of its study design, the article presents inadequate size of study sample, inappropriate measurement methods and statistic, absence of method error analysis and absence of blinding in measurements.

Case 1, a 35-year-old woman, had been taking Fosamax for 16 months before the orthodontic treatment. Orthodontic treatment lasted 30 months and a conservative unilateral extraction pattern, consisting of the maxillary right and the mandibular right first premolars, was planned in conjunction with full banded/bonded orthodontic treatment to correct the Class II Division 1 subdivision

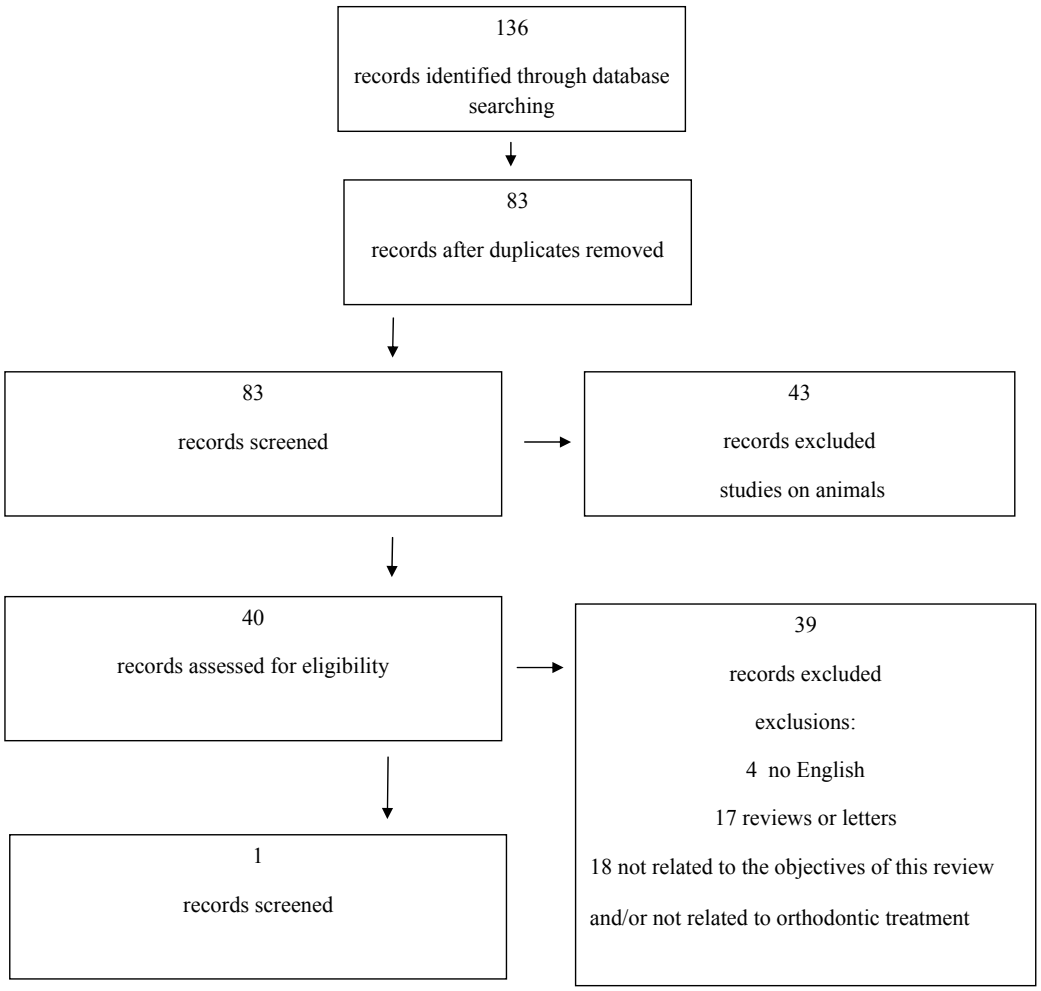

Fig.1. *Flow diagram of data searching and screening*

right malocclusion (Class II on the right and Class I on the left). Treatment phases and appliances are not specified.

Case 2, a 77-year-old man, had been on IV Zometa for 11 months before orthodontic treatment, consisting of placement of canine-to-canine ceramic brackets in the mandible to close 2 mm of residual space after the extraction of an ectopic mandibular. Closure of the extraction space lasted 13 months and was attempted with both a tight-chain elastic over a round 0.016-in stainless steel archwire and by an orthodontic elastic threadunder-tie.

Both patients experienced impeded tooth movement, and 1 patient also suffered osteonecrosis of the mandible. Space closure was extremely difficult in both cases.

The author sustains that bisphosphonates can impact orthodontic treatment by impeding tooth movement due to osteoclast destruction and decreased microcirculation, limiting bone turnover and remodeling. The conclusions of the article selected should be considered with caution due to the low methodological level of quality.

Because of the low level of evidence found, the results of this review are inconsistent to confirm in humans the effects of bisphosphonates observed on animals (5).

The lack of data about the effects of bisphosphonates on orthodontic therapy in humans can be related to several factors.

The introduction of bisphosphonate and the knowledge of their effects are recent.

Description of administration dose and regimen of bisphosphonate is difficult to determine in experimental human studies rather than in experimental animal studies. In fact, the use of bisphosphonate is often discontinuous and its half-life is extremely long (10 years or longer) (1).

Table I. *Summary of the article included in the review*

Author	Sample	Bisphosphonate admistration	Method	Tests	Conclusions
Rinchuse et al.	2 subject	Case 1:Alendronate sodium (Fosamax; 70 mg orally once per week for 16 months before treatment); Case 2: Zoledronic acid (Zometa, 500 mg infusion once per Month for 11 months before treatment).	Fixed orthodontic treatment	No specified	Bisphosphonates can impact orthodontic treatment by impeding tooth movement due to osteoclast destruction and decreased microcirculation, limiting bone turnover and remodeling

Table II. *Article included in the review and quality assessment*

Table II – Article included in the review and quality assessment								
Article	Sample size	Predetermined sample size	Measurement methods	Appropriate statistic	Method error analysis	Blinded measurement	Loss of subjects	Quality
Rinchuse et al.	Small	No	Inappropriate	No	No	No	No	Low

Description of direction and magnitude of the orthodontic forces are hardly determined in humans, especially if fixed orthodontic appliances and continuous arches are applied.

CONCLUSION

Based on the available results, there is no evidence showing that bisphosphonates influence orthodontic treatment in humans.

The main limit of this review article had been the scarcity of papers with an adequate methodology and the lack well-designed long-term trials on a large sample size. These findings suggest that more studies, especially RCTs, should be conducted.

REFERENCES

1. Rinchuse DJ, Sosovicka MF, Robison JM, Pendleton R. Orthodontic treatment of patients using bisphosphonates: A report of 2 cases. Am J Orthod Dentofacial Orthop 2007; 131(3):321-326.
2. Zahrowski JJ. Optimizing orthodontic treatment in patients taking bisphosphonates. Orthod Fr. 2011; 82(3):279-298
3. Kobayashi Y, Hiraga T, Ueda A, Wang L, Matsumoto-Nakano M, Hata K, Yatani H, Yoneda T. Zoledronic acid delays wound healing of the tooth extraction socket, inhibits oral epithelial cell migration, and promotes proliferation and adhesion to hydroxyapatite of oral bacteria, without causing osteonecrosis of the jaw, in mice. J Bone Miner

Metab 2010; 28(2):165-175.
4. Zahrowski JJ. Bisphosphonate treatment: an orthodontic concern calling for a proactive approach. Am J Orthod Dentofacial Orthop 2007; 131(3):311-320.
5. Iglesias-Linares A, Yáñez-Vico RM, Solano-Reina E, Torres-Lagares D, González Moles MA. Influence of bisphosphonates in orthodontic therapy: Systematic review. J Dent 2010; 38(8):603-611.
6. Higgins JPT, Green S, editors. Cochrane handbook for systematic reviews of interventions 4.2.5 (updated May 2005). Available at :http://www.cochrane.org/resources/handbook/hbook.htm.
7. Graham JW. Bisphosphonates and Orthodontics: Clinical Implications. J Clin Orthod 2006; 40(7):425-428.
8. Coulthard P, Esposito M, Worthington HV, Jokstad A. Therapeutic Use of Hyperbaric Oxygen for Irradiated Dental Implant Patients: A Systematic Review. J Dent Educ 2003; 67(1):64-68.

ENDODONTIC-ORTHODONTIC RELATIONSHIPS: EXPRESSION OF NO SYNTHASE IN HUMAN DENTAL PULP DURING ORTHODONTIC TOOTH MOVEMENT.

M. D'ATTILIO[A], F. DE ANGELIS [B], M. VADINI[B], D. RODOLFINO[A], O. TRUBIANI[C], F. DI NARDO DI MAIO[B], C. D'ARCANGELO[B]

[A]Unit of Orthodontics, Department of Medical, Oral and Biotechnological Sciences, "G. D'Annunzio" University of Chieti-Pescara, Chieti, Italy;
[B]Unit of Restorative Dentistry, Department of Medical, Oral and Biotechnological Sciences, "G. D'Annunzio" University of Chieti-Pescara, Chieti, Italy;
[C]Department of Medical, Oral and Biotechnological Sciences, "G. D'Annunzio" University of Chieti-Pescara, Chieti, Italy;

Inflamed human pulp tissue presents an increase in the level of nitric oxide synthase (NOS). The aim of this study is to verify the presence of NOS in human pulp of teeth that are subject to orthodontic force. 20 healthy subjects, wearers of fixed braces on the upper arch, were selected. An open coil-spring in NiTi was applied on the upper premolar test tooth (TT); the controlateral control tooth (CCT) was subjected to orthodontic treatment but not to the further force of the open coil-spring; the antagonist control tooth (ACT) did not undergo any orthodontic treatment. Pulps were taken from test, contralateral control and antagonist control teeth immediately after the extractions which were done at 15 and 30 days from the start of application of the orthodontic force. The pulp tissue was analyzed through immunohistochemical and molecular biology examinations. The results showed tooth pulps subject to orthodontic treatment were very inflamed in the first 15 days with high levels of iNOS and low levels of eNOS; after 30 days a decrease of the inflammation and an increase of the pulp vascularization were observed together with a reduction of iNOS and an increase of eNOS respectively.

Orthodontic tooth movement can cause reduced oxygen levels of the pulp [1,2], cell damage and circulatory disturbances [3,4] and inflammatory changes. The impact of the tooth movement on the pulp is focused primarily on the neurovascular system, in which the release of specific neuropeptides can influence both blood flow and cellular metabolism. Dental pulp inflammation is characterized by changes in blood flow [5], immunocompetent cell function and neuronal activity [6]. Several mediators including histamine, prostaglandins and neuropeptides have been shown to be involved in one or more of these processes [7,8], while all steps may involve nitric oxide (NO) [9]. NO is an intracellular messenger molecule with important cardiovascular, neurological and immune functions [9]. It is produced by a group of isoenzymes collectively termed NO synthases (NOS) [10]. Three distinct isoforms of NOS have been cloned to date: the endothelial (eNOS), neuronal (nNOS) and inducible (iNOS) NOS [9]. The eNOS and nNOS are constitutive isoforms that can rapidly synthetize small amounts of NO following receptor stimulation [11]. The iNOS is mainly involved in the inflammatory processes. Proinflammatory stimuli trigger resident and immigrant inflammatory cell populations, inducing iNOS [12]. The iNOS produces a large amount of NO for sustained periods of time, which has a role in a non-specific immune response, acting as a toxic agent in infections [9,12].

Histochemical identification of nicotinamide-adenine-dinucleotide-phosphate-diaphorase (NADPH-d), one possible marker of NOS [13] and immunohistochemical detection of NOS were used for localization of NOS in rodent, feline, canine, and human dental pulp and periodontal tissues, as well as in rat pulp after tooth preparation [14-17].

Key words: nitric oxide synthase, human dental pulp, orthodontic, inflammation, endothelial cells.

Mailing address: Prof. Camillo D'Arcangelo, Unit of Restorative Dentistry, Department of Medical, Oral and Biotechnological Sciences, "G. D'Annunzio" University of Chieti-Pescara, Via dei Vestini 31, 66100, Chieti, Italy.
E-mail: cdarcang@unich.it
Phone: +39(0)85.4549652 Fax: +39(0)85.4541279

0393-974X (2012)

The literature reviewed supports the presence of nitric oxide synthase in healthy and inflamed human dental pulp: the eNOS in odontoblasts and in endothelial cells is shown in healthy human pulp as is the presence of iNOS in macrophages, natural killer and T cells are shown in inflamed human pulp [17,18]. The high rate of the iNOS-produced NO formation can play a dual role in pulpitis. On the one hand NO has beneficial effects, because NO is an antimicrobial agent, since it decreases the viability of cariogenic bacteria [19]. Furthermore, NO acts as an immune modulator and inhibits formation of microvascular thrombi [20]. On the other hand NO has detrimental effects as well, because the exaggerated production of NO can cause toxic actions against the pulpal tissues. Furthermore, the excessive vasodilatation and increased vascular permeability elicited by local high NO can raise the intrapulpal hydrostatic pressure, because the pulp is a low-compliance system and is located in a closed and rigid dental chamber [21]. The increased intrapulpal pressure may consequently compress the pulpal venules and thus significantly impair the pulpal perfusion that insults the pulp tissue and might even cause pulp necrosis.

The aim of the present study was to examine the pulpal response to orthodontic force by evaluating and comparing the histopathological aspect and the eNOS and iNOS expression in human dental pulps collected from orthodontically treated and untreated teeth. The localization of eNOS and iNOS was performed by immunohistochemistry, their mRNA expression was identified by RT-PCR and their protein levels were detected by Western blot analysis.

MATERIALS AND METHODS

Twenty orthodontic patients, ten females and ten males (ages: 14.6 - 21.2 years; mean 17.4 ±1.8 years) at the Unit of Orthodontics, Department of Oral Sciences, G. D'Annunzio University (Chieti), who were diagnosed as requiring the extraction of their first premolars because of dental crowding, participated in this study. The following inclusion criteria were observed: 1) the need for fixed-appliance therapy involving distal retraction of one maxillary canine; 2) a healthy systemic condition; 3) no use of anti-inflammatory drugs in the month preceding the beginning of the study; 4) a full-mouth plaque score (FMPS) and a full-mouth bleeding score (FMBS) ≤ 20%. Informed consent was obtained from the patients and the parents of patients under 18 years of age prior to the commencement of the study, and the protocol was reviewed and approved by the Medical Faculty Ethical Committee of the G. D'Annunzio University.

Clinical procedures

In each patient, orthodontic brackets (MBT,3M-Unitek) were placed on the buccal surfaces of the teeth in the maxillary arch, including the incisors, the canines, and all premolars; the bands were bonded on the first molars. A straight-wire fixed orthodontic appliance (MBT 3M Unitek) was used only on the maxillary arch. The maxillary first premolar was chosen as the test tooth (TT), and force was applied by a steel archwire, 0.019-in circular cross-sectional dimension, and an open coil spring in NiTi (American Orthodontic) which applied a constant distalizing force of 250 grams on the tooth. The controlateral control tooth (CCT) was included in the orthodontic multibrackets appliance but it was not subject to the force of the open coil-spring. The antagonist control tooth (ACT) was not subjected to any force.

The twenty patients were randomly divided into two equal groups on the base of the time of extractions.

In Group I the test and control teeth were extracted 15 days after the start of the orthodontic treatment; in Group II the test and control teeth were extracted 30 days after the start of the orthodontic treatment.

All test (TT) and control (CCT and ACT) teeth from the same subject were extracted on the same day.

After extractions, the dental pulps were harvested by tooth fracturing, immediately frozen and kept at –80°C for 24-48 hours. Then longitudinal serial sections of about 7 µm were cut with a cryostat (Reichert-Jung Frigocut 2800).

Histopathological and Immunohistochemical analysis

For histopathological and immunohistochemical analysis a Leitz Dialux 22 (Leica, Heidelberg, Germany) microscope was used. Three slides from 5 pulps in each group were stained with hematoxylin-eosin. These slides were used to measure the arteriolar diameter and to localize the odontoblasts and the inflammatory cells at different magnifications Arteriolar diameter evaluation was performed on 20 randomly chosen arterioles in the hematoxylin-eosin stained pulps. The blood vessels selected were of homogenous appearance, free of apparent artifact, and perpendicular to the plane of section [16]. The immunohistochemical localization of eNOS and iNOS was performed using primary rabbit anti-eNOS (1:100) or primary rabbit anti-iNOS (1:100) antibodies (Santa Cruz Biotech Inc., Santa Cruz, California) as previously described [17].

Biochemical identification of eNOS and iNOS

The eNOS and iNOS mRNA were demonstrated from homogenizates of 30 dental pulps (10 TT, 10 CCT and 10 ACT) from each group by RT-PCR using 5'-TGTCTGTCTGCTGCTAG-3' (sense) and 5'-CTCTCCAGGCACTTCAGGC-3' (antisense) for human eNOS and 5'-AGTGATGGCAAGCACGACTTC-3' (sense) and 5'-TCTGTCACTCGCTCACCACGG-3' (antisense) for human iNOS primer pairs as published by Felaco *et al.* [17]. The eNOS and iNOS protein expressions were detected from equal amounts of protein (50 µg, obtained by homogenizing 30 premolar pulps from each group with lysis buffer (Sigma-Aldrich Co., St. Louis, MO., USA) by Western blots with primary anti-eNOS or iNOS antibodies (Santa Cruz Biotech Inc., Santa Cruz, California) as described in detail by Felaco *et al.* [17].

Image processing, image analysis and statistical evaluation

The stained sections of the pulps were examined using a Leitz Dialux 22, LEICA (Heidelberg, Germany) microscope. The

quantitative evaluation of the immune reactions was performed by determination of the integrated optical density (I.O.D.) changes with a digital image analysis. Three investigated areas were randomly selected and recorded on each slide. For data processing each experimental frame was digitized into 512x512 pixels by a Sony videocamera connected to a LEICA Quantimet 500 plus (LEICA Cambridge Ltd, Cambridge, England) and the change in I.O.D. was determined using ISO Transmission Density (Kodak CAT 152-3406, Eastman Kodak Company, Rochester, U.S.A.) as a standard. Results were expressed as mean±standard deviation (SD).

RESULTS

The histological evaluation of the samples was based on the inflammatory response of the cells and on the organization of the pulp tissue. A careful observation through an optical microscope highlighted the differences between the TTs, CCTs and ACTs and cellular evolution at 15 and 30 days after the beginning of treatment.

Pulp of the test teeth

In Group I, after 15 days, a strong inflammatory infiltration was observed with a predominance of polymorphonucleates and lymphocytes; the odontoblast layer was not particularly altered, while the blood vessels were altered, above all, in the third apical. eNOS was not very evident in the endothelial cells (Fig. 1). iNOS was notably evident, above all, in the area of the strong inflammatory infiltration (Fig. 2).

In Group II, after 30 days, there was a regression of the inflammatory phenomena and the pulp tissue showed histology almost equal to that of healthy pulp (some neutrophils present). eNOS was increased together with the number of endothelial cells (Fig. 3). iNOS, instead, was notably decreased (Fig. 4).

Pulp of the controlateral control teeth

In Group I, after 15 days, the presence of a slight inflammatory infiltration was observed with a predominance of polymorphonucleates and lymphocytes; the odontoblast layer was not particularly altered. The blood vessels did not present localized alterations, differently from the pulp of the test teeth, but there was however, a slight hyperemia. e-NOS, in the endothelial cells, was slightly more evident than what observed in the pulp of the teeth that had not undergone orthodontic treatment (ACTs). i-NOS was present, but in a lesser extent than that found in teeth that had been subject to a greater force (TTs).

In Group II, after 30 days, the inflammatory phenomena regressed and the pulp tissue presented only a few inflammatory cells. eNOS appeared increased, while iNOS decreased, compared to what observed in the CCTs of Group I.

Pulp of the antagonist control teeth

The histopathologic analysis with hematoxylin-eosin of the pulp tissue of ACTs showed linear layers of long odontoblasts in column form along the tissue periphery; inside there were star-shaped cells of connective tissue,

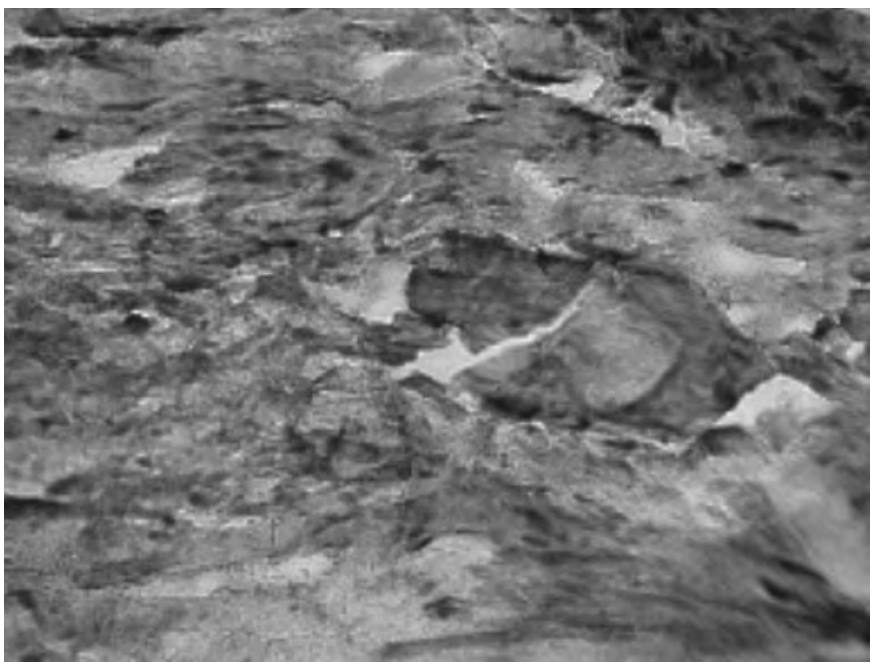

Fig 1. *After 15 days in the test teeth eNOS was not very evident in the endothelial cells.*

Fig 2. *After 15 days iNOS was notably evident in test teeth, above all, in the area of the strong inflammatory infiltration.*

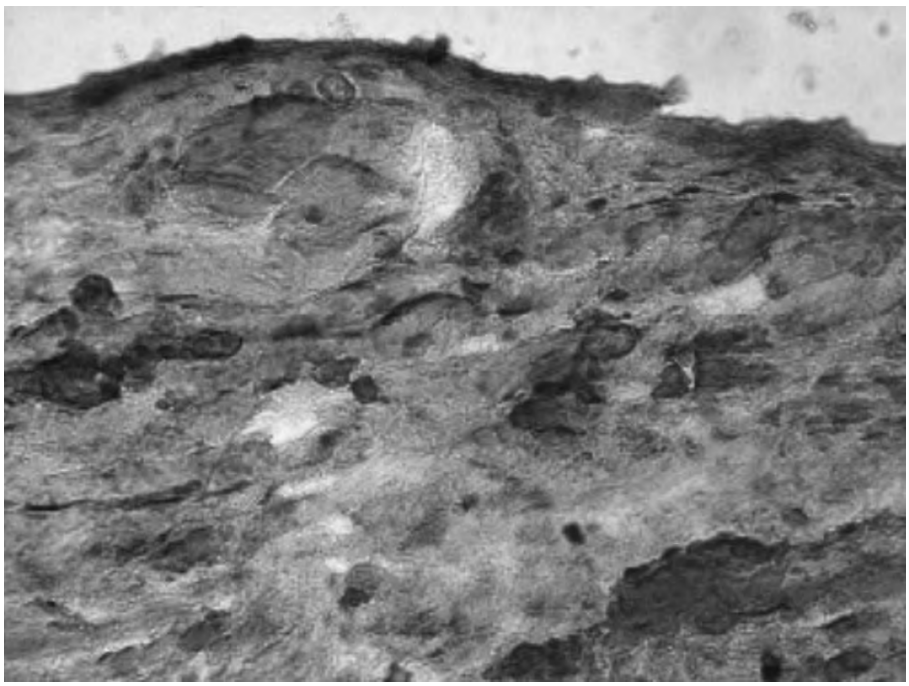

Fig 3. *After 30 days eNOS was increased in test teeth together with the number of endothelial cells.*

nerve fibers, blood vessels and lymphocytes. The immunohistochemical analysis demonstrated the presence of eNOS*:* the endothelial and fibroblast cells, under the optical microscope, were intensely colored and the odontoblasts were also colored. This confirms that these cells synthesize eNOS. No differences were found for the quantity of e-NOS in the pulp tissue between Group I (15 days) and Group II (30 days). iNOS, was totally absent

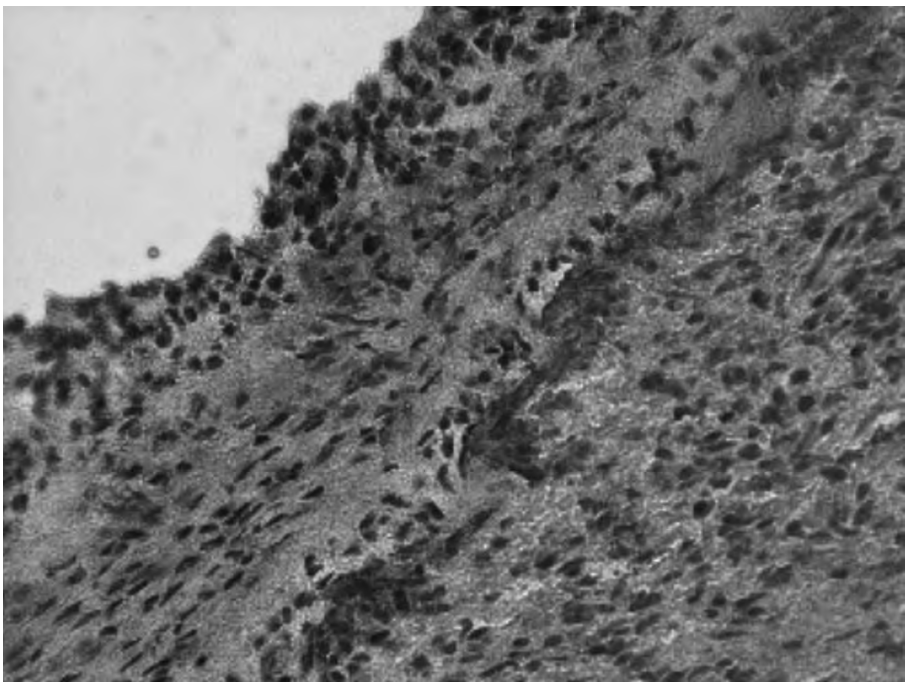

Fig 4. *After 30 days iNOS appeared notably decreased in test teeth.*

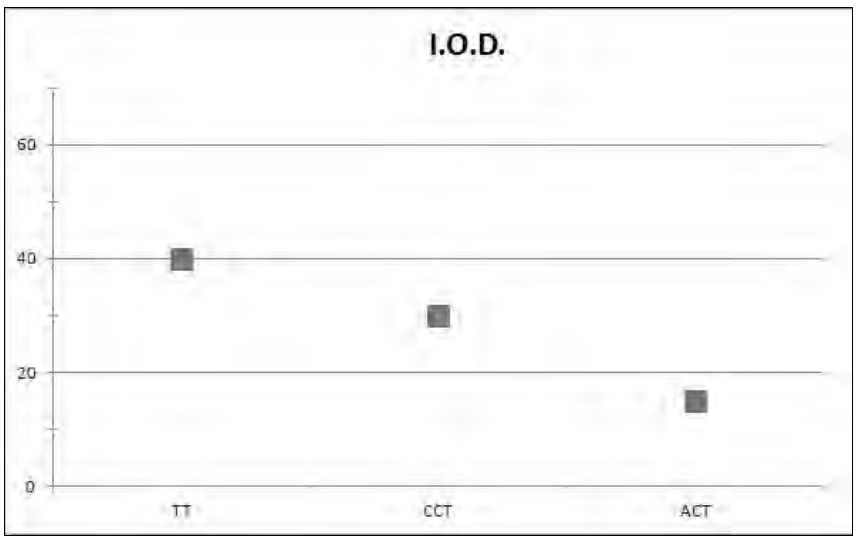

Fig 5. *Graph showing the mean results achieved in test teeth (TT), contralateral control teeth (CCT) and antagonistic control teeth (ACT) with the Integrated Optical Density analysis, performed for eNOS on samples belonging to Group I (extraction after 15 days).*

in the teeth that had not undergone orthodontic treatment.

Biochemical analysis

The results of the rt-PCR biochemical evaluation and of the Western blots for the eNOS and iNOS enzymes confirmed the localization and expression of the enzymes obtained by immunohistochemical techniques: the highest values of iNOS were found in the pulp of TTs and the

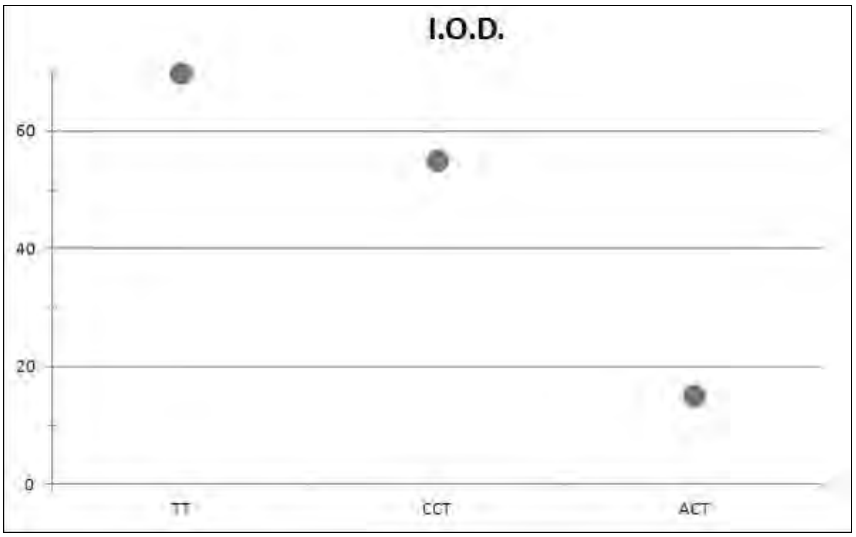

Fig 6. *Graph showing the mean results achieved in test teeth (TT), contralateral control teeth (CCT) and antagonistic control teeth (ACT) with the Integrated Optical Density analysis, performed for eNOS on samples belonging to Group II (extraction after 30 days).*

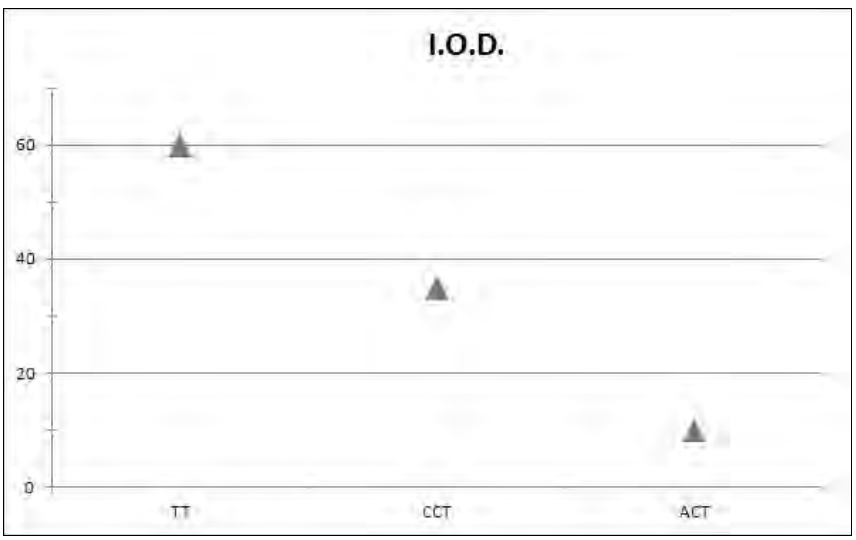

Fig 7. *Graph showing the mean results achieved in test teeth (TT), contralateral control teeth (CCT) and antagonistic control teeth (ACT) with the Integrated Optical Density analysis, performed for iNOS on samples belonging to Group I (extraction after 15 days).*

CCTs after 15 days, while the highest values of eNOS were found in the pulp of the TTs and the CCTs after 30 days; in the pulp of the ACTs only eNOS was present and in similar quantities in the two different groups (15 and 30 days).

Integrated optical density

Changes of the I.O.D., determined on a surface of 512x512 pixel, using an ISO standard transmission density, graphically demonstrated the variations of expression of the enzymes in the different groups. The results were expressed as mean ± standard deviation (SD) and are displayed in Figures 5-8.

DISCUSSION

Although several experimental models have been employed to evaluate pulp tissue responses to mechanical stimuli [1,22,23] only a limited number of studies have been carried out on human subjects; thus, most of the

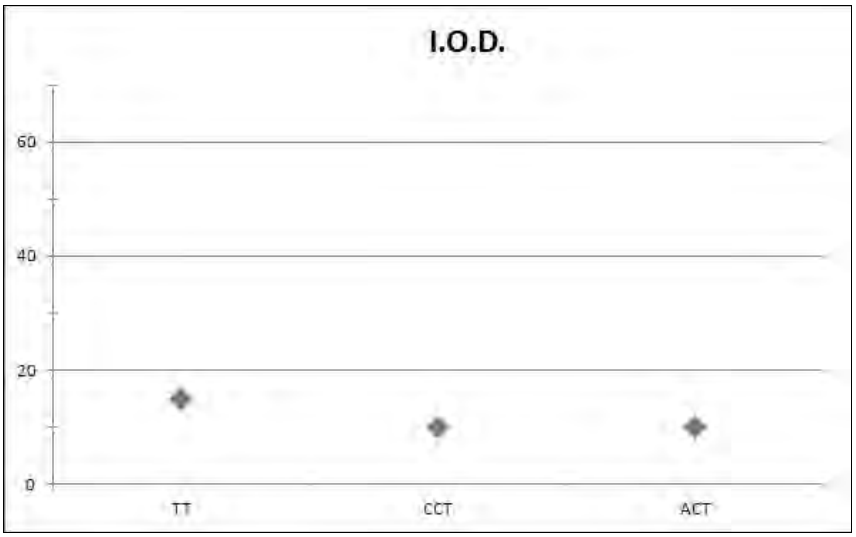

Fig 8. *Graph showing the mean results achieved in test teeth (TT), contralateral control teeth (CCT) and antagonistic control teeth (ACT) with the Integrated Optical Density analysis, performed for eNOS on samples belonging to Group II (extraction after 30 days).*

data available has been obtained from animal models. Nixon *et al.* [4], using the rat model, found that there was a significant vascular change with an increased number of functional pulp vessels as related to the specific forces applied. Derringer *et al.* [22] observed a significantly greater number of microvessels at day 5 and day 10 of culture in pulp explants from orthodontically moved teeth than in the control teeth. These findings support not only the presence of significant angiogenesis in the pulp, but also the presence of the necessary angiogenic growth factors such as PDGF (platelet-derived growth factor), EGF (epidermal growth factor) and TGF-b (transforming growth factor beta) which have been identified in pulp following endodontic injury as well as during orthodontic tooth movement in cats.

An initial hyperemic response was visible following application of force considering the increase in cellular activity taking place around the tooth during appositional and resorptive processes, it is biologically conceivable that blood flow in the pulp would also increase to support the demand from these dividing and multiplying cells in the area.

The suggestion has also been made that the application of orthodontic force had a direct effect without site specificity [4].

However, enzymatic monitoring during alterations of the pulp of teeth supporting an orthodontic force has not been used to date. Even less are the studies on the expression of nitric oxide synthase in human pulp of teeth subject to orthodontic traction.

Previous studies, as well as our findings suggest that all 3 isoforms of NOS can be expressed in the dental pulp [15,16,17].

The present study confirmed that eNOS is present in healthy pulp tissue and that it is also found in teeth subject to orthodontic traction and in particular in endothelial cells, fibroblasts, and odontoblasts, whereas iNOS is never expressed under normal condition. Furthermore, it was found that hyperaemia is accompanied by an elevation of the eNOS, where the dilated vessels maintain an increased blood circulation in the pulp tissue. After 15 days the orthodontic force lowers the eNOS level and elevates the expression of iNOS. The above changes mainly occur in the resident and infiltrating macrophages and PMNs. The decrease of eNOS after 15 days, compared with the increase after 30 days, can be explained by the negative feedback that is elicited by the large amount of NO produced by the significantly upregulated iNOS [24].

Evidence of NADPH-d reactivity, eNOS mRNA and protein in pulpal vessels is coexistent with the role of NO as a mediator of blood flow regulation [14,15,16,17]. Indeed, systemic infusion of the NOS inhibitors markedly reduces basal blood flow and can also inhibit cholinergic-induced vasodilatation in the pulp [14,21,25]. Furthermore, administration of an NO donor compound significantly decreases pulpal vascular resistance [21]. These data indicate that apart from an NO-dependent basal vasodilator tone, the control of the dental pulp

vascular tone can be regulated via a stimulated release of endogenous NO [21].

The functions of NOS in the odontoblasts are still unknown [17]. NO produced by eNOS in the odontoblasts may regulate the vascular tone of the adjacent vessels. Furthermore, NO may modulate the nociceptive input to both directions as low levels of peripherally generated NO are algestic, while high levels of NO were found analgestic. It is conceivable that according to the hydrodynamic pain sensation theory the dentinal fluid movement in the tubules induces shear stress of the odontoblasts which may activate eNOS as the blood flow alterations can activate eNOS in the endothelial cells. Thus, the odontoblasts operate as receptor cells and are responsible for dentine sensitivity. Through this mechanism NO may act as a coupling mechanism between the dental sensory input and the blood flow increase of the pulp. On the other hand, NO may downregulate sensitized nociceptors as well, as in the management of dentine hypersensivity by potassium ion the putative second messenger is NO produced by eNOS or iNOS in the odontoblasts [26]. The exact role of NO in the intradental sensory unit needs to be clarified in later studies. Furthermore, the large amount of NO synthesized by iNOS in the odontoblasts under pathological conditions may have not only an analgestic effect but may dilate local vessels and/or it is possible that the iNOS derived NO in caries is part of the first line of defense in the hard dental tissues against invading oral microorganisms [19].

Inflammation models in the literature show that constitutive NOS accounts for most NOS activity at the onset of the process [27,28]. It is likely that NO formed by constitutive eNOS plays an anti-inflammatory role in healthy pulp and during the early stages of inflammation in hyperaemic pulp; this mechanism is aimed at limiting the process by inhibiting leukocyte and platelet adhesion/ aggregation of the endothelial surface and by increasing tissue perfusion [27,28]. In contrast to the eNOS, our data suggest that iNOS is not present in the healthy pulp of teeth not subject to orthodontic force, it is induced only after orthodontic traction. The progress of inflammation in the dental pulp is accompanied by a marked enhancement of the total NOS activity, most of which is attributed to iNOS of the activated leukocytes.

In conclusion, in the present study different expressions and localizations of eNOS and iNOS have been found in human dental pulp when teeth subject to orthodontic traction were compared to teeth not subjected to it.

The results showed that the pulp of teeth subject to orthodontic treatment are highly inflamed in the first 15 days with high levels of iNOS and slight eNOS; after 30 days there is a regression of inflammation and an increase in the vascularization of the pulp accompanied by a reduction in iNOS and an increase in eNOS.

REFERENCES

1. Hamersky PA, Weimer AD, Taintor JF. The effect of orthodontic force application on the pulpal tissue respiration rate in the human premolar. Am J Orthod 1980; 77:368-78.
2. Unsterseher RE, Nieberg LG, Weimer AD, Dyer JK. The response of human pulpal tissue after orthodontic force application. Am J Orthod Dentofacial Orthop 1987; 92:220-4.
3. Mostafa YA, Iskander KG, El-Mangoury NH. Iatrogenic pulpal reactions to orthodontic extrusion. Am J Orthod Dentofacial Orthop 1991; 99:30-4.
4. Nixon CE, Saviano JA, King GJ, Keeling SD. Histomorphometric study of dental pulp during orthodontic tooth movement. J Endod 1993; 19:13-6.
5. Olgart L, Edwall L, Gazelius B. Involvement of afferent nerves in pulpal blood-flow reactions in response to clinical and experimental procedures in the cat. Arch Oral Biol 1991; 36:575-81.
6. Bergenholtz G. Iatrogenic injury to the pulp in dental procedures: aspects of pathogenesis, management and preventive measures. Int Dent J 1991; 41:99-110.
7. Hirafuji M, Satoh S, Ogura Y. Prostaglandins in rat pulp tissue. J Dent Res 1980; 59:1535-40.
8. Grutzner EH, Garry MG, Hargreaves KM. Effect of injury on pulpal levels of immunoreactive substance P and immunoreactive calcitonin gene-related peptide. J Endod 1992; 18:553-7.
9. Nathan C. Nitric oxide as a secretory product of mammalian cells. FASEB J 1992; 6:3051-64.
10. Bredt DS, Hwang PM, Snyder SH. Localization of nitric oxide synthase indicating a neural role for nitric oxide. Nature 1990; 347:768-70.
11. Carmignani M, Volpe AR, Boscolo P, Qiao N, Di Gioacchino M, Grilli A, Felaco M. Catcholamine and nitric oxide systems as targets of chronic lead exposure in inducing selective functional impairment. Life Sci 2000; 68:401-15.
12. Nussler AK, Billiar TR. Inflammation, immunoregulation, and inducible nitric oxide synthase. J Leukoc Biol 1993; 54:171-8.
13. Hope BT, Michael GJ, Knigge KM, Vincent SR. Neuronal NADPH diaphorase is a nitric oxide synthase. Proc Natl Acad Sci U S A 1991; 88:2811-4.
14. Kerezoudis NP, Olgart L, Fried K. Localization of NADPH-diaphorase activity in the dental pulp, periodontium and alveolar bone of the rat. Histochemistry 1993; 100:319-22.
15. Lohinai Z, Székely AD, Benedek P, Csillag A. Nitric oxide

synthase containing nerves in the cat and dog dental pulp and gingiva. Neurosci Lett 1997; 227:91-4.
16. Law AS, Baumgardner KR, Meller ST, Gebhart GF. Localization and changes in NADPH-diaphorase reactivity and nitric oxide synthase immunoreactivity in rat pulp following tooth preparation. J Dent Res 1999; 78:1585-95.
17. Felaco M, Di Maio FD, De Fazio P, D'Arcangelo C, De Lutiis MA, Varvara G, Grilli A, Barbacane RC, Reale M, Conti P. Localization of the e-NOS enzyme in endothelial cells and odontoblasts of healthy human dental pulp. Life Sci 2000; 68:297-306.
18. Di Nardo Di Maio F, Lohinai Z, D'Arcangelo C, De Fazio PE, Speranza L, De Lutiis MA, Patruno A, Grilli A, Felaco M. Nitric oxide synthase in healthy and inflamed human dental pulp. J Dent Res 2004; 83:312-6.
19. Silva Mendez LS, Allaker RP, Hardie JM, Benjamin N. Antimicrobial effect of acidified nitrite on cariogenic bacteria. Oral Microbiol Immunol 1999; 14:391-2.
20. Albina JE, Henry WL Jr. Suppression of lymphocyte proliferation through the nitric oxide synthesizing pathway. J Surg Res 1991; 50:403-9.
21. Lohinai Z, Balla I, Marczis J, Vass Z, Kovách AG. Evidence for the role of nitric oxide in the circulation of the dental pulp. J Dent Res 1995; 74:1501-6.
22. Derringer KA, Jaggers DC, Linden RW. Angiogenesis in human dental pulp following orthodontic tooth movement. J Dent Res 1996; 75:1761-6.
23. Kvinnsland I, Heyeraas KJ. Effect of traumatic occlusion on CGRP and SP immunoreactive nerve fibre morphology in rat molar pulp and periodontium. Histochemistry 1992; 97:111-20.
24. Buga GM, Griscavage JM, Rogers NE, Ignarro LJ. Negative feedback regulation of endothelial cell function by nitric oxide. Circ Res 1993; 73:808-12.
25. Olgart L, Kostouros GD, Edwall L. Local actions of acetylcholine on vasomotor regulation in rat incisor pulp. Acta Physiol Scand 1996; 158:311-6.
26. McCormack K, Davies R. The enigma of potassium ion in the management of dentine hypersensitivity: is nitric oxide the elusive second messenger? Pain 1996; 68:5-11.
27. Kubes P, Suzuki M, Granger DN. Nitric oxide: an endogenous modulator of leukocyte adhesion. Proc Natl Acad Sci U S A 1991; 88:4651-5.
28. Santamaria M Jr, Milagres D, Stuani AS, Stuani MB, Ruellas AC. Initial changes in pulpal microvasculature during orthodontic tooth movement: a stereological study. Eur J Orthod 2006; 28:217-20.

MICROARRAY EVALUATION OF GENE EXPRESSION PROFILES IN INFLAMED AND HEALTHY HUMAN DENTAL PULP: THE ROLE OF IL1β AND CD40 IN PULP INFLAMMATION.

V. GATTA[1,2], V.L. ZIZZARI[3], V. D'AMICO[1], L. SALINI[4], M. D'AURORA[2,5], S. FRANCHI[1], I. ANTONUCCI[1,2], M.T. SBERNA[6], E. GHERLONE[6], L. STUPPIA[1,2], S. TETÈ[1]

[1]Department of Medical, Oral and Biotecnological Sciences, "G. d'Annunzio" University, Chieti-Pescara, Italy
[2]Center of Excellence on Aging (Ce.S.I.), "G. d'Annunzio" Foundation, Chieti-Pescara, Italy
[3]Department of Drug Sciences, University "G. d'Annunzio", Chieti, Italy
[4]Base Sanitary District (D.S.B), Francavilla al Mare, Chieti, Italy
[5]Department of Neuroscience and Imaging, University "G. D'Annunzio", Chieti, Italy
[6]Department of Oral Science, University "Ateneo Vita-Salute San Raffaele," Milan, Italy

Dental pulp undergoes a number of changes passing from healthy status to inflammation due to deep decay. These changes are regulated by several genes resulting differently expressed in inflamed and healthy dental pulp, and the knowledge of the processes underlying this differential expression is of great relevance in the identification of the pathogenesis of the disease. In this study, the gene expression profile of inflamed and healthy dental pulps were compared by microarray analysis, and data obtained were analyzed by Ingenuity Pathway Analysis (IPA) software. This analysis allows to focus on a variety of genes, typically expressed in inflamed tissues. The comparison analysis showed an increased expression of several genes in inflamed pulp, among which IL1β and CD40 resulted of particular interest. These results indicate that gene expression profile of human dental pulp in different physiological and pathological conditions may become an useful tool for improving our knowledge about processes regulating pulp inflammation.

Microarray technology represent a useful approach in the study of gene function in human cells and tissues. Due to the unique ability to simultaneously analyze the expression levels of thousands genes in a single experiment, this approach provides a very high throughput tool in the identification of genes involved in different physiological and pathological conditions and has been largely used in the molecular characterization of different diseases (1).

A previous report of our group demonstrated the usefulness of the microarray technology in the study of the gene expression profiles in healthy and decayed dental pulp (2). Thus, this approach would likely represents an useful tool also in the study of pathological processes involving human dental pulp, such as inflammation.

The general meaning of any inflammatory response is to deal with and eliminate the source of tissue damage, and establish protective mechanisms (3). The inflammatory process uses specific chemical mediators, which can be classified as *Vasoactive amines, Complement system, Kinin system, Coagulation pathway, Fibrinolytic pathway, Arachidonic acid metabolites, Platelet activating factor, Cytokines, Nitric oxide* (4, 5, 6). Among these, a key role is played by IL1β and CD40 genes, as directly involved in the inflammatory process.

IL1 is a primarily proinflammatory cytokine able to regulate the expression of genes associated with inflammation and autoimmune diseases (7). IL1β plays a crucial role in systemic inflammation due to its ability to induce the expression of a large panel of pro-

Key words: CD40, human dental pulp, IL1β, inflammation, microarray analysis

Corresponding author:
Prof. Stefano Tetè
Department of Medical, Oral and Biotecnological Sciences
"G. d'Annunzio" University
Via dei Vestini, 31 – 66100 Chieti, Italy
Tel./Fax: +39 08713554095
Email: tete@unich.it

0393-974X (2012)

inflammatory genes, as type 2 cyclooxygenase (COX-2), type 2 phospholipase A, and inducible nitric oxide synthase (iNOS) (8).

CD40 is a receptor expressed on a wide range of cells such as leukocytes and endothelial cells, belonging to the TNF superfamily (9). Its activation by CD40-ligand (CD40L) plays a crucial role for the development and progression of a variety of inflammatory processes. CD40/CD40L interaction induces E-selectin dependent adhesion of leukocytes to human endothelial cells and reduces endothelial cell migration by inhibiting the Akt/eNOS signaling pathway (10). Thus, both genes perform their function by interacting with other molecules, and in these cases classical expression studies based on the analysis of single transcripts can only provide information about the up- and down-regulation of the selected genes, but are not able to show a global picture of the different pathways involved.

For this reason, a study aimed to the identification of genes involved in the inflammatory process should be based on the study of the expression levels of several genes and on the dissection of their interaction driving to the process of inflammation.

The aim of this study was to evaluate the gene expression profiles of inflamed and healthy human dental pulp by microarray technology using total RNA amplification, with particular attention to IL1β and CD40 gene expression, in order to clarify the molecular mechanisms involved in the pulp inflammatory response to tooth decay.

MATERIAL AND MHETODS

Pulp Samples

A total of eight subjects were recruited in the clinics of the Department of Medical, Oral and Biotechnological Sciences, at the "G. d'Annunzio" University of Chieti after informed consent.

Dental pulp samples were obtained from third molars subjected to extraction. Four patients were subjected to third molar extraction because of pain or high sensibility due to deep decay (Test Group); the other four subjects received third molar extraction for orthodontic reasons (Control Group). All the teeth belonging to Control Group were impacted and did not show any sign of tooth decay or other diseases.

The age range for Test Group was 30-36 yrs (mean age 34 yrs), while for Control Group it was 24-36 yrs (mean age 28.5 yrs).

After the extraction, all the remnants soft tissues were mechanically removed and the external tooth surfaces were cleaned with a solution of clorhexidine 0.2%. Within 5 minutes from extraction, the teeth were sliced in order to obtain dental pulp samples, by using a diamond cutter, making a 2-3 mm groove around the tooth and avoiding pulp exposure. Then, teeth were fractured off through the cutting line with a surgical lever, and pulp samples removed from the pulp chambers.

RNA Isolation and Amplification

After collection, both inflamed and healthy pulp tissue specimens were immediately stored at -20°C in RNA Later (Ambion Austin, TX, USA). Samples were then homogenized using an hand glass potter, and total RNA was extracted using the SVtotal RNA Isolation System kit (Promega, Madison, WI, USA). The purity and quantity of RNA was assessed using the Agilent 8453 Spectrophotometer (Agilent, Santa Clara, CA, USA). Extracted RNA was linearly amplified and fluorescently labeled using the Amino Allyl MessageAmp™ II aRNA Amplification Kit according to the manufacturer's instruction (Ambion).

Microarray Expression Profiling

The amplified aRNA (5-10 μg) was fluorescently labeled with Cy3-Cy5 cyanins (Amersham; Pharmacia Biotech, Buckinghamshire, UK) and then hybridized on high-density array Human Whole Genome OneArray™ Microarray V5, (30,275 total probe; Biosense, Italy). Each MicroArray experiment was carried out on RNA pools from the four inflamed pulp samples hybridized vs the RNA pools from the four healthy pulp samples as control, in order to increase the homogeneity of the results. Three technical replicates (dye swaps) were performed for each experiment.

After hybridization, Cy3-Cy5 fluorescent signals were captured by a Confocal Laser Scanner "ScanArray Express" (Perkin Elmer, Massachusetts, USA) and analyzed using the software "ScanArray Express - MicroArray Analysis System" version 3.0 (Perkin Elmer). For each slide, after local background subtraction, a LOWESS algorithm was used for row data normalization to evaluate signal to noise ratio and generate log ratios of sample vs reference signal. A gene was considered to be differentially expressed when showing an absolute value of log-ratio higher or equal to 0.5, an index that translates to a fold-change of 1.4 in transcript quantity. Data analysis was based on hierarchical gene clustering using Cluster 3.0 (open source 2006) and TreeView (Stanford University Labs) software. Only spots with a present call in at least 80% of experiments and being > 1.7 fold up-or down regulated were included in the clustering analysis. Identified clusters were analyzed by the Ingenuity Pathways Analysis (IPA) software (Ingenuity Systems, Redwood City, CA), in order to classify genes based on their biological functions and disclose the functional networks connecting specific genes.

TaqMan real-time quantitative PCR (qRT-PCR)

Microarray results for IL1β and CD40 were verified by qRT-PCR analysis using an ABI 7900HT Sequence Detection System (ABI). Triplicate PCR reactions were run for each gene in three independent experiments. The housekeeping gene GAPDH was used as an internal control to normalize the expression of target genes. Relative expression levels were calculated for each

sample after normalization against GAPDH, using the ΔΔCt method for comparing relative fold expression differences, as previously described (11). The T student test was performed to correlate fold change differential expression detected by qRT-PCR in inflamed pulp samples respect to healty pulp samples.

RESULTS

Microarray Analysis

Cluster analysis showed a total of 834 *up regulated* (582 mapped, 252 unmapped) and 159 *down regulated* (140 mapped, 19 unmapped) genes in inflamed pulp as compared to healthy pulp . The list of up-regulated genes in inflamed pulp samples with their specific functions is reported in Table I. IPA analysis was carried out to identify the genetic networks involving the up-regulated genes. Among the different network evidenced, particular interest was devoted to two networks involving IL1β and CD40 genes, known as largely affecting pulp inflammation.

IL1β network resulted to be significantly up regulated

Table I. *list of up-regulated genes in inflamed pulp samples*

Category	p-value	Molecules
Cell-To-Cell Signaling and Interaction	1,34E-04-1,48E-02	GTPBP1, IL27, TRIM35, IL24, PKN1, NDN, AREG, GAST, CDH5, **CD40**, CDK4, SF3A2, POLL, DHFR, IL3, KLC2, MEST, TRAF2, PMP22, KIF20B, RASGRP1, NFE2, MAZ, CAT**, IL1β**, PSMC3, CHN2, MMP9, MUL1
Inflammatory Response	2,24E-04-1,36E-02	LIF, DDIT4, HMGA1, PLAUR, NRF1, GGT1, GSR, HMOX1, SOD2, **CD40**, CYBA, NFE2, PPBP, CAT, IL1B, DNAJB1
Cell Morphology	4,16E-04-1,48E-02	CD2, IL5, PTHLH, HMGA1, NRF1, PLAUR, ALOX12, AREG, GSR, KITLG, HMOX1, SOD2, **CD40**, MT1E, NFE2, PPBP, CAT, PRKCE, **IL1β,** IL3, HFE, HMGB2
Humoral Immune Response	4,53E-04-1,48E-02	LIF, IL5, CD2, SOD2, PRKCE, NKX6-1, DNAJB1, VAX2, PHB (includes EG:5245), SLC1A6,CD19, LETM1, RACGAP1, M1, IL24, KITLG, TRAF2, **CD40**, CDK4, CAT, IL1β, IL3, ESR2
Gene Expression	4,53E-04-8,16E-03	STAT5A, CD19, CD320, IL5, PTPN2, PHC1, HMGA1, HSPD1, BCL6, IL24, FLT3LG, KITLG, TRAF2, CD40, MYB (includes EG:4602), **IL1β**, IL3, MOG
Cell-mediated Immune Response	1,05E-03-1,52E-02	STAT5A, CD19, LIF, IL5, CD2, RACGAP1, HMGA1, IL27, ZFPM1 (includes EG:161882), HSPD1, BCL6, NOG, KITLG, **CD40**, MYB (includes EG:4602), IL1β, IL3, EBI3
Inflammatory Disease	5,53E-03-1,48E-02	KLC1, LETM1, CHGA, MYO7A, HMGA1, HEXA, NRF1, HOOK3, SOD2, NDEL1, PRKCE, **IL1β**, MAP1LC3B, MOG, PEX12, **CD40**

Table II. *Representative up and down genes data.*

	ID	Log2 Ratio*	qRT-PCR**
IL1B	**NM_000576.2**	**4.278**	**8.88**
CD40	**NM_001250.3**	**1.758**	**1.06**

** mean expression level of selected genes in inflamed pulp samples over mean expression level in healthy pulp samples evaluated by microarray method.*

*** mean mRNA levels of selected genes in inflamed pulp samples vs healthy pulp samples measured by real-time PCR.*

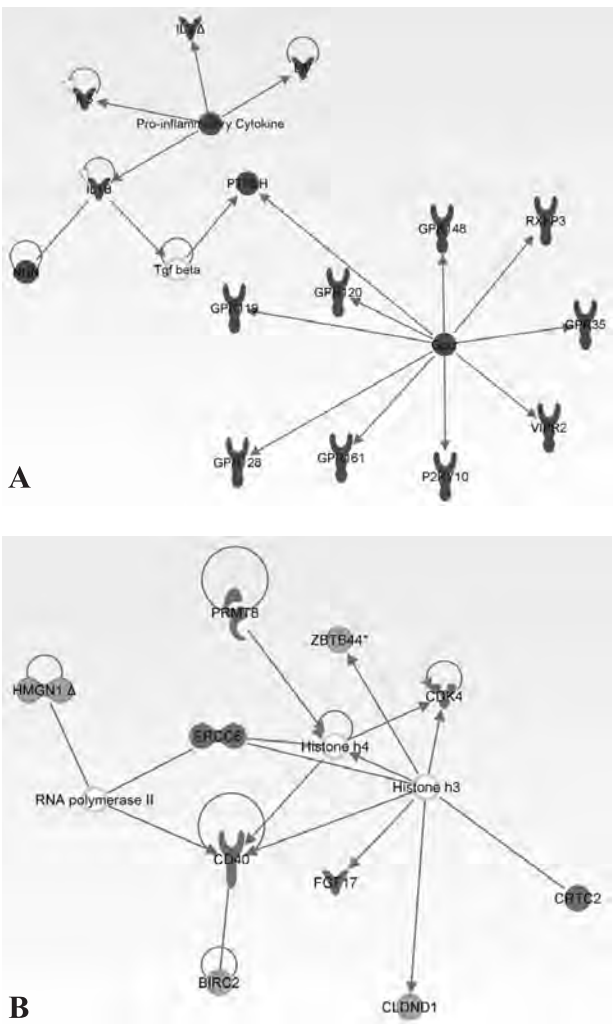

Fig. 1. *Genes networks. 1a: IL1B network; 1b: CD40 network Genes in red show increased expression in inflamed pulp samples compared with control samples. Arrows indicate that a molecule acts on another while lines indicate that a molecule binds to another.*

in samples from inflamed pulp as compared to healthy tissue, showing a very high level of expression of all the other genes present in the network (Fig. 1a). Also CD40 resulted up regulated in inflamed pulp as compared to healthy pulp, but in this case some genes present in the network centered on CD40 resulted to be under expressed (Figure 1b).

To validate the microarray data, TaqMan real-time quantitative PCR analyses were performed on selected genes (Fig. 2, Table II). This analysis confirmed the differential expression of the investigated genes as predicted by microarray data showing a $p<0.05$ with a fold change of 8.88 for IL1B and 1.06 for CD40.

DISCUSSION

Several studies addressed the problem of the inflammation process and many of them focused on the important role of IL1β and CD40 as molecules able to induce the expression of a large panel of pro-inflammatory genes, affecting various target organs and involved in cell apoptosis stimulation (12, 13, 14)

In our research, high levels of IL1β gene expression were found in inflamed pulp samples, while this gene showed a significantly lower expression in dental pulp under physiological conditions, thus confirming the important role played in the beginning and progression of dental pulp inflammation.

CD40 is essential in mediating a broad variety of immune and inflammatory responses including T cell-dependent immunoglobulin class switching, memory B cell development, and germinal center formation (15). This gene is expressed on activated T-cells, endothelial cells, macrophages, vascular smooth muscle cells, and activated platelets (16). So the high levels of expression of this gene as evidenced by microarray analysis in inflamed dental tissue il likely related to its important role in cell-mediated immune response and in the cell-

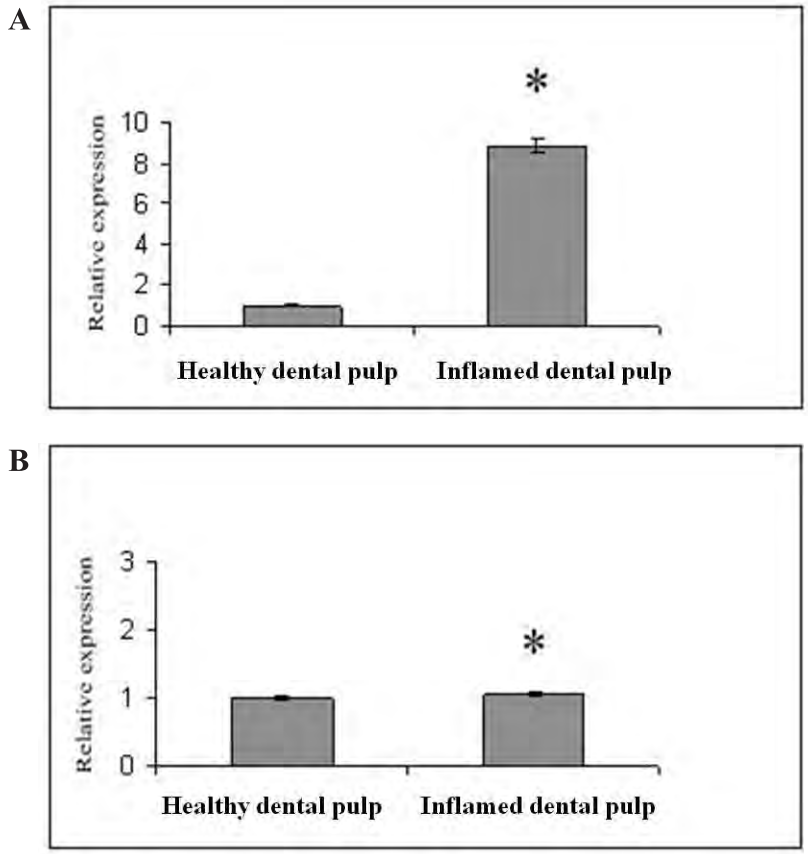

Fig. 2. *qRT-PCR analysis of IL1B (2a) and CD40 genes (2b).*

to-cell signalling and interaction during the inflammatory process.

The microarray analysis allowed us to evidence other interesting features associated with the gene expression of these genes. IL1β gene appeared involved in a network showing all over expressed genes, while CD40 showed both over and under expressed genes in its network. In fact, IL1β gene network involved other interleukine genes such as IL3 and IL5, suggesting that their over expression may be related to a global up regulation of the pro-inflammatory cytokines. Moreover, also other genes involved in the network resulted up regulated, such as several genes of the G-protein coupled receptors (GPCRs) family.

As concerning CD40 gene, in the network centered on this transcript it was possible to evidence the over expression of some genes, such as FGF17, ERCC6, PRMT8, CDK4 and CD40, and the under expression of other genes, such as ZBTB44, CLDND1, BIRC2 and HMGN1. Interesting, it has been demonstrated a deficiency the BIRC2 gene product impair caspase-1 activation after spontaneous or agonist-induced inflammasome assembly (18). These data suggests that the inflammatory process within human pulp is based not only on the activation of inflammation related genes, but also on the under expression of other genes. Once again, this study confirm that the use of microarray technology may provide useful information about the genetic networks involved in the inflammation processes, although there is still much to learn about the beginning and progression of inflammation in human dental pulp. Moreover, this method permits to compare inflamed and physiological tissues, finding the genes involved in this pathological process, for the best understanding of cells interaction.

REFERENCES

1. Chaudhuri JD. Genes arrayed out for you: the amazing world of microarrays. Med Sci Monit 2005;11:RA52-62.
2. Tranasi M, Sberna MT, Zizzari V, et al. Microarray evaluation of age-related changes in human dental pulp. J

Endod 2009; 35: 1211-7.
3. McLachlan JL, Smith AJ, Bujalska IJ, et al. Gene expression profiling of pulpal tissue reveals the molecular complexity of dental caries. Biochim Biophys Acta 2005;1741:271-81
4. Shirinskiy VS. Autoimmune Diseases: Problems of Pathogenesis, Diagnostics and Treatment. Russ J Immunol 1999;4:261-3.
5. Levin ME, Jin JG, Ji RR, et al. Complement activation in the peripheral nervous system following the spinal nerve ligation model of neuropathic pain. Pain 2008;137:182-201.
6. Fathallah DM, Cherif D, Dellagi K, et al. Molecular cloning of a novel human hsp70 from a B cell line and its assignment to chromosome 5. J Immunol 1993;151: 810–3.
7. Beadling C, Johnson KW, Smith KA. Isolation of interleukin 2-induced immediate-early genes. Proc. Nat. Acad. Sci. U.S.A. 1993;90:2719–23.
8. Datta De D, Bhattacharjya S, Maitra M, et al. IL1B induced Smad 7 negatively regulates gastrin expression. PLoS One 2011;6:e14775.
9. Jéru I, Amselem S. Inflammasome and interleukin IL1. Rev Med Interne 2011;32:218-24.
10. Hassan GS, Merhi Y, Mourad W. CD40 Ligand: A neo-inflammatory molecule in vascular diseases. Immunobiology 2012; 217:521-532.
11. Urban D, Thanabalasingam U, Stibenz D, et al. CD40/CD40L interaction induces E-selectin dependent leukocyte adhesion to human endothelial cells and inhibits endothelial cell migration. Biochem Biophys Res Commun 2011;404:448-52.
12. LivaK KJ, Schmittgen TD. Analysis of relative gene expression data using real-time quantitative PCR and the 2-(Delta Delta C(T)). Methods 2001;25:402-8.
13. Jéru I, Amselem S. Inflammasome and interleukin IL1. Rev Med Interne 2011;32:218-224.
14. McMahan CJ, Slack JL, Mosley B, et al. A novel IL-1 receptor, cloned from B cells by mammalian expression, is expressed in many cell types. EMBO J 1991;10:2821-32.
15. Dinarello CA. The IL-1 family and inflammatory diseases. Clin Exp Rheumatol 2002;25:S1-13.
16. Speirs RS, Speirs E, Ponzio NM. A Role for Eosinophils in Adaptive Humoral Immunity. The Open Immunology Journal 2009; 2:168-186.
17. Borrow P, Tough DF, Eto D, et al. CD40 ligand-mediated interactions are involved in the generation of memory CD8+ cytotoxic T lymphocytes (CTL) but are not required for the maintenance of CTL memory following virus infection. J. Virol 1998;72:7440-9.
18. Labbé K, McIntire CR, Doiron K, Leblanc PM, Saleh M. Cellular Inhibitors of Apoptosis Proteins cIAP1 and cIAP2 Are Required for Efficient Caspase-1 Activation by the Immunity. 2011 Dec 23;35(6):897-907.

THERMAL ANALYSIS OF LASER-SOFTENED GUTTA-PERCHA

M. PETRINI, M. FERRANTE, P. TRENTINI, G. PERFETTI, P. DOTTORE, G. SPOTO

Department of Medical, Oral and Biotechnological Sciences, University of Chieti - Italy

The aim of this work is to examine the behaviour of laser treated gutta-percha (a–b) after heating, to test the validity of a new obturation technique. Samples of laser- and no laser- treated gutta-percha have been examined by the thermal/thermogravimetric analysis and compared. All samples have been submitted to four runs of heating from the temperature of 25–130 °C, followed by spontaneous cooling. It was found that some samples have shown the typical behaviour of the α-gutta-percha; others have shown characteristics similar to the conventional β-gutta-percha. The laser treated gutta-percha has shown a significant mass loss after the first run of heating, while the mass tends to stabilize after the third run. It has been demonstrated that the 980 nm diode laser used with cited parameters does not alters thermal behaviour of gutta-percha cones.

The inflammation of dental pulp is characterized by a succession of cellular, vascular and immunological processes; monitoring the level of such mediators, like prostaglandins E2 it is possible to investigate the severity of the pulpitis and to assess if it is irreversible. (1-2)

The treatment of irreversible pulpitis is the extraction of the tooth or the endodontic therapy, in order to obtained effective elimination of bacteria and the complete filling of the root canal system, which are essential to provide a biological environment for healing of the periradicular tissues. (3)

A proper canal cleaning, shaping and irrigation is essential to significantly reduce bacteria from canals, but, many studies demonstrated that laser irradiation has an adjunctive bactericidal effect in conventional endodontic therapy. (4-5-6)

The material most widely used for endodontic obturation is the dental gutta-percha: it has been shown to be approximately 18 to 22% gutta-percha polymer and 37 to 75% zinc oxide. (7)

Currently a variety of gutta-percha obturation techniques exist, like lateral condensation and of heat-softened vertical condensation. (8) Studies have shown that plasticized gutta-percha can easily be moved into the canal irregularities, thus replicating the intricacies of the root canal system. (9)

Laser softened gutta-percha provides procedural simplification of the root filling and less time consumption. (10) The assessment of the thermal behaviour of softened gutta-percha is critical for ensuring that laser treatments do not pose a risk to alter its physical and mechanics characteristics.

The aim of this work was to compare thermal behaviour of 980 nm laser-softened gutta-percha and commercial gutta-percha.

MATERIALS AND METHODS

The measurements were carried out on a thermogravimetric/differential thermal analyser (Model TG/DTA 6300, Seiko Instruments USA Inc. Torrance, CA, USA).

56 gutta-percha Points (Inline) ISO 40 were randomly divided into two groups: 32 Test and 24 Control.

The coronal portion of gutta-percha points of both Group Test and Control, were split with a scalpel and eliminated, so samples of 5 mm long were obtained from their apical portion (Fig. 1).

Group Test was irradiated by a 980 nm diode laser at 3.0W for 20 sec in continuous mode. (11)

The laser used was the 980-nm diode (G-Laser 25, Galbiati srl, Italy), with flexible fibber optic 600 μm in diameter at a distance of 1 cm.

The measurements were carried out on a thermogravimetric/differential thermal analyser (Model TG/DTA 6300, Seiko Instruments USA Inc. Torrance, CA, USA).

Samples were heated in the analyser to determine the occurrence of endothermic peaks;

20 samples of each group were analyzed (40 samples total

Keywords: laser, gutta-percha, endodontology, thermal analysis, inflammation

Corresponding author address
Spoto Giuseppe, Full Professor of Dental Materials
Address: Via Vestini 31, 66013 Chieti, Italy
Phone: +39 0871 355 4066
Email : spoto@unich.it

0393-974X (2012)

analyzed); for each sample of gutta-percha the following cycle of heating and cooling experiments was carried out four times (12):

a. Analysis of the sample at standard temperature (25° C):
b. Evaluation of the mass (mg).
c. Heating from the temperature of 30° C to 70°C with an increase of 1° C/min.
d. Heating from the temperature of 70° C to 130°C with an increase of 5° C/min with maintenance of the final temperature for 10 minutes.
e. Cooling of the sample with spontaneous decrement up to the temperature of 30°C.

Simultaneously, thermogravimetric analysis was carried out to determine the weight loss, if any, during the heat cycles. This analysis consists in eliminating the organic compounds present in the analysed material, and observing its degradation behaviour toward the heat treatment. (7)

Statistical analysis

The TGA data collected for each sample were entered into a spreadsheet and analyzed statistically using Stat View 4.0 (Abacus Concepts, Berkeley, USA). Fisher's PLSD, Scheffe and Bonferroni/Dunn methods were used to evaluate the presence of statistically significant differences (significance level < 0.05).

RESULTS

All samples presented a thermal behaviour characterized by a peak comprised between 53 and 59°C, which is the conversion of the α-phase into amorphous gutta-percha (Fig. 2). On the contrary the peak between 42 and 49 °C, corresponding to the transformation from β-gutta-percha to the α-gutta-percha, characterized only few samples of both groups. In Group Test there was a slight increase in the percentage of β gutta-percha, however Bonferroni, Scheffé, and Fisher's LSD did not show significant differences than Group Control (Fig. 3).

Indeed thermogravimetric analysis registered a different behaviour between Group Test and Control (Fig 4). The percentage of loss of weight after the thermal cycle was higher in samples irradiated by laser (3.89%) than controls (2.26%). Bonferroni, Scheffé, and Fisher's LSD have confirmed that there were significant differences (p=0.0258; significance level < 0.05) between the two groups.

DISCUSSION

A thermal/thermogravimetric comparison between commercial gutta-percha (Group Control) and laser treated gutta-percha (Group Test) has been conducted. The 980-nm diode laser is characterized by small wavelengths, belonging to the infrared region –close to the electromagnetic spectrum. It is thought that the pink-orange colour of gutta-percha points is a target of the 980 nm diode laser; in this way the energy is mainly absorbed and converted into heat and gutta-percha softens.

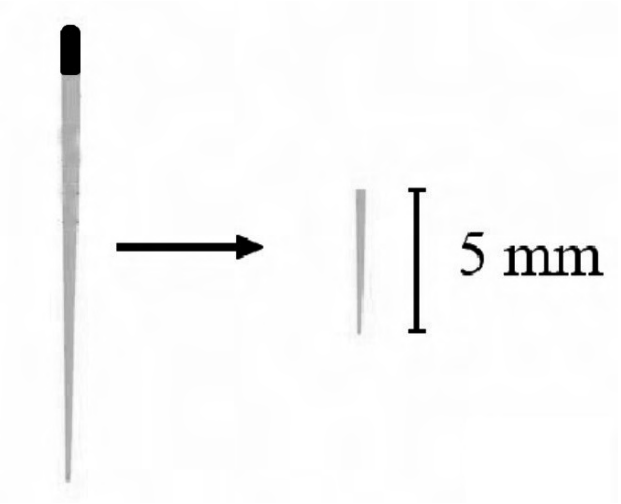

Fig. 1 *shows the samples preparation: gutta-percha cones were split with a scalpel and only samples of 5 mm obtained from the apical portion were considered.*

The polymer of the gutta-percha (trans-polysoprene) can exist in two crystalline forms a and ß: they differ by the distance between two consecutive -CH3 groups placed on the same side in relation to the carbons engaged in the double bonds ("molecular repeat distance") and the two phases (a and β) are inter-convertible. (12)

Results showed a slight increase in the percentage of β gutta-percha in Group Test. This change, however, is not significant respect group Control. Authors believe that the presence of β gutta-percha in both groups is attributable to the different crystal structures that already, without laser treatment is present in the commercial form of gutta-percha tips.

Many studies indeed disagree about the composition of the gutta-percha in endodontic tips. Maniglia-Ferreira found that the majority of the analyzed endodontic cones showed thermal behaviour typical of β-gutta-percha, with two endothermic peaks. (13)On the contrary Ferrante registered only one endothermic peak, corresponding to the conversion from the α- to the amorphous gutta-percha. (12) Basing on thermal results this study showed that 980 nm diode laser can be safety used also during endodontic obturation.

The thermogravimetric differences between Group Test and Control are very important. The weight of loss in laser treated gutta-percha polymer could make the cone more porous and reduce its root canal sealing property, essential for the success and durability of the endodontic treatment. (14)

However also commercial gutta-percha cones during clinical treatment, are often plasticized by a heat carrier

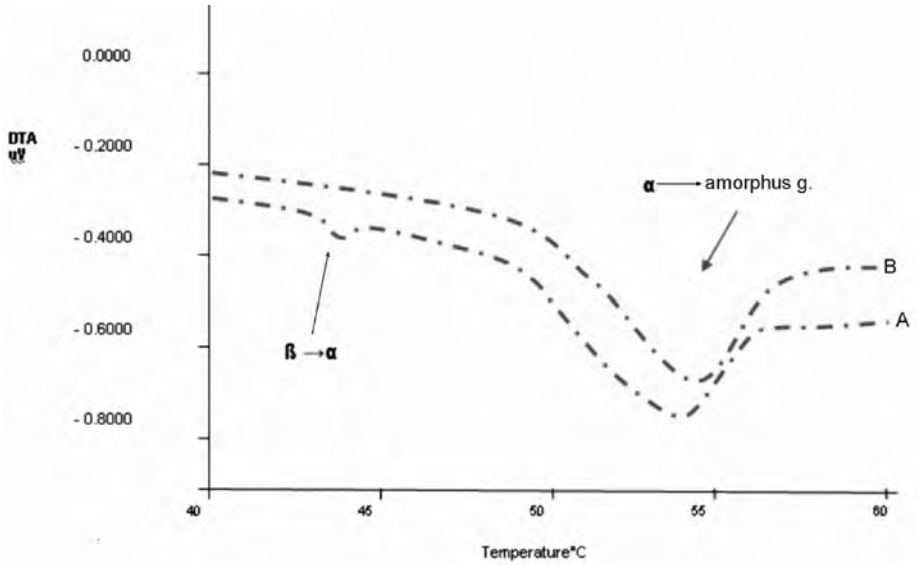

Fig. 2. *shows the differential thermal analysis of 2 different samples. The curve relatives sample A presents two typical major endothermic peaks (40.0 and 53 °C), indicating that the material was in β form. The curve relatives sample B shows only one endothermic peak (ca. 53 °C), which corresponds to the conversion of the α-phase into amorphous gutta-percha.*

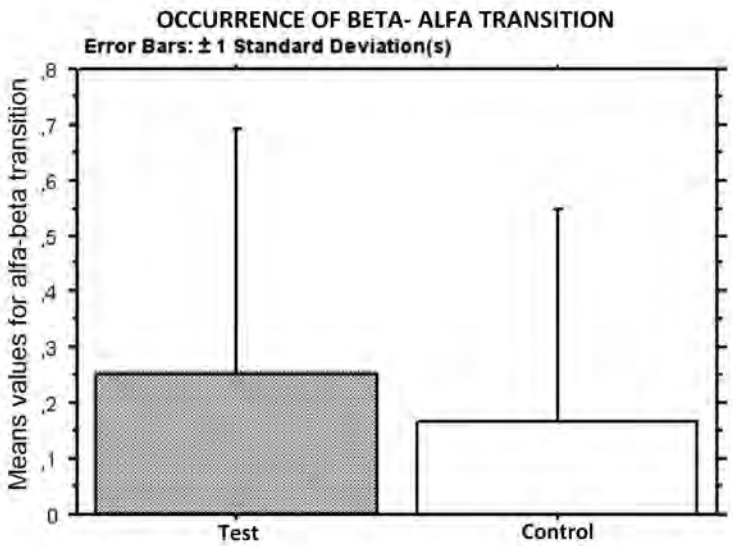

Fig. 3 *shows different occurrence of βàα transition in Group Test and Control. In samples irradiated by laser there is a slight increase in the percentage of β gutta-percha. Bonferroni, Scheffé, and Fisher's LSD, however, did not show significant differences between Group Test and Control (significance level < 0.05).*

or by thermo mechanical compaction, which if used improperly may cause partial decomposition if the heat generated exceeds 100°C, according to the Merck index. (15)

Nevertheless, the use of this device in endodontics is recently supported by many studies. Bahcall has demonstrated that there is a low increment of temperature using a 980 nm diode laser when compared with a 1064 nm Nd:YAG laser (3 W/30 s), with the same potency value and mode of operation.(16-17)

Hmud has demonstrated that this device is able to induce cavitation bubbles in water and weak hydrogen peroxide solutions, for enhance the removal of debris and smear layer in the root canal. (18)

These protocols are safe in terms of thermal insult to adjacent tissues, provided that the fibber is moved and irrigation is used between laser exposures. (19)

Also Garcia supported the use of 980 nm diode laser

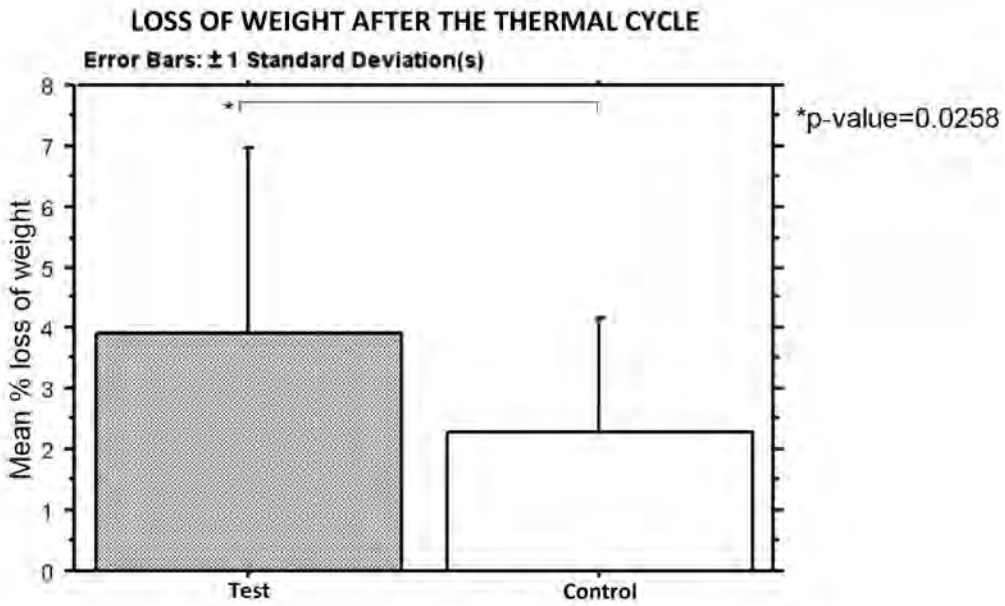

Fig. 4. *Shows the percentage of loss of weight after thermal cycle. Group Test is characterized by a higher loss of weight than Group Control. Bonferroni, Scheffé, and Fisher's LSD have registered significant difference between two groups (p-value=0.0258; significance level < 0.05).*

in endodontics; in fact he stated that this device promotes an increase in bond strength of the self-adhesive resinous cement to root dentin. (20)

Other studies have been undertaken, seeking to correlate physical properties, chemical composition and clinical behaviour to the 980 nm diode laser application to different root canal materials readily available to the clinician.

CONCLUSIONS

It has been demonstrated that:

1. 980 nm diode laser used with cited parameters does not alters thermal behaviour of gutta-percha cones.
2. Laser treatment modifies thermogravimetric behaviour of endodontic cones but other studies are needed to compare this technique with others plasticizer methods.

ACKNOWLEDGEMENTS

The authors would like to thank Galbiati srl (Italy) for the concession of the 980-nm diode laser (G-Laser 25).

REFERENCES:

1 M Petrini M, Ferrante L, Ciavarelli A, Ceccarini L, Brunetti M, Vacca G. Spoto. Prostaglandins E2 for diagnosis between reversible and irreversible pulpitis. Int J Immunopathol Pharmacol 2012; 25:157-163.

2 Waterhouse PJ, Whitworth JM, Nunn JH. Development of a method to detect and quantify prostaglandin E2 in pulpal blood from cariously exposed, vital primary molar teeth. Int End. J 1999; 32, 381-87.

3 Longman LP, Preston AJ, Martin MV, Wilson NH. Endodontics in the adult patient: the role of antibiotics. J Dent. 2000; 28, 539-48

4 Kovac J, Kovac D. Effect of irrigating solutions in endodontic therapy. Bratisl Lek Listy. 2011;112:410-5.

5 Nagayoshi M, Nishihara T, Nakashima K, Iwaki S, Chen KK, Terashita M, KitamuraC. Bactericidal Effects of Diode Laser Irradiation on Enterococcus faecalis Using Periapical Lesion Defect Model. ISRN Dent. 2011;2011:870364.

6 Rios A, He J, Glickman GN, Spears R, Schneiderman ED,

Honeyman AL. Evaluation of photodynamic therapy using a light-emitting diode lamp against Enterococcus faecalis in extracted human teeth. J Endod. 2011 Jun;37(6):856-9.

7 Maniglia-Ferreira C, Silva Jr JBA, Paula RCM, Feitosa JPA, Cortez DGN, Zaia AA et al. Brazilian gutta-percha points. Part I: chemical composition and X-ray diffraction analysis. Braz Oral Res. 2005;19(3):193-7.

8 Anić I, Matsumoto K. Comparison of the sealing ability of laser-softened, laterally condensed and low-temperature thermoplasticized gutta-percha. J Endod. 1995 Sep;21(9):464-9.

9 Gençoğlu N. Comparison of 6 different gutta-percha techniques (part II): Thermafil, JS Quick-Fill, Soft Core, Microseal, System B, and lateral condensation. Oral Surg Oral Med Oral Pathol Oral Radiol Endod. 2003 Jul;96(1):91-5.

10 Rocca JP, Bertrand MF, Curti M. Er:Yag laser as an aid in filling root canals in three dimensions. J Oral Laser Applications 2002;2; 101-105.

11 Alfredo E, Marchesan MA, Sousa-Neto MD, Brugnera-Júnior A, Silva-Sousa YT. Temperature variation at the external root surface during 980-nm diode laser irradiation in the root canal. J Dent. 2008 Jul;36(7):529-34.

12 Ferrante M. , Trentini P., Croce F., Petrini, M. , Spoto G. Thermal analysis of commercial gutta-percha. J Therm Anal Calorim 2011, 103:563-567

13 Maniglia-Ferreira C, Gurgel-Filho ED, Silva JB Jr, Paula RC, Feitosa JP, GomesBP, Souza-Filho FJ. Brazilian gutta-percha points. Part II: thermal properties. Braz Oral Res. 2007 Jan-Mar;21(1):29-34.

14 Joa˜o Batista A. Silva Jr., Regina C. M. de Paula, Judith P. A. Feitosa, Eduardo Diogo Gurgel-Filho, Claudio Maniglia-Ferreira, Francisco Jose de Souza Filho. In Vivo Aging of Gutta-Percha Dental Cone. J Appl Pol Sc 2006; 100;5:4082-4088

15 Budavari S, ed. The Merck index: an encyclopedia of chemicals, drugs, and biologicals. 12th ed. Whitehouse Station: Merck; 1996.

16 Bahcall J, Howard P, Miserendino L, Walia H. Preliminary investigation of the histological effects of laser endodontic treatment on the periradicular tissues in dogs. J Endod. 1992;18:123–7.

17 Alfredo E., Marchesan M.A.,. Sousa-Neto M.D, Brugnera-Ju´ nior A., Silva-Sousa Y.T.C.. Temperature variation at the external root surface during 980-nm diode laser irradiation in the root canal. J Dent. 3 6 (2 0 0 8) 52 9 – 53 4

18 Hmud R, Kahler WA, George R, Walsh LJ. Cavitational effects in aqueous endodontic irrigants generated by near-infrared lasers. J Endod. 2010 Feb;36(2):275-8

19 Hmud R, Kahler WA, Walsh LJ. Temperature changes accompanying near infrared diode laser endodontic treatment of wet canals. J Endod. 2010 May;36(5):908-11.

20 Garcia LD, Naves LZ, Correr-Sobrinho L, Consani S, Pires-De-Souza FD. Bond strength of a self-adhesive resinous cement to root dentin irradiated with a 980-nm diode laser. Acta Odontol Scand. 2010 Mar 3. (Article in press)

IN VITRO EVALUATION OF MESENCHYMAL STEM CELL ISOLATION POSSIBILITY FROM DIFFERENT INTRA-ORAL TISSUES.

M. ORCIANI[1], R. DI PRIMIO[1], C. FERRETTI[1], G. ORSINI[2], E. SALVOLINI[1], R. LAZZARINI[1], M. MATTIOLI-BELMONTE[1]

[1]Department of Clinical and Molecular Sciences, and [2]Department of Clinical Sciences and Stomatology, Università Politecnica delle Marche, Via Tronto 10/a, 60126 Ancona (Italy).

Mesenchymal stem cells (MSCs) are of great interest for the regeneration of tissues and organs. Bone marrow is the first sources of MSCs, but in the recent years there has been interest in other tissues for the isolation of these pluripotent cells. In this study, we investigated the features of MSCs isolated from different oral regions in order to evaluate their potential application in the regeneration of damaged maxillofacial tissues. Sampling from human periodontal ligament, dental pulp, maxillary periosteum as well as bone marrow were collected in order to obtain different stem cell populations. Cells were morphologically and immunophenotipically characterized. Their proliferation potential and their ability to differentiate in osteoblasts were also assessed. All tested cell population showed a similar fibroblast-like morphology and superimposable immunophenotype. Slight differences were observed in proliferation and differentiation potential. Cells isolated from human periodontal ligament, dental pulp, maxillary periosteum had the characteristics of stem cells. Considering their peculiar feature they may alternatively represent interesting cell sources in stem cell-based bone/periodontal tissue regeneration approaches.

Stem cells are immature and unspecialized cells with the potential to differentiate into many different cell lineages. By the conventional definition, these cells can renew themselves indefinitely through "self-renewal (1), and they vary in terms of their body location and the type of cells that they can generate. Recent studies showed that the oral tissues, which are easily accessible for dentists, may represent an interesting source of stem cells.

Given to their unique abilities, stem cells are particularly attractive for the development of innovative bone tissue engineering strategies (2) and/or tissue regenerative medicine based on in situ cell recruitment also in dentistry (3,4) where, for instance, alveolar bone resorption may occurs after tooth loss/extraction in periodontal disease, severe caries, root fractures or accidental trauma (5). Consequently, stem cell and tissue engineering applications are expected to provide a novel capability to regenerate large defects in periodontal tissues (6) and alveolar bone (7), and to ultimately replace the lost tooth itself (8).

Stem cell-based tissue engineering has already been applied to clinical trials for oro-facial bone tissue regeneration (7) with preliminary promising successes. However, the recent findings that several types of stem cells can be harvested from the oral and maxillofacial regions (9), advocate further investigation on their role in dentistry regenerative biology, in particular with regard to the optimal type of stem cells to be used for a more efficient treatment of injured oral tissues.

In oral and maxillofacial regions, two types of adult stem cells have been characterized: epithelial stem cells (10) and mesenchymal stem cells (MSCs). The latter have long been assumed to exist in dental tissues, because some of these tissues (i.e. periodontal tissues and dental pulp) can regenerate or form reparative dentin by a natural process, if the environmental conditions are suitable after dental treatments (11,12) .

Considering the diverse MSC sources identified and characterized in dental tissues (9,13,14), aim of the present study is to compare cells obtained by different oral regions (i.e. periodontal ligament, dental pulp, maxillary periosteum) with bone marrow (BM) derived stem cells, in order to evaluate their potential application in regenerative medicine for oral tissues.

Keywords: MSCs, Tissue engineering, dentistry

Corresponding author: Monia Orciani
Department of Clinical and Molecular Sciences
Università Politecnica delle Marche,
Via Tronto 10/a, 60126 Ancona, Italy
Phone +39 071 2206078
FAX +39 071 2206073
e-mail: m.orciani@univpm.it

0393-974X (2012)

MATERIALS AND METHODS

Mesenchymal stem cells isolation

Mesenchymal stem cells (MSCs) were isolated from human periodontal ligament (PDL-MSCs), dental pulp (DP-MSCs), maxillary periosteum (PDPCs) and bone marrow (BM-MSCs). Periodontal ligaments and dental pulps were obtained from the third molars of healthy donors after extractions scheduled for orthodontic reasons. Periosteum was harvested from full-thickness biopsy of patients who underwent routine oral surgery procedures. BM was collected from iliac crest and mononuclear cells were obtained by Histopaque® 1077 (Sigma Aldrich, MO, USA) density gradient centrifugation. The study was performed under an institutionally (Università Politecnica delle Marche) approved protocol and all patients gave their informed consent. Both systemic and oral diseases were absent in all subjects. Immediately after extraction, the samples tissue were cut into small pieces, washed in phosphate-buffered saline (PBS) and cultured with the Mesenchymal Stem Cell Growth Medium (MSCGM) bullet kit (Lonza Group® Ltd).

The cultures were maintained in a 5% CO2 humidified incubator at 37°C. After 14 days of culturing, numerous cells forming colonies (CFU-F) migrated from the explants; non-adherent cells and residual tissue were removed and the medium was replaced with fresh one. Subsequently, the medium was changed twice a week. When the adherent cells reached confluence, they were detached by 0.125% trypsin and 1 mM ethylenediamine tetraacetic acid (EDTA) for 3 minutes. The released cells were collected and re-plated for subculture in culture flasks with MSCGM for DP- and PDL-MSCs and with Dulbecco's Modified Eagle Medium: Nutrient Mixture F-12 (DMEM/F-12) supplemented with 10% Foetal Bovine Serum (FBS) and 1% penicillin-streptomicin (100U/ml), all from GIBCO® (Invitrogen, Milan, Italy) for PDPCs (15, 16) and BM-MSCs.

MSCs morphology and characterization

Morphology and cell growth of the MSCs were evaluated by phase contrast microscopy (Leika DM IL, Leika® Microsystems GmbH, Germany) and the viability was assessed by an automated cell counter (Invitrogen®, Milano, Italy).

At 3rd passage, cells isolated from BM, DP, PDL and periosteum were examined for surface antigens specific to stem cells. Cells in culture were trypsinized and stained, in agreement to minimal criteria for identification of human MSCs (17), with fluorescin isothiocyanate (-FITC) conjugated antibodies against: CD90, CD105, CD14, CD19, CD34, CD45 , CD73 and HLA-DR. Flow cytometry analysis was performed with a Becton Dickinson FACScan instrument equipped with an argon ion laser tuned at 488 nm. Data acquisition was done with CellQUEST software (Becton Dickinson, USA). All antibodies were purchased from Becton-Dickinson. Cells were gated according to their scatter light, and fluorescence intensity distribution was analyzed in histograms.

In vitro differentiation into osteocytes

Differentiation was performed using STEMPRO® Osteogenesis Kit (GIBCO, Invitrogen, Milan, Italy). Cells cultured in DMEM/F-12 with 10%FBS were used as negative controls. For osteogenesis cells were seeded at a density 4.5x104cells with appropriate medium for 8-12 days, changing the medium twice a week. Osteogenic differentiation was assessed by Von Kossa and Alkaline phosphatise (ALP) stainings. For Von Kossa stain, cells were fixed in 4% Paraformaldehyde (PFA) for 15 min at Room Temperature (RT) and incubated with 1% silver nitrate solution under UV light for 20 min RT. Unreacted silver was removed with 5% sodium thiosulfate for 5 min. For ALP staining, cells were fixed in 4% PFA for 15 min RT and washed in 100 mM Tris-HCl pH 9.5, 100 mM NaCl and 10 mM MgCl2 buffer for 10 min RT. Cells were then stained with fast 5-bromo-4-chloro-3-indolyl phosphate and nitroblue tetrazolium alkaline phosphate substrate (Sigma-Aldrich, Milan, Italy) for 10 min and rinsed in dH2O. Reaction was observed with a light microscope (Nikon Eclipse 600, Nikon, Milan, Italy).

RESULTS

Mesenchymal stem cells isolation

BM was collected from iliac crest and mononuclear cells were obtained by a density gradient centrifugation. Cells were plated in culture flasks and maintained till near-confluence that they reached around day 14.

DP- and PDL-MSCs were obtained from the third molars of healthy donors; after 7 days of culturing, some cells with a fibroblastoid morphological aspect appear near the explants. A confluent cell monolayer was reached by day 14 when cells were detached and splitted for the second passage. Cells showed a fast doubling population time and appeared morphologically more homogeneous than first passage.

Minced explants of maxillary periosteum were positioned with their cambium side placed against the dishes. Cells were then allowed to adhere in standard cell culture condition and cells with a fibroblast-like morphology (PDPCs) migrating from the explants were observed after 10-12 days. Confluence was reached within 20 days.

Figure 1 depicts the fibroblastoid morphological aspect of cells isolated from the different selected sources with no differences among cells. On the contrary the proliferation rate of PDPCs and of MSCs isolated from BM was lower in comparison with that observed for PDL- and DP-MSCs (Fig. 2). For three months, the cell proliferation follows an exponential growth curve; after this time the growth rate decreased (Fig. 2).

Immunophenotypical characterization

BM-,DP-, PDL-MSCs, and PDPCs were immunophenotypically analyzed by flow cytofluorimetry to confirm that the isolated cell displayed phenotypic characteristics usually described for MSCs.

The analyses revealed that cells appeared to be strongly positive for CD73, CD90 and CD105 and negative for

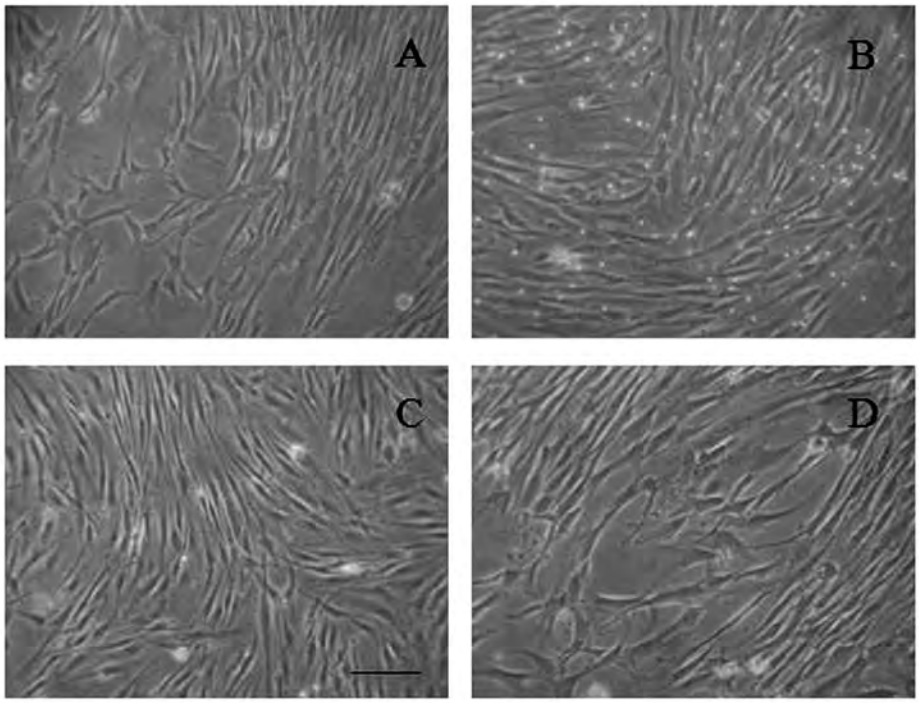

Fig. 1. *Morphology of MSCs. Phase-contrast images of MSCs derived from bone marrow (A), dental pulp (B), periodontal ligament (C) and periostium (D) at 10 days of culture. Scale bar, 100 μm.*

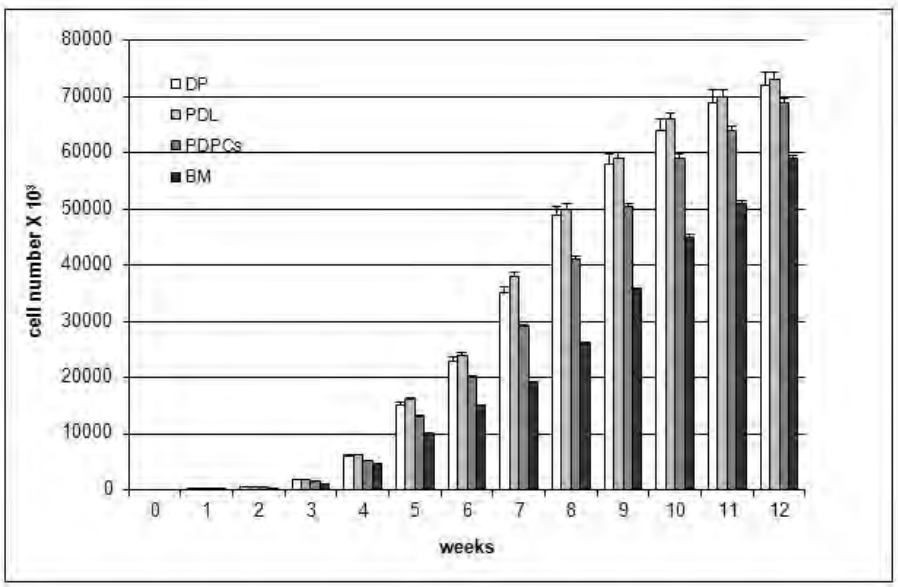

Fig 2. *Cell growth .Cell number was assessed by an automated cell counter at every passage during 12 weeks of culture. The proliferation rates of BM-MSCs and PDPCs were significantly lower than the others.*

HLA-DR, CD14, CD19, CD34 and CD45 (Fig. 3). This MSCs-like immunophenotype was comparable to that of BM-MSCs and confirmed in all tested sample of PDL, DP and PDPCs.

To evaluate any possible changes in their phenotype linked to culture conditions, cytofluorimetric analysis was repeated on proliferating cells after 8 or 16 weeks. The expression profile of mesenchymal markers on these

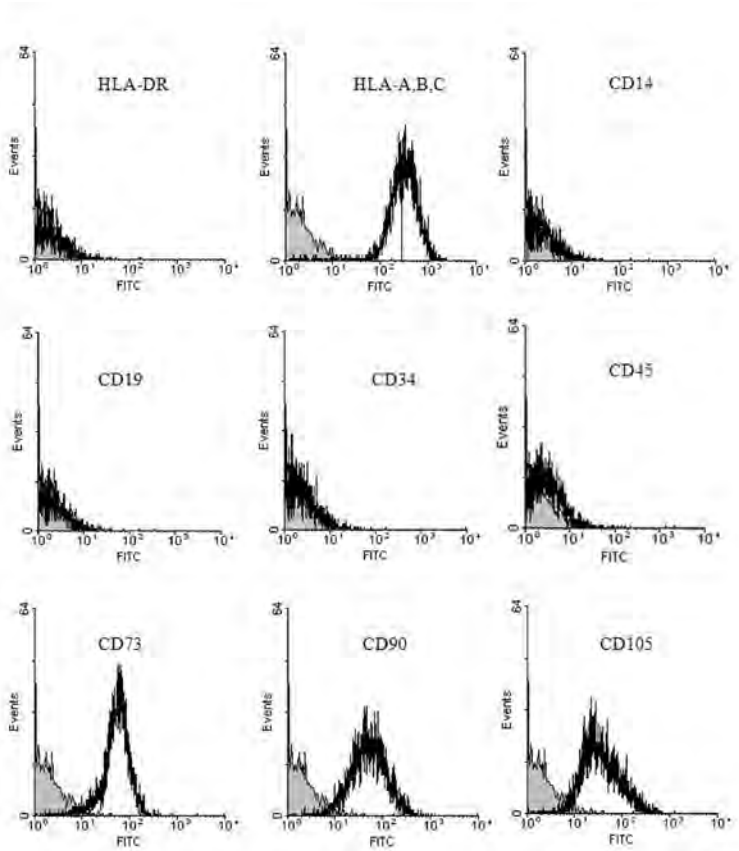

Fig. 3. *Representative FACScan analyses of cell-surface antigen expression. Solid grey fluorescence histograms, negative control (IgG1 isotype control-FITC labeled). The data are representative of BM-, DP- and PDL-MSCs and of PDPCs, each performed in duplicate. No differences were observed.*

cell populations was not significantly different from that observed in earlier expanded cells (data not shown).

Cell differentiation

BM-, DP-, PDL-MSCs and PDPCs osteogenic differentiation was detected after 10 days of culture for BM-MSCs and PDPCs, with cells strongly positive for alkaline phosphatase (Fig 4) and aggregates of mineralized matrix as shown by Von Kossa staining (Fig 4). Differentiation for DP- and PDL-MSCs occurs after 12 days.

DISCUSSION

Tissue engineering approach for bone regeneration and repair is a new challenge in oral and maxillofacial surgery and many therapeutic attempts have been reported (18). In view an efficient treatment for regeneration of these tissue is however represented by a correct selection of the appropriate cytotype since cells from diverse sources may show different in vivo results (19).

MSCs are among the most promising adult stem cells for clinical applications; they were originally found and isolated from the bone marrow and more recently from some other tissues including skin (20), amniotic fluid (21,22), periosteum (16), adipose tissue (23) and various dental tissues (13,24). In cell culture, MSCs can be identified and isolated on the basis of their adhesion to tissue-culture-treated plastic (25). This concept was originally reported in 1970 by Friedenstein et al (26) and gave rise to the concept of MSCs (27). In 1999, Pittenger et al. (28) characterized human MSCs from iliac crest bone marrow (BM-MSCs) as multipotent stem cells by demonstrating their isolation, expansion in culture and directed differentiation to osteogenic, adipogenic and chondrogenic lineages. Since then, extensive studies on MSCs have demonstrated their robust multipotency and even "stem cell plasticity", as demonstrated by the MSCs ability to differentiate into lineages that are not typical mesenchymal derivatives (29,30).

Although the iliac crest has served as the primary source of BM-MSCs, at present they can also be isolated from orofacial (maxilla and mandible) bone marrow aspirates obtained during dental different surgical procedures (e.g. dental implant, wisdom tooth extraction). Clinical observations (31) and experimental animal

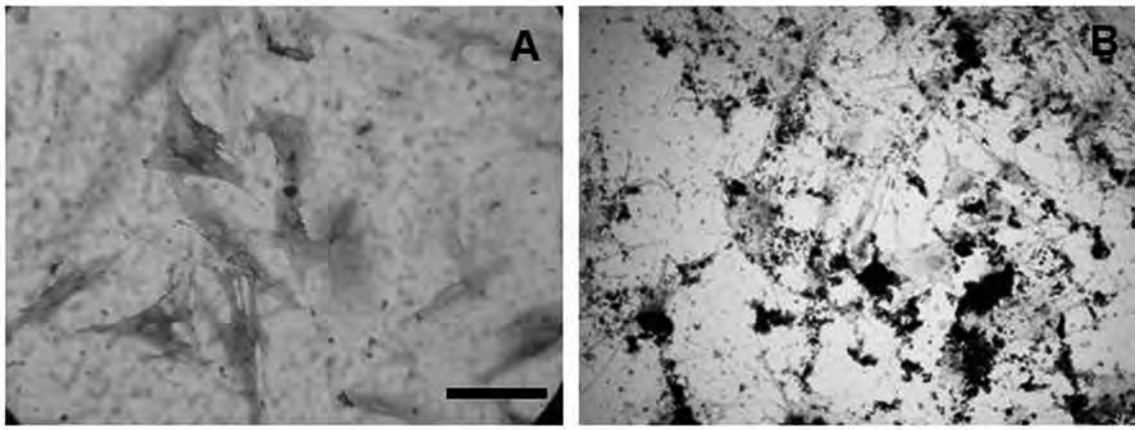

Fig 4. *Representative osteogenic differentiation assessment by ALP staining (a) and identification of CaPO4 crystals by von Kossa reaction (b). Scale bar, 50 μm.*

studies (32) have indicated that grafted bone obtained from the craniofacial area (membranous bone) for autologous bone grafting at craniofacial sites provides better results and significantly higher resultant bone volume than bone harvested from the iliac crest or rib (endochondral bone). These observations suggest that different skeletal donor tissues possess site-specific regenerative properties. From an embryological point of view, the maxilla and mandible bones originate from cranial neural crest cells (33), whereas the bone of iliac crest is formed by mesoderm. As a consequence, these differences may result in functional differences between orofacial and iliac crest human BM-MSCs (34, 35). Indeed, the collectable volume of orofacial bone marrow is less than that of iliac crest bone marrow (36) and therefore it is interesting to identify alternative MSCs accessible oral cavity sources of cell populations specifically suitable for facial bone regeneration.

In this respect we decided to investigate the applicability of mesenchymal stem cells derived from different tissues of the oral cavity (i.e. PDPCs from maxillary periostium; dental pulp and periodontal ligament) using culture conditions comparable to that used for the cultivation of BM-MSCs. In our study the cultured cells were adherent and fibroblastoid in shape, remarkably similar to one another and just the same as BM-MSCs. In addition, an analysis of their surface phenotype conducted using antibodies recognizing multiple putative markers of "mesenchymal stem cells" revealed a virtually identical profile. The self-renewal potential of cell tested was comparable with cultured BM-MSCs only for PDPCs, while DP-and PLD-MSCs showed an higher proliferation rate.

Our data are in agreement with previous studies on DP-MSCs (37, 38), PDL-MSCs and maxillary periosteum (39) and suggest different oral tissues suitable for isolating stem cells. This could allow the surgeon to reduce tissue loss, trauma, complications and discomfort for the patients in view of clinical practice requiring stem cell-based bone/periodontal tissue regeneration. Further studies are however necessary to establish evidence-based practices to educate dentists and patients regarding the use of stem cells in autologous regenerative therapies.

REFERENCES

1. Slack M. Origin of stem cells in organogenesis. Science 2008; 322:1498–1501
2. Langer R, Vacanti JP. Tissue engineering. Science 1993; 260:920–926
3. Kaigler D, Mooney D. Tissue engineering's impact on dentistry. J Dent Educ 2001; 65:456–462
4. Koyano K. Toward a new era in prosthodontic medicine. J Prosthodont Res 2012; 56:1–2
5. Atwood DA. Reduction of residual ridges: a major oral disease entity. J Prosthet Dent 1971; 26: 266–279
6. Yamada Y, Ueda M, Hibi H, Baba S. A novel approach to periodontal tissue regeneration with mesenchymal stem cells and platelet-rich plasma using tissue engineering technology: a clinical case report. Int J Periodontics Restorative Dent 2006; 26:363–369
7. Yamada Y, Nakamura S, Ito K et al. Injectable tissue-engineered bone using autogenous bone marrow-derived stromal cells for maxillary sinus augmentation: clinical application report from a 2–6-year follow-up. Tissue Eng

2008; 14: 1699–1707
8. Oshima M. Mizuno M, Imamura et al. Functional tooth regeneration using a bioengineered tooth unit as a mature organ replacement regenerative therapy. PLoS One 2011; 6:e21531
9. Egusa H, Sonoyama W, Nishimura M, Atsuta I, Akiyama K. Stem cells in dentistry - Part I: Stem cell sources. J Prosthodont Res. 2012; 56:151-165.
10. Harada H, Kettunen P, Jung HS, Mustonen T, Wang YA, Thesleff I. Localization of putative stem cells in dental epithelium and their association with Notch and FGF signaling. J Cell Biol 1999; 147:105–120
11. Ruch JV. Odontoblast commitment and differentiation Biochem Cell Biol 1998; 76:923–938
12. Kao DW, Fiorellini JP. Regenerative periodontal therapy Front Oral Biol 2012; 15:149–159
13. Orciani M, Trubiani O, Vignini A, Mattioli-Belmonte M, Di Primio R, Salvolini E. Nitric oxide production during the osteogenic differentiation of human periodontal ligament mesenchymal stem cells. Acta Histochem. 2009; 111:15-24
14. Trubiani O, Zalzal SF, Paganelli R et al.Expression profile of the embryonic markers nanog, OCT-4, SSEA-1, SSEA-4, and frizzled-9 receptor in human periodontal ligament mesenchymal stem cells. J Cell Physiol. 2010; 225:123-131
15. Pal R, Hanwate M, Jan M, Totey S. Phenotypic and functional comparison of optimum culture conditions for upscaling of bone marrow-derived mesenchymal stem cells. J Tissue Eng Regen Med 2009; 3:163-174
16. Ferretti C, Borsari V, Falconi M, Gigante A, Lazzarini R, Fini M, Di Primio R, Mattioli-Belmonte M. Human periosteum-derived stem cells for tissue engineering applications: the role of VEGF. Stem Cell Rev. 2012; 8:882-890
17. Dominici M, Le Blank K, Muller I et al. Minimal Criteria for deifying multipotent mesenchymal stem cells. The International Society for Cellular Therapy position statement. Cytotherapy 2006; 8: 315-317.
18. Yamada Y, Ueda M, Naiki T, Nagasaka T. Tissue-engineered injectable bone regeneration for osseointegrated dental implants. Clin Oral Implant Res 2004;15:589-97.
19. Choi YS, Noh SE, Lim SM, et al. Multipotency and growth characteristic of periosteum-derived progenitor cells for chondrogenic, osteogenic, and adipogenic differentiation. Biotechnol Lett 2008; 30593-601
20. Orciani M, Gorbi S, Benedetti M, Di Benedetto G, Mattioli-Belmonte M, Regoli F, Di Primio R. Oxidative stress defense in human-skin-derived mesenchymal stem cells versus human keratinocytes: Different mechanisms of protection and cell selection. Free Radic Biol Med. 2010; 49:830-8
21. Orciani M, Emanuelli M, Martino C, Pugnaloni A, Tranquilli AL, Di Primio R. Potential role of culture mediums for successful isolation and neuronal differentiation of amniotic fluid stem cells. Int J Immunopathol Pharmacol. 2008; 21:595-602
22. Antonucci I, Iezzi I, Morizio E et al. Isolation of osteogenic progenitors from human amniotic fluid using a single step culture protocol. BMC Biotechnol. 2009; 9:9
23. Augello A, Kurth TB, De Bari C. Mesenchymal stem cells: a perspective from in vitro cultures to in vivo migration and niches. Eur Cell Mater. 2010; 20:121-133
24. Trubiani O, Cataldi A, De Angelis F, D'Arcangelo C, Caputi S. Overexpression of interleukin-6 and -8, cell growth inhibition and morphological changes in 2-hydroxyethyl methacrylate-treated human dental pulp mesenchymal stem cells. Int Endod J. 2012; 45:19-25
25. Horwitz EM, Le Blanc K, Dominici M et al. Clarification of the nomenclature for MSC: the International Society for Cellular Therapy position statement. Cytotherapy 2005; 7:393–395
26. Friedenstein AJ, Chailakhjan RK, Lalykina KS. The development of fibroblast colonies in monolayer cultures of guinea-pig bone marrow and spleen cells. Cell Tissue Kinet 1970; 3:393–403
27. Caplan AI. Mesenchymal stem cells. J Orthop Res 1991; 9:641–650
28. Pittenger MF, Mackay AM, Beck SC et al. Multilineage potential of adult human mesenchymal stem cells. Science 1999; 284:143–147
29. Peran M, Marchal JA, Rodriguez-Serrano F, Alvarez P, Aranega A. Transdifferentiation: why and how. Cell Biol Int 2011; 35:373–379
30. Scuteri A, Miloso M, Foudah D, Orciani M, Cavaletti G, Tredici G. Mesenchymal stem cells neuronal differentiation ability: a real perspective for nervous system repair? Curr Stem Cell Res Ther. 2011; 6:82-92
31. Crespi R, Vinci R, Cappare P, Gherlone E, Romanos GE. Calvarial versus iliac crest for autologous bone graft material for a sinus lift procedure: a histomorphometric study. Int J Oral Maxillofac Implants 2007; 22: 527–532
32. Zins JE, Whitaker LA. Membranous vs endochondral bone autografts: implications for craniofacial reconstruction. Surg Forum 1979; 30:521–523
33. Chai Y, Jiang X, Ito Y et al. Fate of the mammalian cranial neural crest during tooth and mandibular morphogenesis. Development 2000; 127:1671–1679
34. Akintoye SO, Lam T, Shi S, Brahim J, Collins MT, Robey PG. Skeletal site-specific characterization of orofacial and iliac crest human bone marrow stromal cells in same individuals. Bone 2006; 38:758–768
35. Chung IH, Yamaza T, Zhao H, Choung PH, Shi S, Chai Y. Stem cell property of postmigratory cranial neural crest cells and their utility in alveolar bone regeneration and tooth development. Stem Cells 2009; 27: 866–877

36. Matsubara T, Suardita K, Ishii M et al. Alveolar bone marrow as a cell source for regenerative medicine: differences between alveolar and iliac bone marrow stromal cells. J Bone Miner Res 2005; 20:399–409
37. Gronthos S, Mankani M, Brahim J, Robey PG, Shi S. Postnatal human dental pulp stem cells (DPSCs) in vitro and in vivo. Proc Natl Acad Sci USA 2000; 97:13625–13630
38. Shi S, Robey PG, Gronthos S. Comparison of human dental pulp and bone marrow stromal stem cells by cDNA microarray analysis. Bone 2001; 29:532–539
39. Cicconetti A, Sacchetti B, Bartoli A et al. Human maxillary tuberosity and jaw periosteum as sources of osteoprogenitor cells for tissue engineering. Oral Surg Oral Med Oral Pathol Oral Radiol Endod. 2007; 104:618.e1-12.

ANTIBIOTIC-MODIFIED HYDROGEL COATINGS ON TITANIUM DENTAL IMPLANTS

S. COMETA[1], M. MATTIOLI-BELMONTE*[2], D. CAFAGNA[3], R. IATTA[4], E. CECI[5], E. DE GIGLIO[3]

[1] *Department of Chemistry & Industrial Chemistry, University of Pisa, S. Piero a Grado -Pisa (Italy)*
[2]*Department of clinical and Molecular Sciences, Università Politecnica delle Marche, Ancona (Italy)*
[3]*Department of Chemistry, University of Bari Aldo Moro, Bari (Italy)*
[4]*Department of Biomedical Sciences and Human Oncology, University of Bari Aldo Moro, Bari (Italy)*
[5] *Department of Public Health, Faculty of Veterinary Medicine, University of Bari Aldo Moro, Bari (Italy)*

Implant-associated infections represent an occasional but serious problem in dental and/or orthopaedic surgery. A possible solution to prevent the initial bacterial adhesion may be the coating of the implant surface with a thin layer of antibiotic-loaded biocompatible polymer. Hydrogels are one of the promising and versatile materials as antibiotic controlled release systems. In this work, antibiotic-modified poly(ethylene-glycol diacrylate) hydrogel coatings on titanium substrates were prepared by electrochemical polymerization and tested against methicillin resistant Staphylococcus aureus (ATCC 33591). Two different methods to load vancomycin and ceftriaxone were used. We show that the proposed titanium coatings displayed an interesting antibacterial activity, however, further studies on their effective cytotoxicity will furnish evidence of their real clinical efficacy.

The success of a dental implant is hugely related to a good osseointegration as well as to the long term prevention of bacterial infections [1]. In general, biomaterial implantation into the human body increases infection susceptibility [2] and activates host defences, stimulating the release of inflammatory mediators, including oxygen radicals and lysosomal enzymes [3-5].

The microflora of dental peri-implantitis is predominantly based on anaerobic Gram-negative bacilli (i.e. *Porphyromonas gingivalis* and *Prevotella intermedia*) or anaerobic Gram-negative cocci (*Veillonella spp*. and spirochaetes including *Treponema denticola)* [6]. The role of *Staphylococcus aureus,* that is typically encountered in orthopedic infections is also controversial in dental infections [7]. Indeed, the primary cause of implant associated infections is related to the presence of an extracellular matrix serum protein that covers the implant. The latter provides an ideal environment for bacterial adhesion and proliferation that, in turn, determines biofilm formation [8].

A systemic treatment of infected implants with antibiotics is often difficult [9], therefore the use of local antimicrobial prophylaxis may represent a useful tool for infection prevention. One of the major advantages of this approach is the stable and extended antibiotic release directly to infected tissue, at an adequate local bactericidal concentration and without systemic toxicity. In this respect the development of controlled release systems for bioactive agents (e.g. drugs, peptides and proteins) is, today, one of the major research driving forces in pharmaceutical industry.

Hydrogels are three-dimensional polymer networks able to absorb extremely large amounts of water [10,11], the ideal environment for many bioactive molecules. Several studies report drug release and/or tissue engineering applications of hydrogel networks obtained by UV irradiation or cross-linking, either chemical or physical [12-14]. For hydrogel coatings onto a metal substrates (e.g titanium), a very promising alternative synthetic route is represented by an electrochemical polymerization, which leads to thin coatings firmly attached to the substrate, that in the electro-synthetic process is used as working electrode [15-22].

This work represents a further development of previous studies devoted to the identification of possible modification of titanium (Ti) implant surfaces for the delivery of active molecules directly at the site of infection, through a polymeric coating [18-20, 22].

On the basis of these former experiences, here we

Key words: hydrogel, electrosynthesis, titanium, antibiotic, dental infections.

*Corresponding author:
Monica Mattioli-Belmonte
Department of Clinical and Molecular Sciences
Università Politecnica delle Marche,
Via Tronto 10/a, 60126 Ancona, Italy
Phone +39 071 2206077 FAX +39 071 2206073
e-mail: m.mattioli@univpm.it

0393-974X (2012)

chose a lower molecular weight poly(ethylene glycol diacrylate) (PEGDA) macromer as a potential carrier for vancomycin, an effective drug against methicillin-resistant *S. aureus* (MRSA) [23] and ceftriaxone (a third-generation cephalosporin) [24], since cephalosporins are the most frequently used antibiotics in dental postoperative prophylaxis.

Antibiotic loadings within hydrogel coatings were obtained using two different procedures: 1) entrapment of the antibiotic during electrosynthesis, i.e. adding the drug to the monomer solution; 2) post-electrosynthesis antibiotic loading, dipping the hydrogel coated Ti sheets in a solution containing an appropriate antibiotic amount.

X-ray Photoelectron Spectroscopy (XPS) and High Performance Liquid Chromatography (HPLC) were employed to perform coating characterization and to estimate the amount of antibiotic released from the hydrogel networks. Microbiological tests were carried out on MRSA ATCC 33591 strain, evaluating the antibiotic growth inhibition properties and the coating efficacy as drug delivery systems.

MATERIAL AND METHODS

Chemicals

Hydrogels were obtained on titanium substrates by electrosynthesis of poly(ethylene-glycol diacrylate) with average M_n = 575 g/mol (PEGDA) (SIGMA). Titanium (SIGMA) electrodes were mechanically polished by fine diamond paper and then by Al_2O_3 powder (50 μm). After this treatment, before polymer deposition, each electrode was cleaned by an ultrasonic bath using ethanol and successively triply distilled water. Reticulated vitreous carbon (RVC) was cut to size and used as the anode in all electropolymerizations, without further modification.

Vancomycin hydrochloride (Sigma Aldrich) MW = 1485.71 g/mol and ceftriaxone disodium salt hemi(heptahydrate) MW = 661.60 g/mol (Sigma Aldrich), were stored at 4°C and used without further modification. The chemical structure of the employed antibiotics is reported in Figure 1.

Apparatus

All electrochemical experiments were carried out using a PAR 273 potentiostat-galvanostat (EG&G Princeton Applied Research) and a three-compartments cell. A schematic description of the cell was already reported [16]. Cathodic and anodic compartments were connected by a glass frit of medium porosity. Titanium sheets (10x10 mm^2) were used as working electrodes and dipped into the cathodic side cell compartment, while the RVC auxiliary electrode was secured in the anodic one. The Ag/AgCl (KCl sat.) reference electrode was introduced in close proximity to the working electrode by a Luggin's capillary. In the present work, all potentials are referred to the reference system used: Ag/AgCl (KCl sat.) (0.199 V vs. SHE).

Electrochemical polymerization

Electrochemical polymerizations were carried out accordingly to a procedure described in previous works [16,18]. Briefly, the cathodic compartment was filled with 0.1 M $(NH_4)_2S_2O_8$ aqueous electrolyte solutions containing 0.1 M of macromer, whilst the anolyte was 0.025 M H_2SO_4. The potential was cycled between 0.0 V and a final potential of -0.9V or -1.2V (see below), using 20 cycles (scan rate 100 mV/s).

The catholyte was purged with nitrogen for 10 minutes before any electrosynthesis. During the electrosynthesis, carried out at room temperature, nitrogen purged the air above the catholyte. At the end of electrosynthesis, Ti working electrodes were removed immediately, washed with distilled water and then dried with a nitrogen flux.

XPS analysis

X-ray Photoelectron Spectroscopy (XPS) spectra were obtained using a ThermoVG Thetaprobe spectrometer, equipped with a microspot monochromatised AlKα source. The AlKα line (1486.6 eV) was used throughout the work and the base pressure of the instrument was 10^{-9} mbar. Survey scans (binding energy range 0-1200 eV, FAT mode, pass energy = 150 eV) and detailed spectra (FAT mode, pass energy = 50 eV) were recorded for each sample. Data analysis of the latter was performed using the Avantage software package, which consists of a non-linear least-squares fitting program. In all the cases the experimental points of the detailed spectra were fitted by gaussian-lorentzian peaks having the same full width at half maximum, starting from

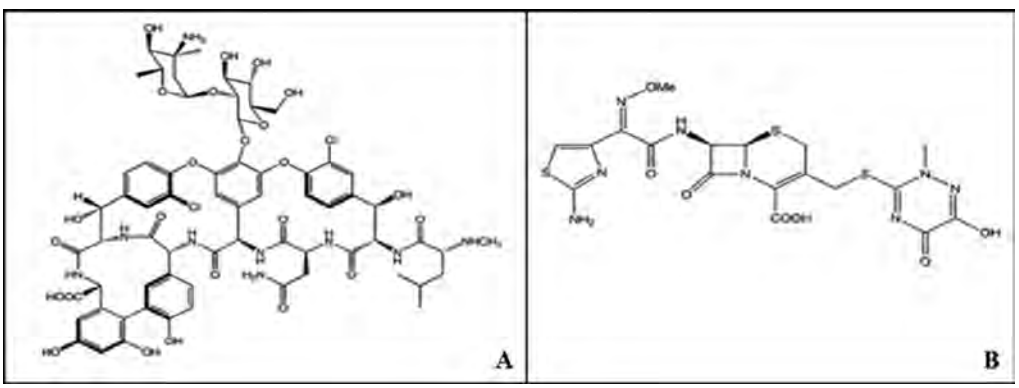

Fig. 1. *Chemical structure of vancomycin (A) and ceftriaxone (B).*

models already applied. Quantification was performed using peaks areas; comparison between data from different elements was possible after correction (division) by empirically derived atomic sensitivity factors [25].

Antibiotics loading in hydrogel coatings

When molecules were loaded in the hydrogel coatings during their growth (i.e. during electrosynthesis), antibiotics were added in the catholyte with a concentration of 100 ppm. In this case, the electrochemical parameters were accurately chosen in order to found the best conditions for the integrity of these drugs during the electrosynthesis. In particular, for vancomycin, the final potential was -0.9V while for ceftriaxone was -1.2V.

An alternative, post-electrosynthetic antibiotic loading procedure was also evaluated. In this case, the electrosynthesized hydrogel films were dipped in an aqueous solution containing a 100 ppm of antibiotic for 2 hours.

HPLC analysis of the antibiotic release from antibiotic-modified hydrogel coatings

Preliminary HPLC measurements have been performed on vancomycin- or ceftriaxone-loaded samples. The HPLC experiments were carried out using a liquid chromatograph at high performance (*Agilent Technologies Ltd*) Model 1100, having a mobile phase degassing module, a pump, an auto-sampler in which the injector *Rheodyne* with a 100 µl loop was accommodated. The chromatographic separation was allowed by a *Restek RP-C18* analytical column (5 µm, 250 mm x 4.6 mm internal diameter). The detector used was a DAD (*Agilent Technologies Ltd. mod. 1100*) with BIORAD software for signal analysis.

As far as vancomycin detection is concerned, isocratic elution was carried out thermostating the column at 30 °C, for a flow rate of 1.5 mL/min. Mobile phase was PBS (0.05 M): ACN: methanol (84: 8: 8), while the DAD was set at a wavelength of 215 nm [26].

For ceftriaxone detection, the mobile phase was composed by PBS (0.1M): ACN (10:90). The pH of the mobile phase was adjusted to 7.5 using ammonia solution. The DAD was set at a wavelength of 270 nm [27].

Evaluation of in vitro antibacterial activity

Samples were previously sterilized by UV radiation for 1 h/sheet side. Antibiotic-modified Ti sheets were immersed in a bacteria suspension that has been performed adding one to two colonies of MRSA ATCC 33591 culture into 2 mL of 8.5% NaCl physiological solution, in order to get an initial concentration of colony-forming units (CFU)/mL of 2.9 x 10^8. Bacterial suspension was then diluted 1:10, and a sterile swab soaked in this suspension was streaked on plate count agar (Oxoid) in Petri dishes. Each different antibiotic-modified hydrogel Ti coating sheet was dispensed onto the agar plate. Unmodified hydrogel Ti coating sheet was used as negative control. The bacteria were grown overnight at 37°C and then the antibiotic release was verified evaluating the inhibition zone diameter after 24h.

Vancomycin and ceftriaxone sensitivity was preliminary assessed measuring zones of inhibition on agar plates. These tests have not been utilised to obtain a quantitative information on the amount of drug released, but just to have an on/off response of the effectiveness of the antibiotic-modified drug delivery systems developed. For each antibiotic-modified Ti sheets, three experiments were performed in the same conditions; the inhibition zone diameter was calculated as the mean value and error was estimated by standard deviation.

RESULTS AND DISCUSSION

XPS analysis

A detailed XPS characterization of the electrosynthesized PHEMA- and PEGDA-based hydrogel films has been carried out in a previous work [18]. In particular, using a PEGDA macromer with a mean molecular weight of 700 g/mol, it was expected the obtainment of an average presence of 13 ethylene glycol units in each macromer. In contrast, XPS analysis demonstrated that the electrosynthesized hydrogel was constituted by macromers with shorter PEG chains (equal to 10.1 ± 1.6 EG units/macromer).

On the basis of this consideration, in this work, in order to obtain more compact and adherent hydrogel coatings, a PEGDA macromer with shorter PEG chains (mean molecular weight 575 g/mol) has been used, with a theoretical average ethylene glycol (EG) units of 10. The obtained PEGDA coatings appeared more adherent and underwent no peeling-off with respect to the previous investigated PEGDA system [18]. XPS analysis was employed to estimate the average PEG chain length. The PEGDA C1s signal curve fitting analysis is shown in Figure 2. C1s signal was fitted with four components, whose attributions were reported in Table 1. The area ratio between peaks A:B:C:D was 2.7 : 1.0 : 7.4 : 1.0 and indicated that XPS stoichiometric value relevant to macromer EG units (peak C) was equal to 7.4 ± 0.7. This finding suggests that the electrosynthesized hydrogel was obtained by macromers with shorter PEG chains (i.e. containing 7.4 *vs* 10 EG units).

HPLC detection

A quantitative detection of the vancomycin released from the hydrogel coatings was obtained by HPLC analysis. UV-detection HPLC without pre- or post-column derivatization was employed. Six replicates for all the investigated systems were prepared, using both the during- and the post-electrosynthesis loading procedures. The amount of vancomycin released from antibiotic-loaded PEGDA coatings in PBS solution (pH= 7.4) has been evaluated after 24h. A blank experiment was performed by analysing solution after 24h of immersion of unloaded PEGDA covered Ti sheets. HPLC results, were summarized in Table 2.

At this stage of our investigations, the quantitative information obtained by the *in vitro* simulation of the

drug release was used to verify a possible relationship between the amount of antibiotic released and MRSA growth inhibition. Work is in progress to investigate both vancomycin and ceftriaxone release kinetics from PEGDA coating by HPLC analysis and to determine a quantitative relationship that could clarify how the inhibition of MRSA growth is affected by the concentration of each antibiotic employed.

In vitro antibacterial activity

The screening of the efficacy of the two different antibiotics, vancomycin and ceftriaxone, and the release properties of PEGDA electrosynthesized hydrogel coatings were performed by *in vitro* tests against MRSA ATCC 33591.

Unloaded PEGDA thin hydrogel coatings on Ti sheets were exposed to bacteria suspension in the same experimental condition adopted for antibiotic-loaded hydrogel coatings. It can be observed that any biological activity can be ascribable to the sole polymer matrix. The results obtained from the two antibiotic loaded PEGDA-modified Ti sheets are reported in Table 3.

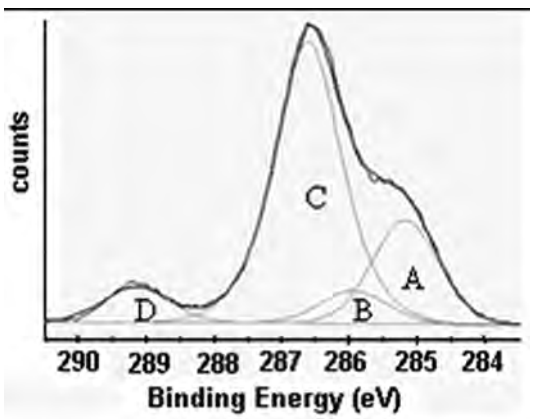

Fig. 2. *Typical Carbon 1s XPS signal recorded on PEGDA hydrogel coating electrosynthesized on titanium. Components and resultant obtained from curve fitting analysis are also shown.*

In Figure 3 the MRSA inhibition growth haloes due to the antibiotics release at 24h from PEGDA-modified Ti sheets have been reported. It can be underlined that, as suggested by Clinical and Laboratory Standards Institute (CLSI-Document M100), the vancomycin minimal inhibition concentration (MIC) against MRSA is lower than that of ceftriaxone.

In this study, it was observed that in the case of vancomycin, positive results were obtained irrespectively to the antibiotic loading procedure employed (see Figure 3 A and B). This suggests that the vancomycin amount loaded "during" or "post" electrosynthesis is enough to inhibit the bacterial growth. Anyway, in agreement with our previous experience [19], the "post" electrosynthesis antibiotic loading procedure is more effective than the "during" one.

As far as ceftriaxone-loaded coatings are concerned, no inhibition in MRSA growth was detected when the antibiotic was loaded during electrosynthesis, revealing that this loading method is not effective for the entrapment in the hydrogel coating of a ceftriaxone concentration able to kill the tested bacteria. In this respect, a possible structure modification of the entrapped ceftriaxone molecules in the "during-electrosynthesis" loading could not be excluded, even if this procedure has been accurately chosen taking into account the electrochemical parameters able to avoid any electroactivity of this molecule . On the other hand, employing the "post electrosynthesis" loading method for ceftriaxone, a significant inhibition zone was detected.

Moreover, these *in vitro* antibacterial tests resulted in good agreement with the above reported antibiotic release analyses performed by HPLC.

We can conclude that vancomycin-loaded coatings represent the most interesting local antibiotic release system, independently from the loading method employed. Alternatively, the hydrogel coating modified by ceftriaxone "post electrosynthesis" could be a potential antimicrobial coating for dental prosthetic devices.

Table I. *Attributions and binding energy values relevant to C1s signal curve-fitting analysis reported in Figure 2.*

Attribution	*B.E: (eV) (PEGDA)*
A: –**C**Hx	285.0
B: –**C**-C(=O)OR	285.7
C: –**C**OC	286.5
D: –**C**(=O)OR	289.0

Table II. *HPLC detection of vancomycin and ceftriaxone amounts (μg/mL) released from PEGDA hydrogel coatings after 24h.*

Antibiotic loading procedure	***Vancomycin loaded-PEGDA***	***Ceftriaxone loaded-PEGDA***
During electrosynthesis	4.0 ± 1.9	0.29± 0.13
Post electrosynthesis	10.0 ± 1.4	5.5 ± 1.6
Data are reported as mean ± SD		

Table III. *Diameter of inhibition zone (cm) of the different drug loading procedures and antibiotics employed against MRSA.*

Antibiotic loading procedure	***Vancomycin*** inhibition haloe	***Ceftriaxone*** inhibition haloe ***)***
During electrosynthesis	2.0±0.2	no halo
Post electrosynthesis	3.0 ±0.7	2.5±0.2
Data are reported as mean ± SD of three experiments performed in the same conditions.		

Overall these results, even though stimulating from a microbiological point of view, needs to be further investigated tacking into account problems related to the surrounding oral tissue, which could be affected by antibiotic release. Our previous experiences [19, 20] on the use of this type of hydrogels and of another antibiotic (i.e. ciprofloxacin) showed a good biocompatibility of MG63 osteoblast-like cells. During implantation, cells that could be affected by the presence of coatings endowed with an antibacterial activity are, however, not only that involved in bone remodelling (i.e. osteoblasts, pre-osteoblasts and mesenchymal stem cells [28]) but other cells of the oral cavity, such as gingival fibroblasts and cells from periodontal ligament [29]. Therefore, further studies are necessary to validate the clinical efficacy of the proposed antibacterial coatings.

CONCLUSION

In this work a new electrosynthesized polyacrylic hydrogel film has been proposed as a bioactive titanium implants coating. Two antibiotics, vancomycin and ceftriaxone, which are frequently used in orthopedic an dental postoperative antibiotic prophylaxis, were successfully entrapped into hydrogel coatings electrosynthesized onto titanium substrates. The release and efficacy of these local antibiotic delivery systems have been also evaluated by *in vitro* test against MRSA, confirming that antibiotic-modified hydrogel coatings, especially with vancomycin, could represent an effective approach in order to prevent oral bacterial infections frequently related to oral and maxillofacial surgery. HPLC data showed the efficacy of the antibiotic amount released from the hydrogel network.

As future perspective, the toxic properties of PEGDA will be investigated in order to ascertain the biocompatibility of these electrosynthesized hydrogels. In this way, it will be possible to obtain a biocompatible coating endowed with antibacterial activity and able to support cell functions pertinent to bone remodelling

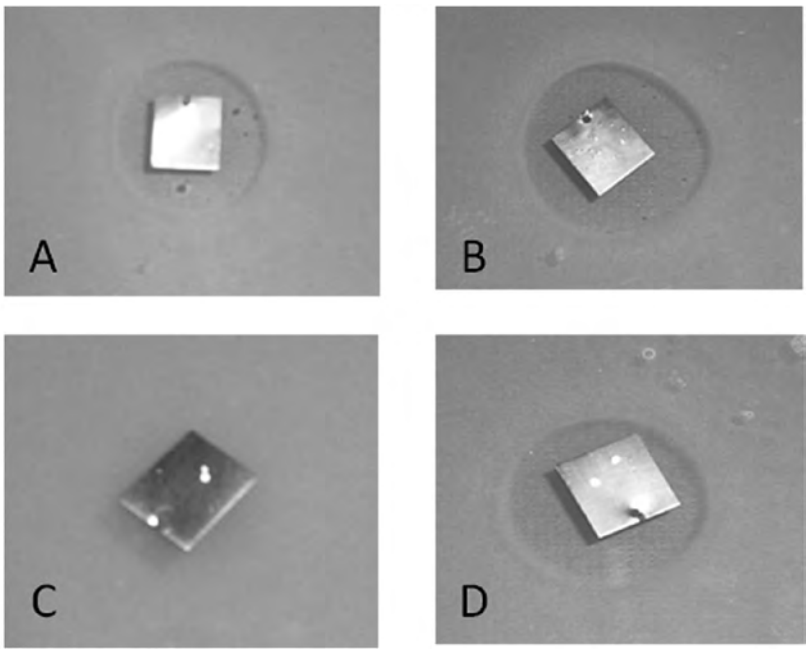

Fig. 3. *MRSA inhibition growth zones obtained by vancomycin (A, B) and ceftriaxone (C, D) loaded PEGDA coatings modified "during" (A, C) and "post" electrosynthesis (B, D), respectively.*

during implant osseointegration.

REFERENCES

1. Lian, Z., Guan, H., Ivanoski, S., et al. Effect of bone to implant contact percentage on bone remodelling surrounding a dental implant. Int. J. Oral. Maxillofac. Surg. 2010; 39; 690-8.
2. Elek S D, Conen PE. The virulence of Staphylococcus pyogenes for man: a study of the problems of wound infection. Br J Exp Pathol 1957; 38:573–86.
3. Merritt K, Dowd JD. Role of internal fixation in infection of open fractures: studies with Staphylococcus aureus and Proteus mirabilis. J Orthopaed Res 1987;5: 23–8.
4. Dickinson G, Bisno AL. Infections associated with indwelling devices: infections related to extravascular devices. Antimicrob Agents Chemother 1989; 33:597–601.
5. Gristina AG. Implant failure and the immuno-incompetent fibroinflammatoryzone. Clin Orthop Rel Res 1994;298: 106–18.
6. Bergbundh T et al. A Systematic review of the incidence of biological and technical complications in implant dentistry. J Clin Periodontol 2002; 29: 197-212.
7. Smith AJ, Robertson D, Tang MK et al. *Staphylococcus aureus* in the oral cavity: a three-year retrospective analysis of clinical laboratory data. Br Dent J 2003; 195: 701-3.
8. Dunne WM Jr. Bacterial adhesion: seen any good biofilms lately? Clin Microbiol Rev 2002; 15: 155–66.
9. Stewart PS, Costerton JW. Antibiotic resistance of bacteria in biofilms. Lancet 2001; 358, 135–8.
10. Peppas NA, Mikos AG. Preparation methods and structure of hydrogels in: N.A. Peppas(Ed), Hydrogels in Medicine and Pharmacy. Boca Raton FL: CRC Press; 1986; pp. 2–23
11. Brannon-Peppas L. Preparation and characterization of crosslinked hydorphilic networks in Brannon-Peppas R.S. Harland (Eds), Adsorbent Polymer Technology. Amsterdam: Elsevier; 1990; pp. 45–66.
12. Scott RA, Peppas NA. Highly crosslinked, PEG-containing copolymers for sustained solute delivery. Biomaterials. 1999;20: 1371-80.
13. Burdick JA, Mason MN, Hinman AD, Thorne K, Anseth KS. Delivery of osteoinductive growth factors from degradable hydrogels influences osteoblast differentiation and mineralization. J Control Release. 2002; 83:53-63.
14. Kiyonaka S, Sada K, Yoshimura I et al. Semi-wet peptide/protein array using supramolecular hydrogel. Nature Materials. 2004; 3:58-64.
15. De Giglio E, Guascito MR, Sabbatini L, et al. Electropolymerization of pyrrole on titanium substrates for the future development of new biocompatible surfaces. Biomaterials 2001; 22:2609-16.
16. De Giglio E, Cometa S, Spoto G, et al. Electrosynthesis

and analytical characterization of PMMA coatings on titanium substrates as barriers against ion release. Anal Bioanal Chem. 2005; 381:626-33.

17. De Giglio E, Cometa S, Calvano CD, et al. A new titanium biofunctionalized interface based on poly(pyrrole-3-acetic acid) coating: Proliferation of osteoblast-like cells and future perspectives. J. Mater. Sci Mater. Med. 2007; 18: 1781-89.
18. De Giglio E, Cometa S, Sabbatini L et al., "Electrosynthesis of hydrogel films on metal substrates for the development of coatings with controlled drug delivery performances", J Biomed Mater Res A 2009; 88:1048-57.
19. De Giglio E, Cometa S, Ricci MA, et al. Ciprofloxacin-modified electrosynthetized hydrogel coatings to prevent titanium-implant-associated infections. Acta Biomaterialia. 2011; 7: 882-91.
20. Mattioli Belmonte M, Orciani M, Ferretti C, et al. Cell behaviour on bioactive polymeric coatings. IJAE. 2010; 115: 127-33.
21. De Giglio E, Cometa S, Ricci MA, et al. Development and characterization of rhVEGF-loaded poly(HEMA-MOEP) coatings electrosynthesized on titanium to enhance bone mineralization and angiogenesis . Acta Biomaterialia 2010; 6:282-90.
22. De Giglio E, Cafagna D, Cometa S, et al. An innovative , easily fabricated, silver nanoparticle-based titanium implant coating: development and analytical characterization. Anal Bioanal Chem *in press*; doi 10.1007/s00216-012-6293-z
23. Niikura T, Tsujimoto K, Yoshiya S, et al. Vancomycin-impregnated calcium phosphate cement for methicillin-resistant *Staphylococcus Aureus* femoral osteomyelitis. Orthopedics 2007; 30: 320-1.
24. Mazza A. Ceftriaxone as short-term antibiotic prophylaxis in orthopedic surgery: a cost-benefit analysis involving 808 patients. J Chemother 2000; 12: 29-33.
25. Cometa S, Chiellini F, Bartolozzi I, et al. Surface Segregation Assessment in Poly(ε–caprolactone)-poly(ethylene glycol) Multiblock Copolymer Films. Macromol. Biosci. 2010; 10: 317–27.
26. Farin D, Piva GA, Gozlan I, et al. A modified HPLC method for the determination of vancomycin in plasma and tissues and comparison to FPIA (TDX) J Pharm Biomed Anal 1998; 18: 367-72.
27. Abdel-Hamid ME. FSQ spectrophotometric and HPLC analysis of some cephalosporins in the presence of their alkali-induced degradation products. Il Farmaco 1998; 53: 132-8.
28. Gigante A, Manzotti S, Bevilacqua C, et al. Adult mesenchymal stem cells for bone and cartilage engineering: effect of scaffold materials. Eur J Histochem. 2008; 52:169-74.
29. Trubiani O, Scarano A, Orsini G, et al. The performance of human periodontal ligament mesenchymal stem cells on xenogenic biomaterials. Int J Immunopathol Pharmacol 2007; 20:87-91.

TWO-STEP IMPRESSION/ INJECTION, AN ALTERNATIVE PUTTY/ WASH IMPRESSION TECHNIQUE: CASE REPORT

S. CAPUTI, G. MURMURA, B. SINJARI, G. VARVARA

Department of Medical, Oral and Biotechnological Sciences, Dental School, "G. d'Annunzio" University of Chieti–Pescara, Italy.

We here describe a new technique for making a definitive impression that we refer to as the two-step impression/ injection technique. This technique initially follows the classical one-step putty/ light-body impression technique with the polymerization of the putty and the light-body compound. This is then followed by the second step: injection of extra-light-body compound into the preparation through a hole in the metal stock tray. The aim of this additional step is to control the wash bulk and minimize the changes that can produce unfavorable impression results. This new two-step impression/injection technique allows displacement of soft tissues, such as the tongue, during the first seating of the putty and wash materials, while in the second step, the extra-light-body compound records all of the finer details without being compressed.

Impression techniques that use dual-phase materials, such as the putty and light-body impression technique, can be accomplished in one or two steps. In these one-step and two-step techniques, only the light-body compound should cover the entire preparation, although this cannot always be accomplished clinically (1,2). The classical two-step putty/ light-body impression technique has been reported to be more accurate than the 1-step putty/ light-body impression technique (2,3). In these two-steps, the light-body stage is carried out after the putty has polymerized and contracted; therefore, any further contraction of the light-body compound leads to minimal dimensional changes (4,5).

The one-step putty/ light-body impression technique has also been criticized because of the uncontrolled bulk of the light-body compound (6-13). By diminishing the volume of the polymerizing compound at each stage, the final contraction will also be reduced, and the accuracy of the impression can be improved (7). The putty in the one-step impression technique also tends to push the light-body wash off the prepared tooth, and thus critical areas, such as the finish line, can be covered by the putty, which cannot record details to a satisfactory level (2,8-11). For this reason, even studies where the one-step impression technique has been seen to be as accurate as the classical two-step impression technique, concerns have been raised about surface defects when using the one-step impression technique (9).

Another difficulty with the one-step impression technique is that once the light body is on the preparation, the putty needs to be brought into position and seated. During this critical phase, the patient's tongue or floor of the mouth can remove the light-body compound from the tooth. The classical two-step impression technique largely allows these problems to be overcome, but it can be associated with the creation of an occlusal step, as some light-body compound can spread along the occlusal surface during the reseating of the putty (10). Moreover, the light-body compound is displaced during this second step, and this can generate distortions that result in reduced dimensional accuracy of the impression. It has also been reported that the wash material can displace the preliminary putty impression during the seating, and afterwards, elastic recovery of the putty can occur upon removal of the impression, resulting in a tendency towards larger inter-abutment distances (9).

Considering the problems that can be associated with these techniques, although the classical two-step impression technique shows a number of advantages, further improvements to dimensional accuracy can be achieved with our novel two-step putty/ light-body impression/ injection technique. We recently described

Keywords: dimensional accuracy, impression technique, injection impression technique, vinyl polysiloxane.

Corresponding author: Giuseppe Varvara
Department of Medical, Oral and Biotechnological Sciences,
University "G. d' Annunzio" Chieti–Pescara
Via dei Vestini 31 66100 Chieti, Italy.
Tel: +39-0871-3554125
Fax: +39-0871-3554148
E-mail: gvarvara@unich.it

0393-974X (2012)

DISCLOSURE: ALL AUTHORS REPORT NO CONFLICTS OF INTEREST RELEVANT TO THIS ARTICLE.

the principles of this new two-step impression/ injection technique in an *in-vitro* study (12). In this previous study, the initial polymerization of the putty and the light-body compound was as for the classical one-step putty/ light-body impression technique, but this was followed by the injection of extra-light-body compound into the preparation through a hole in the metal stock tray. The aim of the present study is to present this alternative two-step putty/ light-body impression/ injection technique in the patient.

CASE DESCRIPTION

The following case report illustrates the use of this new definitive impression technique. A healthy 40-year-old patient came to the Department of Prosthetic Dentistry at the University "G. d'Annunzio" concerned about a restoration on the upper left first molar. Clinical examination and radiographic evaluation were performed. The proposed treatment plan include removing the existing restoration and some decay, followed by endodontic therapy and post-endodontic restoration. A supra gingival Chamfer (# 165 018; Komet, Lemgo, Switzerland) preparation of the margin was then performed (Figure 1A). A temporary crown was seated and an appointment for the impression taking was given for 3 weeks later.

The technique used for capturing the impression of the preparation involved the selection of a stock tray appropriate for the dental arch for the impression. First, a 1-step impression was performed, with the putty and light-body compound (Aquasil; Dentsply, York, Pa), simultaneously (Figure 1B). After removing the preliminary impression tray from the mouth, a hole was made through the polymerized compound with a carbide bur (187 023, Komet, Lemgo, Switzerland). This hole was positioned at the most coronal end (edge) of the prepared abutment, so as to coincide with one of the holes in the stock tray (Figure 2A). The selected hole on the stock tray was circled with ink to facilitate its identification during the following procedures, and a thin section of the inter-dental compound was taken off the impression using the same carbide bur (Figure 2B). After this, extra-light-body compound (Aquasil; Dentsply, York, Pa) was syringed onto the prepared abutment and the adjacent teeth, and into the preliminary impression. Then the impression tray was re-inserted in the same position. Further extra-light-body compound was placed in a syringe (Elastomer, ESPE Dental AG, Seefeld, Germany) and injected through the hole marked on the abutment (Figure 3), while holding down the impression tray, to prevent it from lifting off the teeth. The impression was left *in situ* to polymerize for the time period recommended by the manufacturer. The impression tray was then removed from the mouth and examined for accuracy (Figure 4).

DISCUSSION

In the present study, we can see that in the patient, this new two-step impression/ injection technique allows the displacement of soft tissues, such as the tongue, during the first seating of the putty and wash materials, while in the second step, the super-light-body compound records all of the finer details without being compressed. Another aspect that we believe will also be of advantage is that greater pressure can be created, forcing the super-light-body compound to penetrate into the gingival sulcus more easily. The disadvantage of this technique is that it is time-sensitive and requires coordination between the clinician and dental assistant for the injection of the extra-light-body compound. Also, overall, it is more time-consuming when compared to the classical two-step putty/ light-body impression technique. Despite these timing and time limitations, however, in the patient, this new two-step impression/ injection technique provides much greater

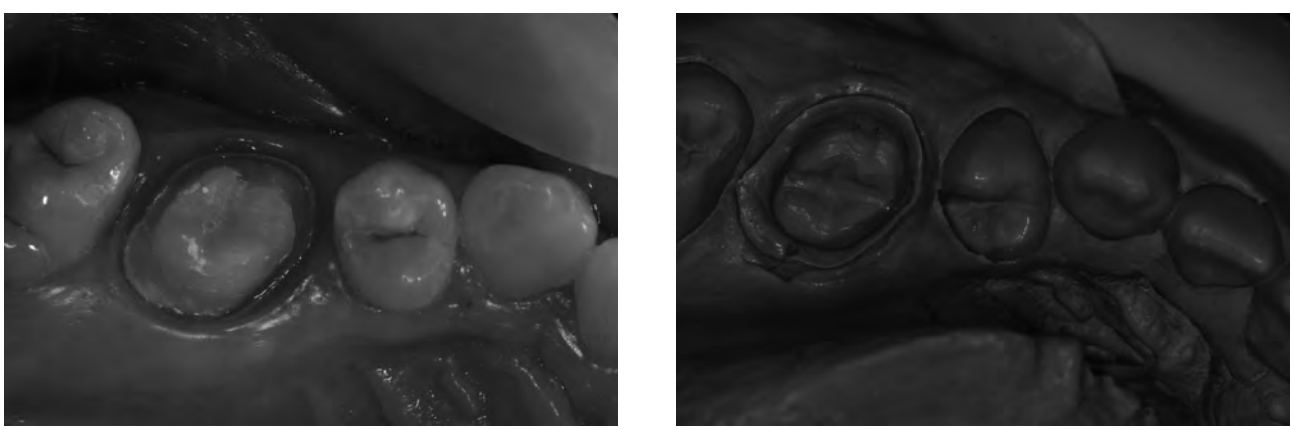

Fig. 1. *The dental preparation (A), and the preliminary impression (B).*

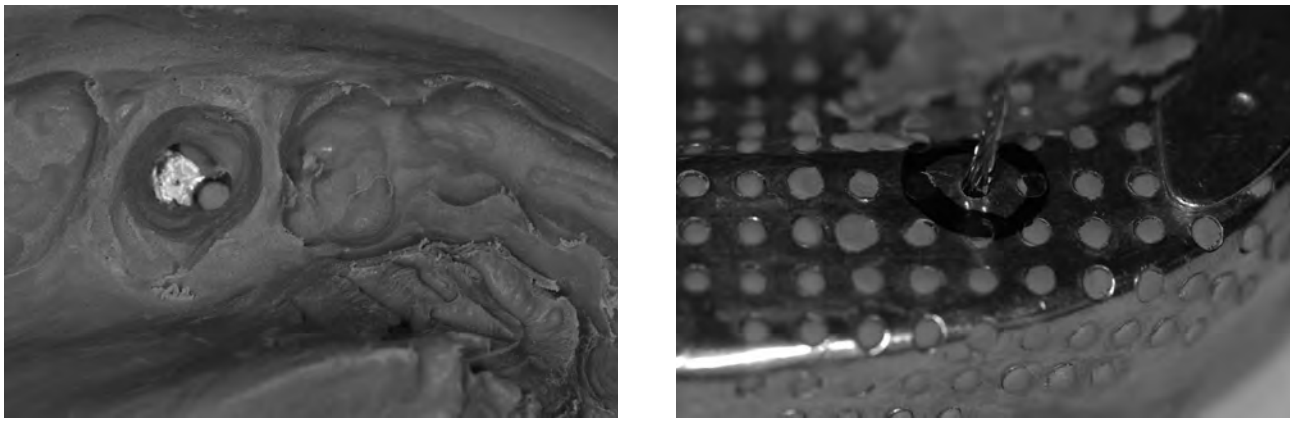

Fig. 2. *A hole is made in the impression compound (A) to correspond with a hole in the stock tray (B).*

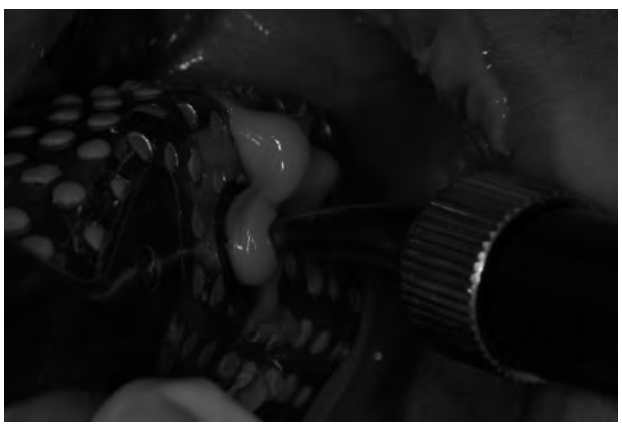

Fig. 3. *The extra-light-body compound is injected through the hole marked on the abutment.*

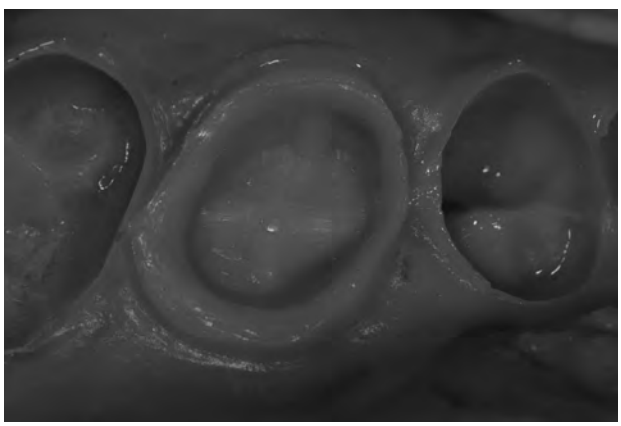

Fig. 4. *Detail of the definitive impression surface of one of the abutment teeth.*

accuracy in the recording of the details due to the use of the very fluid super-light-body compound. Moreover, there is no extra cost involved for the patient and for the clinic, in terms of the use of stock trays.

When making impressions, dimensional accuracy is crucial to the quality of the fixed prosthodontic treatment, and the impression technique is a critical factor that can affect the accuracy. This new two-step impression/injection technique appears to be the most dimensionally accurate impression method in terms of the resultant casts, and it allows a very precise dental prosthesis to be achieved.

ACKNOWLEDGEMENTS

The authors are grateful to Dr Christopher P. Berrie for critical reading of the manuscript.

REFERENCES

1. Hung SH, Purk JH, Tira DE, Eick JD. Accuracy of one-step versus two-step putty wash addition silicone impression technique. J Prosthet Dent 1992; 67:583-9.
2. Morgano SM, Milot P, Ducharme P, Rose L. Ability of various impression materials to produce duplicate dies from successive impressions. J Prosthet Dent 1995; 73:333-40.
3. Millar BJ, Dunne SM, Robinson PB. In-vitro study of the number of surface defects in monophase and two-phase addition silicone impressions. J Prosthet Dent 1998; 80:32-5.
4. Nissan J, Laufer BZ, Brosh T, Assif D Accuracy of three polyvinyl siloxane putty-wash impression techniques. J Prosthet Dent 2000; 83:161-5.

5. Eames WB, Sieweke JC, Wallace SW, Rogers LB Elastomeric impression materials: effect of bulk on accuracy. J Prosthet Dent 1979; 41:304-7.
6. Nissan J, Gross M, Shifman A, Assif D. Effect of wash bulk on the accuracy of polyvinyl siloxane putty-wash impressions. J Oral Rehabil 2002; 29:357-61.
7. Lewinstein I. The ratio between vertical and horizontal changes of impressions. J Oral Rehabil 1993; 20:107-14.
8. Chee WW, Donovan TE. Fine detail reproduction of very high viscosity poly(vinyl siloxane) impression materials. Int J Prosthodont 1989; 2:368-70.
9. Idris B, Houston F, Claffey N. Comparison of the dimensional accuracy of one- and two-step- techniques with the use of putty/wash addition silicone impression materials. J Prosthet Dent, 1995; 74:535-41.
10. Wu AY, Donovan TE. A modified one step putty-wash impression technique. J Prosthet Dent 2007; 98:245-46.
11. Chaimattayompol N, Park D. A modified putty wash vinyl polysiloxane impression technique for fixed prosthodontics. J Prosthet Dent 2007; 98:483-45.
12. Caputi S, Varvara G. Dimensional accuracy of resultant casts made by a monophase, one-step and two-step, and a novel two-step putty/light-body impression technique: An in-vitro study. J Prosthet Dent 2008; 99:274-81.
13. Raigrodski AJ, Dogan S, Mancl LA, Heindl H. A clinical comparison of two vinyl polysiloxane impression materials using the one-step technique. J Prosthet Dent 2009; 102:179-86.

LATE DEVELOPMENT OF A SUPERNUMERARY PREMOLAR IN A 17-YEAR-OLD FEMALE: TIMING OF MINERALIZATION AND MEDICOLEGAL CONSIDERATIONS

V. PINCHI[1], G. VARVARA[2,*], L. FARESE[1], GA. NORELLI[1]

[1]Departmental Section of Legal Medicine, University of Florence, Italy
[2]Department of Medical, Oral and Biotechnological Sciences, Dental School, "G. d'Annunzio" University of Chieti–Pescara, Chieti, Italy.

This report presents a case of a patient who developed a mandibular premolar supernumerary tooth after 14 years of age. Panoramic radiographs show the complete absence of the tooth (or tooth lacuna) at 14 years of age, and the crown as 50% developed at 17 years of age. The panoramic radiograph and computed tomography show dislocation of the roots of the adjacent teeth and a morphology similar to a premolar. Although the patient concluded the orthodontic treatment just before the premolar detection on any panoramic radiograph, the parents of the patient complained about the poor information received from the orthodontist.

Supernumerary teeth are generally defined as teeth formed in excess of the normal configuration and number (1, 2). Single or multiple supernumerary teeth occur more frequently in males than in females (3). They can occur in both arches, but different relative prevalences have been reported in the literature. Some studies have reported that the mandibular premolar area is most frequently affected (2), whilst others have described the highest recurrence of supernumerary teeth as pre-maxilla (4). Therefore, supernumerary premolars are more frequent as mandibular than maxillary, and lower supernumerary teeth mimic the normal shape and volume (5).

Supernumerary bicuspids start late in development and in the literature most reports have described cases of the development of supernumerary teeth in children aged between 7 and 14 years (1-5). Often the precise age of appearance of supernumerary teeth and their rate of development are not recorded due to a lack of close serial X-rays (1-5). Whenever neglected, the development of supernumerary teeth can cause complications, such as root resorption, impaction or malpositioning of the adjacent teeth, and cyst or ameloblastoma formation (6). Hence the age of the possible appearance of a supernumerary tooth and the rate of its mineralization are crucial points for clinicians to plan follow-up examinations and possible interventions.

Although the occurrence of supernumerary teeth is a phenomenon that is well reported in the literature, very few cases have focused on the late development of supernumerary teeth during adolescence (7). The present clinical case describes a supernumerary premolar that started development after the patient had reached 14 years of age. Two series of relatively close radiographic examinations allowed a description of the development timing from stage zero (absence of the tooth lacuna) to the stage of crown mineralized at 50%. This case risked a possible medicolegal claim, so the potential medicolegal issues connected with the appearance of such a supernumerary tooth after the conclusion of orthodontic treatment require specific discussion.

CASE REPORT

A 14-year-old female started orthodontic treatment for a malocclusion. The girl had her first menstruation when she was 12 years old, and the medical and familiar histories were unremarkable. A panoramic radiograph was requested by the orthodontist (Fig. 1), the dental arches were photographed, and the orthodontic procedure provided two arches of full bandage. After three years, when the orthodontic treatment was nearly at a conclusion, the patient went to an osteopath because of some pain in the lumbar region. A new panoramic radiograph was then requested, and a developing supernumerary tooth in

Key words: supernumerary tooth, late developing teeth, orthodontic patient information

Corresponding author: Giuseppe Varvara
Department of Oral, Nano and Biotechnological Sciences
"G. d'Annunzio" University of Chieti–Pescara
Via dei Vestini 31 66100 Chieti, Italy.
Tel: +39-0871-3554125
Fax: +39-0871-3554148
E-mail: gvarvara@unich.it

0393-974X (2012)

mandible region 34-35 was detected (Fig. 2). The tooth crown was shaped as a premolar and the roots of the adjacent teeth were remarkably diverging. The parents of the patient returned to the orthodontist complaining about the lack of information about the presence of the supernumerary tooth. The orthodontist retrieved the panoramic radiograph taken at the beginning of the treatment and explained that the tooth was actually not present at that time. The patient underwent computed tomography (Fig. 3) of the mandible and surgical removal of the tooth was performed without complications. The morphology of the tissues and the histological examination confirmed that they were dental tissues of a tooth.

DISCUSSION

This is a case report of the very late development of a supernumerary lower premolar in a healthy 17-year-old female. At 14 years of age, she had started orthodontic treatment that lasted for three years without any complications, and with the accomplishment of the foreseen results. Then, a panoramic radiograph taken at the age of 17 years revealed the presence of a supernumerary tooth developing in the mandible bone between the roots of the two bicuspids. However, this was not present in the panoramic radiograph taken when the patient was 14 years old. Applying the Moorees scale to assess the stage of dental mineralization, the supernumerary premolar was at stage C ½ (50% of the crown) in the second panoramic radiograph (8). According to Moorees et al., a normal regularly developing premolar crown takes an average of 2.5 years to mineralize from the earliest stages (the tooth lacuna) to stage C ½ in the case of a first premolar, and 1.5 years if it was a second premolar (9). As three years had passed between the first and second panoramic radiographs, the supernumerary tooth appeared to have undergone regular development.

At first glance, this finding is quite different from the case reported by Leonardi et al., who described the rapid development of a supernumerary premolar over nine months (10). Indeed, even in this previous case, the Authors indicated that a more accurate re-examination of the first panoramic radiograph revealed the thin band of dental enamel of the developing supernumerary tooth, so that the appearance of the tooth should be dated earlier.

Supernumerary teeth tend to start their development later than the normal corresponding teeth, and forming supernumerary premolars have been found in subjects aged between 11 and 16 years (4). Therefore, most case reports deal with supernumerary premolars that show an advanced or completed crown in patients younger than 14 years (5). Shneider et al. described two conical supernumerary teeth that erupted in a 16-year-old male, but neither the images nor the description of the case allow it to be inferred whether the teeth were forming or were indeed completely calcified (11). A supernumerary premolar was detected by Gibson in the panoramic radiograph of a 20-year-old female (12). Since the supernumerary bicuspid was completely calcified in the second panoramic radiograph, no discussion about the age when the formation started or the rate of the calcification was possible.

From this point of view, the present case appears relatively rare, as in this female subject, who had reached her puberty peak 2 years before, the supernumerary tooth started to form after 14 years of age. Furthermore, the tooth development appears to have proceeded at a regular

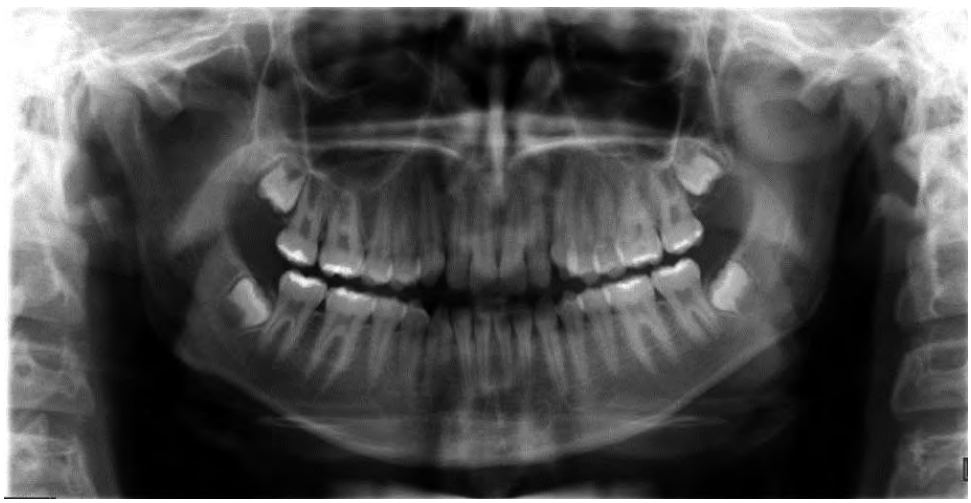

Fig. 1. *The panoramic radiograph taken before the orthodontic treatment (April 2009). The female patient was 14 years old at the time. No evidence of supernumerary teeth can be seen.*

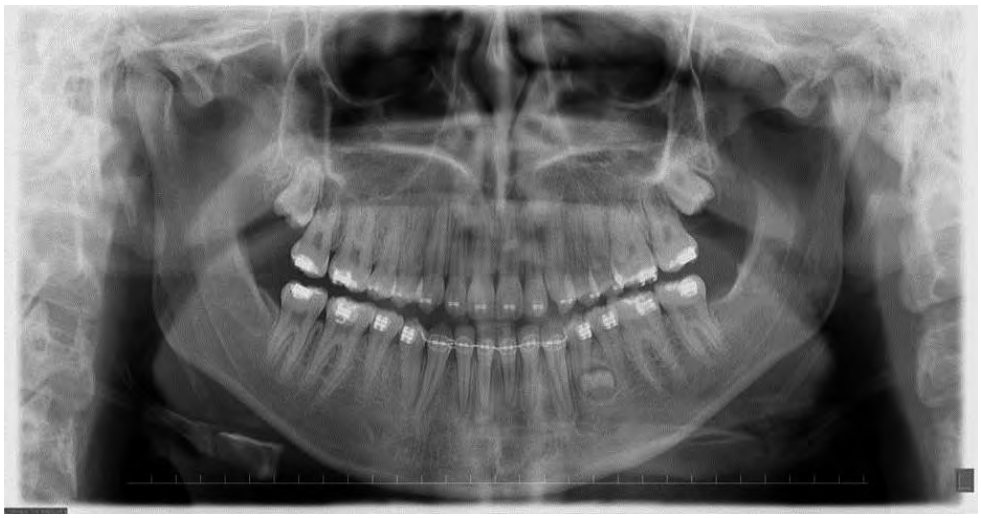

Fig. 2. *The second panoramic radiograph taken after three years (April 2012) reveals the late development of a mandibular supernumerary premolar. The tooth crown shows the early stages of calcification.*

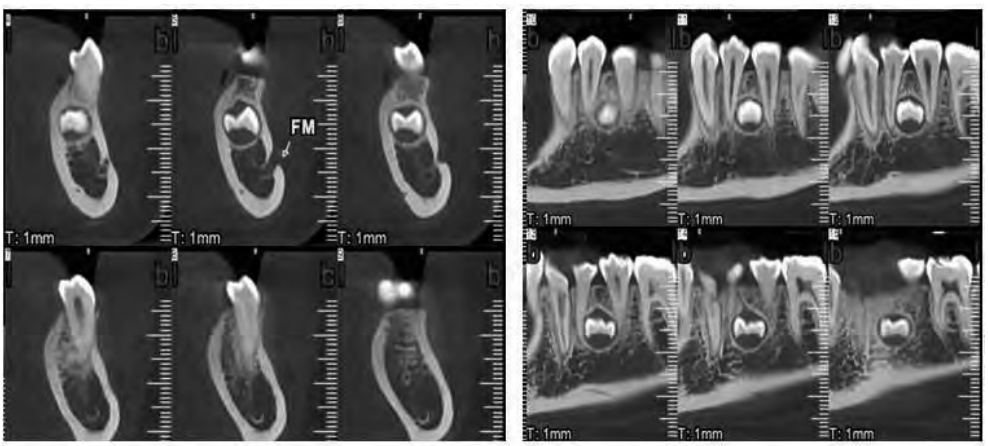

Fig. 3. *The computed tomography cross-sectional images show that the developing crown of the supernumerary premolar had a slight lingual displacement, and that it was moving the roots of the adjacent bicuspids without any remarkable evidence of root resorption. The crown was at a safe distance from the alveolar nerve emergence.*

rate, thus attaining only the first stage of crown formation by 17 years. Moreover, the moment of appearance of this supernumerary tooth was delayed until after the completion of all of the other teeth, except the third molars. In particular, all of the four premolars showed completely built apices in the first panoramic radiograph (Fig. 1). These findings suggest that it is not likely that the supernumerary tooth was the result of dycothomia of the dental tooth bud. On the contrary, the findings of a tooth with a shape and mineralization rate similar to a normal premolar are compatible with possible local hyperactivity in the dental lamina that resulted in post-permanent dentition. The tooth showed a very delayed formation time also with respect to the third molars, and it would have completed the root after the patient reached 25 years of age, as the average time needed for the regular development of a premolar is about 11 years (13).

The management of supernumerary teeth depends on the type, position and the decision whether or not to intervene, with surgical removal resulting from a balance between the possible surgical complications with those connected with the maintenance of the tooth and the periodic radiographic follow-up (14). In this case, no risk increase was deemed to be connected with the actual

germectomy of the supernumerary tooth, which was otherwise moving the adjacent roots.

The disclosure of this forming tooth left the parents of the patient astonished, who argued that this constituted *prima-facie* negligence on the part of the orthodontist. This comes with the assumption that the tooth was previously detectable and that the orthodontist had failed to correctly diagnose it and to properly inform the patient and her family. However, the re-examination of the panoramic radiograph taken before the orthodontic treatment and correctly maintained in the dental files of the patient allowed the demonstration of the occurrence of the rare and very delayed formation of the tooth, and thus to exclude any suspicions of misdiagnosis on the part of the dental practitioner. Furthermore, the abnormal tooth formation cannot have been even remotely foreseen by the orthodontist, so that no specific information had to be provided to the patient.

In this specific case, a detailed explanation supplied to the patient and her parents sufficed to avoid any dispute with the orthodontist, so that the relationship based on trust was quickly re-established and the patient is completing her orthodontic treatment. As reported in the literature that focuses on dental claims, this case demonstrates the need for the maintenance of good patient records, thereby allowing the dentist to explain fully what had happened during the treatment. This allowed full and proper communication with the patient, which can be a tricky point when there is the need to prevent or to better manage the possible of a conflict arising (15, 16).

REFERENCES

1. Meighani G, Pakdaman A. Diagnosis and managment of supernumerary (mesiodens): a review of the literature. J Dent 2010; 7:41-9
2. Jamwal RS, Sharma P, Sharma R. Late-developing supernumerary mandibular premolar: a case report. World J Orthod 2010; 11:94-8.
3. Alvira-González J, Gay-Escoda C. Non-syndromic: multiple supernumerary teeth: meta-analysis. J Oral Pathol Med 2012; 41:361-6
4. Cho SY, So FH, Lee CK, Chan JC. Late forming supernumerary tooth in the premaxilla: a case report. Int J Paediatr Dent 2000; 10:335-40
5. Cochrane SM, Clark JR, Hunt NP. Late developing supernumerary teeth in the mandible. Br J Orthod 1997; 24:293-6
6. Shah A, Hirani S, A late-forming mandibular supernumerary: a complication of space closure. J Orthod 2007; 34:168-72
7. Moore SR, Wilson DF, Kibble J. Sequential development of multiple supernumerary teeth in the mandibular premolar region - a radiographic case report. Int J Paediatr Dent 2002; 12:143-5
8. Panchbhai AS. Dental radiographic indicators, a key to age estimation. Dentomaxillofac Radiol. 2011; 40:199-212
9. Moorrees CF; Fanning EA, Hunt EE. Age variation of formation stages for ten permanent teeth. J Dent Res 1963; 42:1490- 502
10. Leonardi R, Barbato E. A late developing supernumerary premolar. J Clin Orth 2004; 38:331-2
11. Schneir MA, Sampson WJ. Supernumerary teeth: a review of the literature and four case reports. Aust Dent J 1997; 42:160-5
12. Gibson N. A late developing premolar supernumerary tooth. Aust Dent J 2001; 46:51-2
13. Corradi F, Pinchi V, Barsanti I, Garatti S. Probabilistic classification of age by third molar development: the use of soft evidence. J Forensic Sci. 2012 Jul 16. doi: 10.1111/j.1556-4029.2012.02216.x
14. Solares R, Roberto MI. Supernumerary Premolars: A Literature Review . Pediatric Dent 2004; 26:450-8
15. Mizrahi E. Risk Management in clinical practice. Part 7. dento legal aspects of orthodontic practice. Brit Dent J 2010; 209:381-90
16. Villari N, Norelli GA, Corridoni F, Minigrilli M Radiological investigation for expert and medico-legal purposes. Radiol Med 2003; 105:370-5.

MICROMORPHOMETRICAL AND HISTOLOGICAL ANALYSES USING TWO DIFFERENT OSCILLATING OSTEOTOMY TECHNIQUES COMPARED WITH CONVENTIONAL ROTARY OSTEOTOMY.

G. PERFETTI, I. DE TULLIO, D. BERARDI, D. DI IORIO, G. SPOTO, A. SCARANO

Department of Medical, Oral and Biotechnology Sciences, University of Chieti-Pescara, Chieti, Italy.

The recently introduced ultrasonic osteotome procedure is an alternative to conventional rotatory burs. The aim of this study was to establish the differences between two ultrasonic osteotomes and conventional rotatory burs, in order to perform micromorphological and histological analyses of osteotomized bone surfaces. Bony samples were taken from adult bovine ribs including both the cortical and marrow bone. Soft tissues have been removed and the bone pieces were divided into four groups, to test four devices: a conventional osteotomy round bur, a Lindeman bur and piezoelectric osteotomes ES007 and the T-Black. Each device performed cuts that were examined via scanning electron microscope (SEM) and light microscopy (LM) to check respectively cut precision and bone architecture all along the defect borders. SEM analysis of specimens showed that burs created defects of greater width and with irregular edges while those produced by ultrasonic osteotomes were narrow and had mostly smooth cutting surfaces. The edges of incisions made by drills were full of bone fragments while less bone chips were observed on piezoincision's ones. Dimensions of fragments were wider if cuts were made by burs too. LM analysis of samples showed focally, delicate bony trabecules crushed and pressed into the bone marrow in cutting made by burs. Samples cut by ultrasonic devices showed small or no smear layer and only partial or no crushed trabecules. Osteocytes seemed to be intact all along the cutting surface in all samples observed. In the present study, according to literature, ultrasonic surgery's validity is confirmed. As a matter of fact, the greater the number of bone chips products, the greater the magnitude of the inflammatory process induced, as well as the possibility of a greater bone loss and delay in wound healing near the osteotomized area.

Ultrasonic surgery uses modulated ultrasonic vibration to let controlled cutting of bony structures (1). The main advantages of piezosurgery include soft tissue protection, optimal visibility in the surgical field, decreased blood loss, less vibration and noise, increased comfort for the patient and protection of tooth structure. To date it has been indicationed for use in oral and maxillofacial surgery, otorhinolaryngology, neurosurgery, ophthalmology, traumatology and orthopaedics (2). The aim of the study was to establish the differences between two ultrasonic osteotomes and conventional rotatory burs in order to perform micromorphological and histological analyses of osteotomized bone surfaces(3). Qualitative analysis evaluated these parameters: cutting precision, presence of fragments / debris (3,4), architectural integrity of the bone and osteocytes adjacent to the cutting area. Quantitative analysis evaluated these parameters: thickness of the smear layer and bone density percentage of debris on the cut surface.

METHODS

Forty four fresh bony samples were taken from ten adult bovine ribs collected within 1 h post-mortem (4). The samples included both the cortical and marrow bone. Soft tissues have been removed (connective tissue and periosteum) and then samples have been stored for 1-2 days at a temperature of 4 ° C. These were cut along the major axis and then along the minor axis, to obtain 48 pieces of rectangular shape having dimensions of width and height respectively 2cm x 1cm and thickness comprising the two cortical and medulla. The bone pieces were divided into four groups, each group consisting of twelve samples. The cuts were conducted at a distance of 0.5 cm between them and from the lateral margins of the sample, at the depth necessary for reaching up to the bone marrow and in order to cover the

Key words: piezosurgery, osteotomy, histological analysis, micromorphometrical, bone chips

Corresponding auhor:
Prof Scarano Antonio
Department of Medical, Oral and Biotechnology Sciences
University of Chieti-Pescara, Chieti, Italy
tel: 08713554100-08713554099
email ascarano@unich.it

0393-974X (2012)

DISCLOSURE: ALL AUTHORS REPORT NO CONFLICTS OF INTEREST RELEVANT TO THIS ARTICLE.

entire cortex. So we obtained thirty-six cuts for each group. The four groups correspond to four different instruments tested in this study: a conventional osteotomy round bur (Komet, Lemgo, Germany), a Lindeman bur (Komet, Lemgo, Germany) (both used on low-speed hand piece and under constant irrigation) (5) and piezoelectric osteotomes ES007 and the T-Black (the same device ES007 covered in medical polished steel) (ESACROM Surgysonic Moto®). Piezoelectric osteotomes were used under constant irrigation of sterile and refrigerated (4-6°C) saline solution and power and vibration were set respectively to 40 (according to the scale set by the device) and 80 microns (Figure 1). Each device performed three cuts for sample (Figures 2, 3, 4, 5). The samples obtained were fixed in a volume of 10% buffered formalin (4) equal to approximately 5 times its own, for about 18 to 24 hours. The prepared surfaces were examined via scanning electron microscope (SEM) (6) and light microscopy (LM) to check respectively cutting surfaces and cut precision and bone architecture all along the defect borders.

18 histological sections for each instrument were set up to be monitorated at Light Microscope (LM) (Leitz LABORLUX S, Binocular Microscope, Leica, Germany), and 18 samples per instrument to be analyzed at the Scanning Electron Microscope (SEM) (Ages 50 XVP The B6, Carl Zeiss SMT Ltd., Cambridge, UK).

RESULTS

Qualitative analysis

SEM analysis of specimens showed that round burs created defects of greater width and with irregular edges. The edges of incisions made by this drill were full of bone chips and theirs dimensions were wide (Figures 6, 7) . Already looking at the image at low magnification, it's possible to see that round bur has imprinted on cortical grooves (Figure 6). LM analysis of samples showed focally, delicate bony trabecules crushed and pressed into the bone marrow in cutting made by round burs. At higher magnification on the irregular cutting surface was possible to detect fragments of cortical bone and a layer of altered and compressed bone (approximately 45 micron), so as to make osteocytes little discernible (Figure 8). Perpendicular sections to the cutting surface confirmed the presence of bone chips and an irregular surface (Figures 9 and 10). At higher magnification (40x) it is possible to detect portions of torn bone (Figure 10). Finally, always at higher magnification, it is visible a portion of altered bone, with thickness of about 7-8 microns (Figures 11 and 12).

SEM images of sections obtained with the Lindemann bur have detected a cutting surface more regular when compared with that obtained by the cutting of the round bur. The cutting edges are surrounded by cortical bone chips and torn bone (Figure 13). At higher magnification is also visible compression bone generated by the bur during cutting and debris of modest size (Figure 14). LM analysis of samples showed focally, delicate bony trabecules crushed and pressed into the bone marrow but no damaged osteocytes (Figure 15).

Both sections made parallel or perpendicularly showed smear layer on the cutting surface which amount respectively 15 microns and 10 microns (Figures 15, 16).

Samples cut by ultrasonic devices showed more clear and regular edges (cortical ones), free from bone chips (Figures 17, 18, 19, 20). At higher magnification, samples cut by the T-Black osteotome showed the structure of a small blood vessel preserved in its integrity (Figure 20). Under LM samples cut by ultrasonic devices showed only partial or no crushed trabecules and intact osteocytes all along the cutting surface as in all sample observed (Figures 21, 22).

However, samples made by T-Black osteotome, already at low magnification, showed a very thin smear layer on the surface of cortical bone, with thickness of a few microns (about 6-7 microns) (Figure 22). Finally, cutting analyzed in histological perpendicular sections, has revealed smooth and clear edges: there were no bone chips or debris and no crushed trabecules (Figures 23, 24, 25).

Statistical analysis

Analysis of Variance (ANOVA) and, for multiple comparisons, the Bonferroni test were used to analyze data relating to the percentages of debris on each cutting surface (Table I). Figure 26 shows the percentages of bone chips on surfaces cut by different devices, each analyzed at both low and high magnification. There were statistical differences between the percentage of debris created by the two piezoelectric inserts ($P < 0.05$) as well as between the two burs used ($P < 0.05$). Even pair wise comparisons between the different instruments showed statistical differences ($P < 0.05$). In particular, the round bur generated the highest percentage of debris, followed by Lindemann one and, finally, by the piezoelectric inserts, ES007 and then the T-Black one. Figures 27 and 28 show graph about smear layer thickness in respectively parallel LM sections and perpendicular ones.

DISCUSSION

The results reported in this work are consistent with most of the data currently available in the international literature (5, 7, 8). In fact a certain superiority of piezosurgery is showed in the early stages of the healing process of a wound made with the Ultrasonic Surgery Device compared to conventional rotary instruments, both applied in the field of Bone Surgery (8, 9, 10,11,12). This improvement in healing phase is due to the greater precision and regular cut that allow to obtain less or no

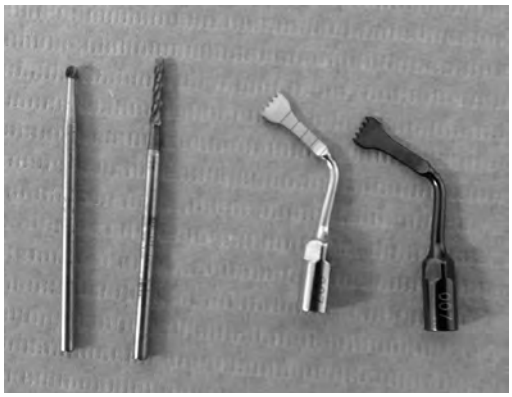

Fig. 1. *From left: round bur, Lindemann bur, piezoelectric insert ES007, piezoelectric insert T-Black.*

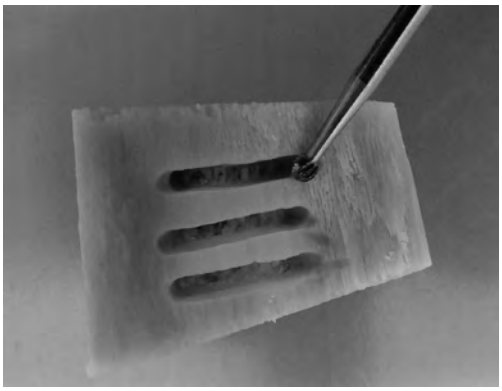

Fig. 2. *Execution of the cuts with round bur.*

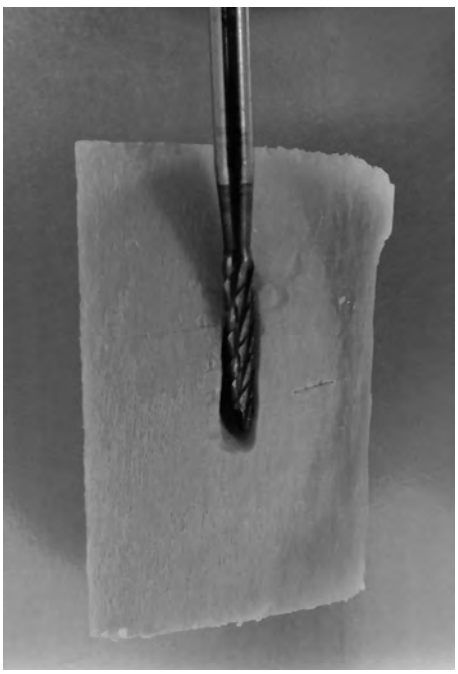

Fig.3. *Execution of the cuts with Lindemann bur.*

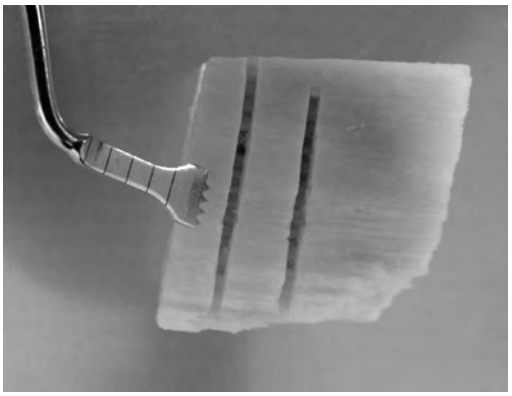

Fig. 4. *Execution of the cut with ES007.*

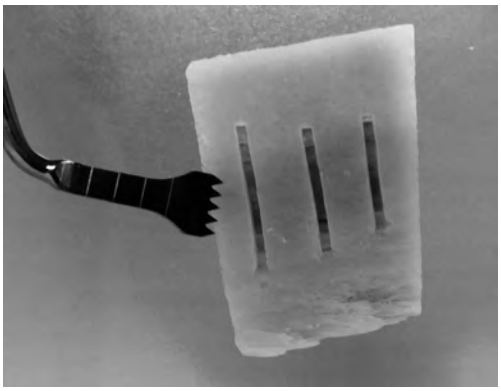

Fig. 5. *Execution of the cut with ES007 T-Black.*

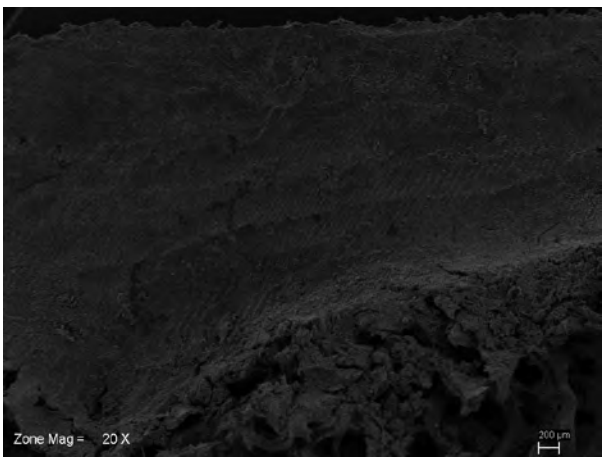

Fig. 6. *Round bur: SEM low magnification.*

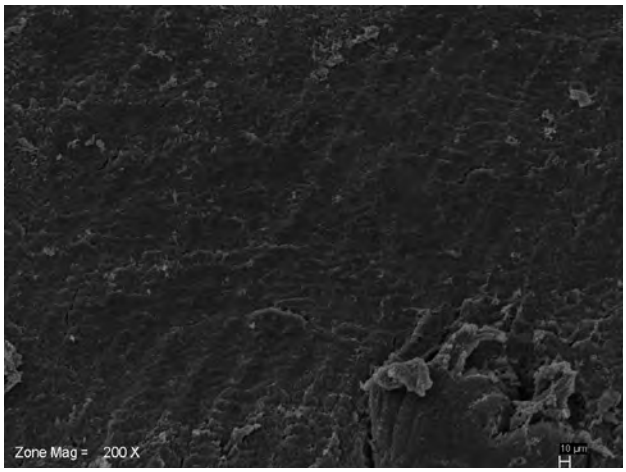

Fig. 7. *Round bur: SEM high magnification.*

Fig. 10. *Round bur, LM image, perpendicular section, high magnification (40x).*

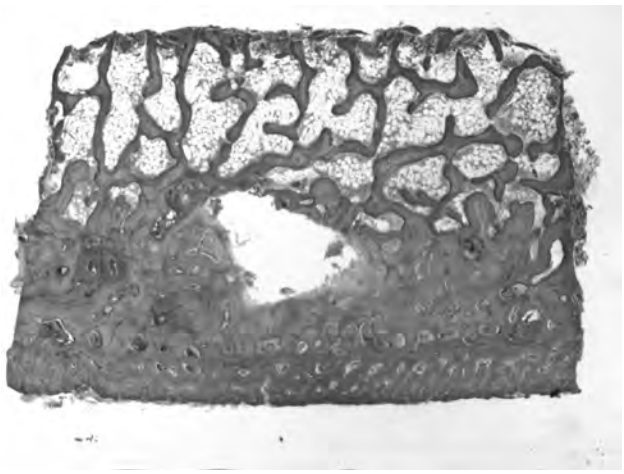

Fig. 8. *Round bur: LM image.*

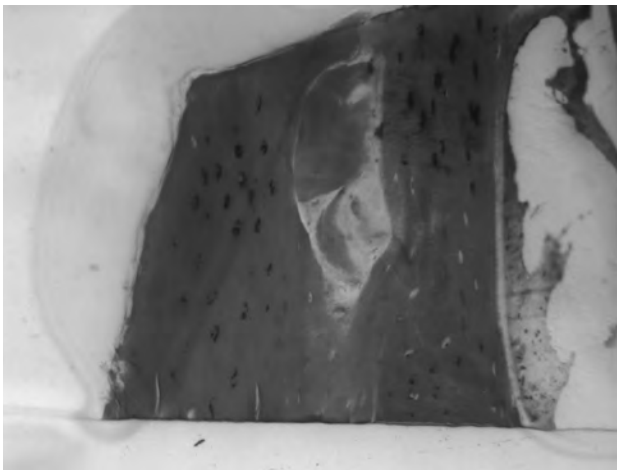

Fig. 11. *Round bur, particular of figure 10.*

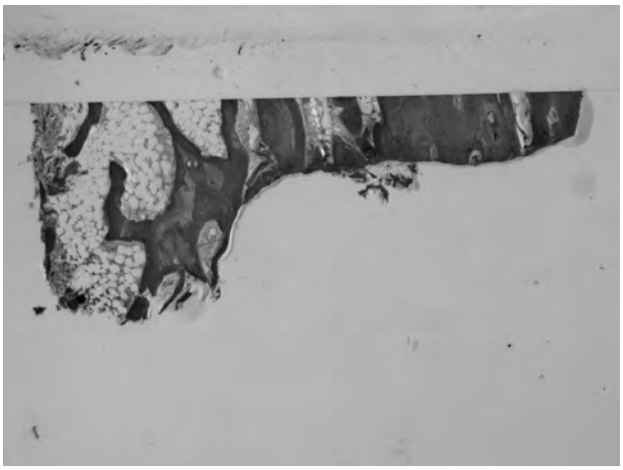

Fig. 9. *Round bur, LM image, perpendicular section.*

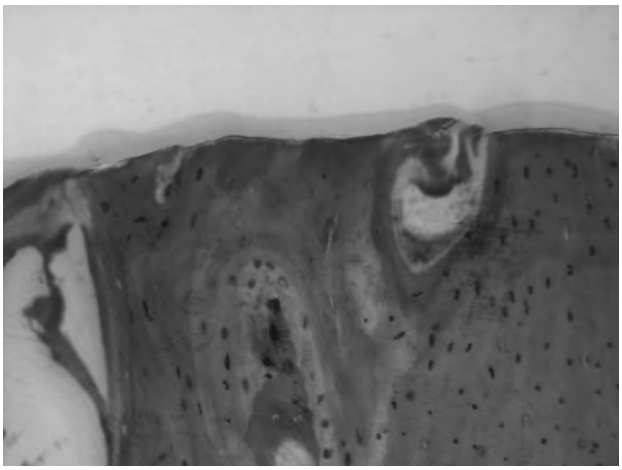

Fig. 12. *Round bur, particular of figure 10.*

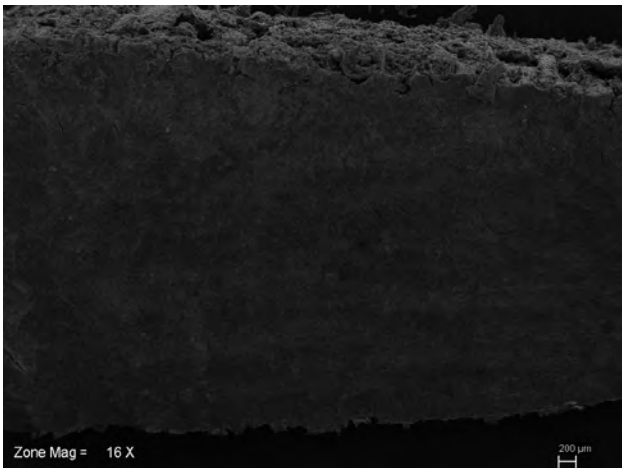

Fig. 13. *Lindemann bur, SEM low magnification.*

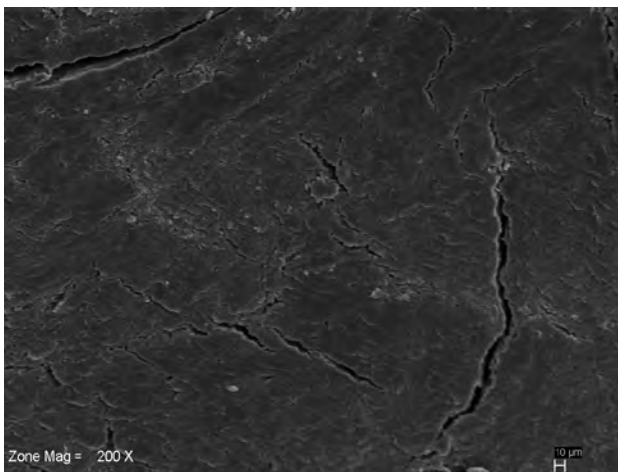

Fig. 14. *Lindemann bur, SEM high magnification.*

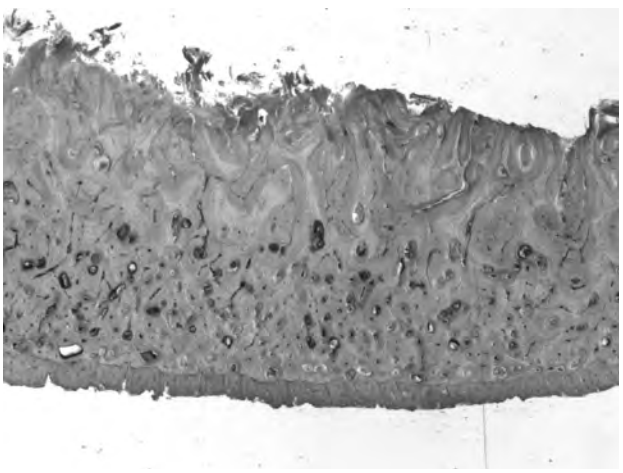

Fig. 15. *Lindemann bur: LM image.*

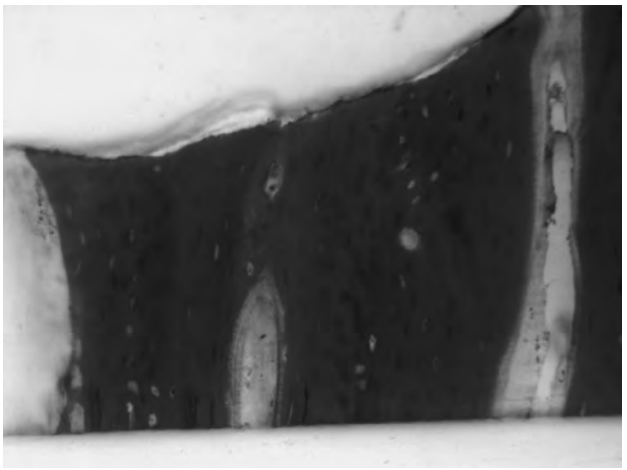

Fig. 16. *Lindemann bur: LM image, perpendicular section.*

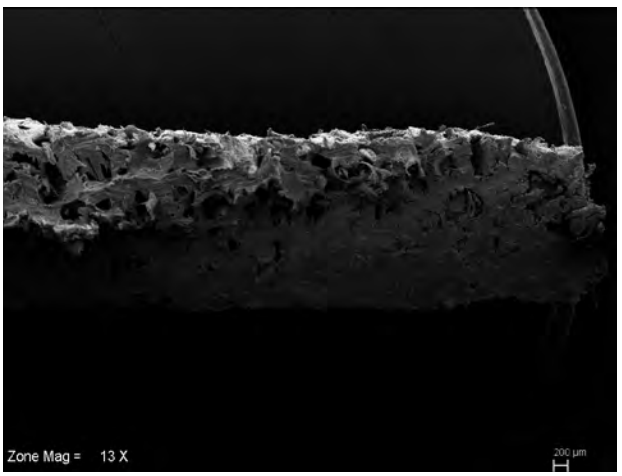

Fig. 17. *Piezoelectric osteotome ES007, SEM low magnification.*

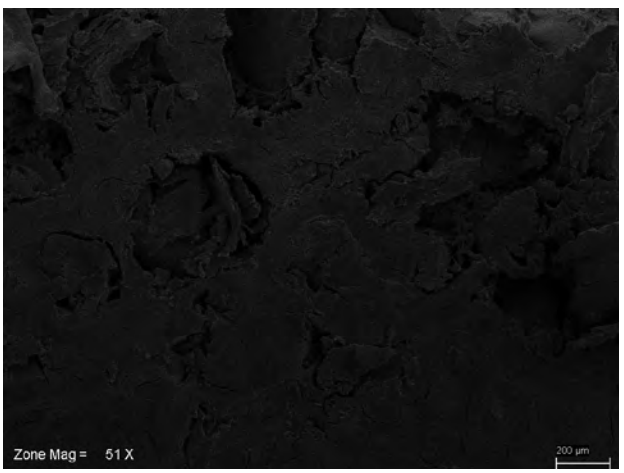

Fig. 18. *Piezoelectric osteotome ES007, SEM high magnification.*

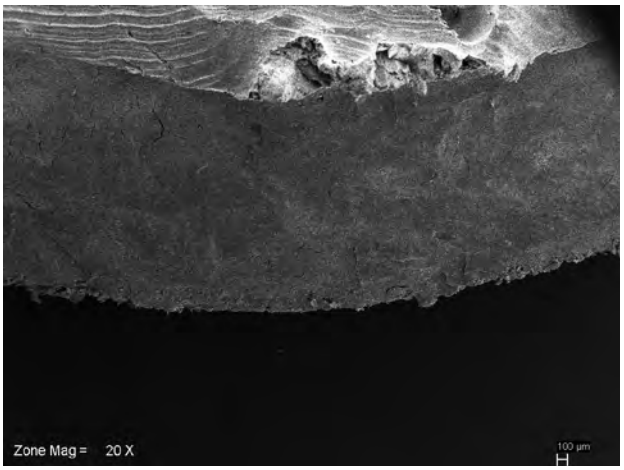

Fig. 19. *Piezoelectric osteotome ES007 T-Black, SEM low magnification.*

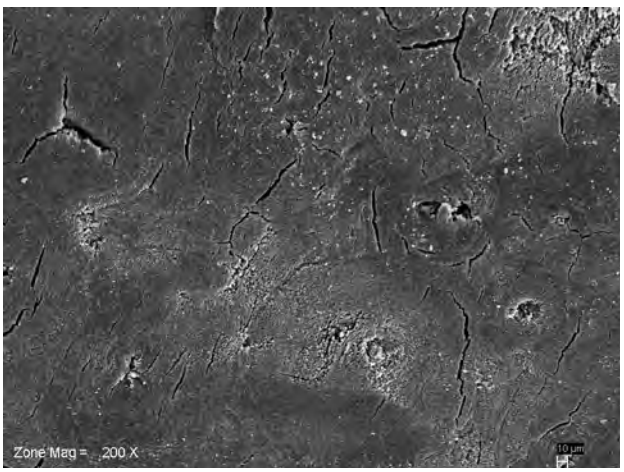

Fig. 20. *Piezoelectric osteotome ES007 T-Black, SEM high magnification.*

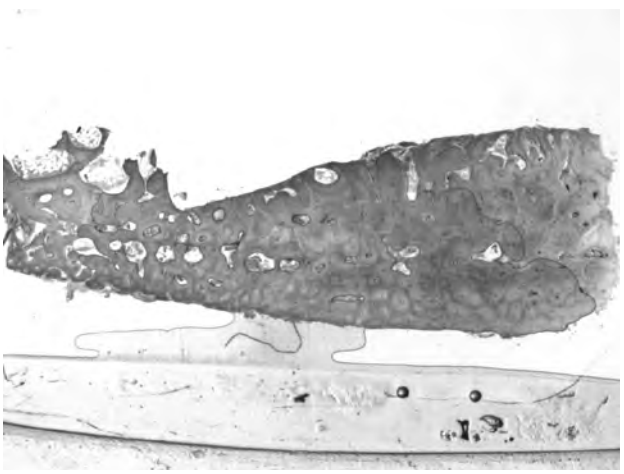

Fig. 21. *Piezoelectric osteotome ES007, LM low magnification.*

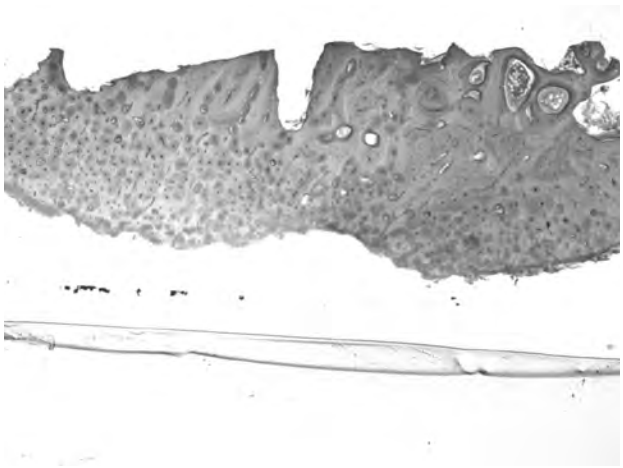

Fig. 22. *Piezoelectric osteotome ES007 T-Black, LM low magnification.*

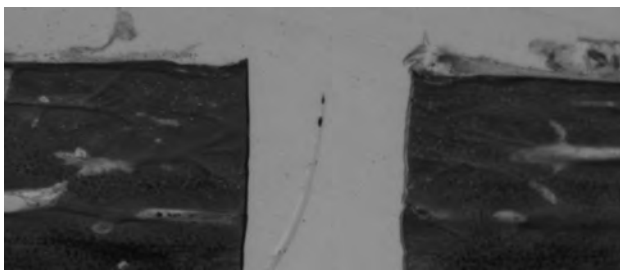

Fig. 23. *Piezoelectric osteotome ES007, LM perpendicular section.*

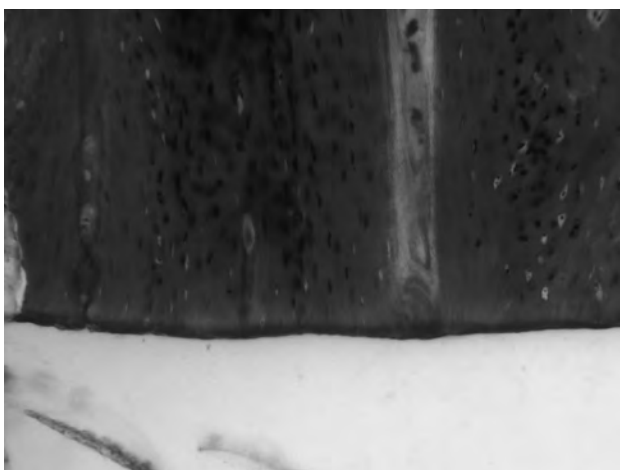

Fig. 24. *Piezoelectric osteotome ES007, LM perpendicular section.*

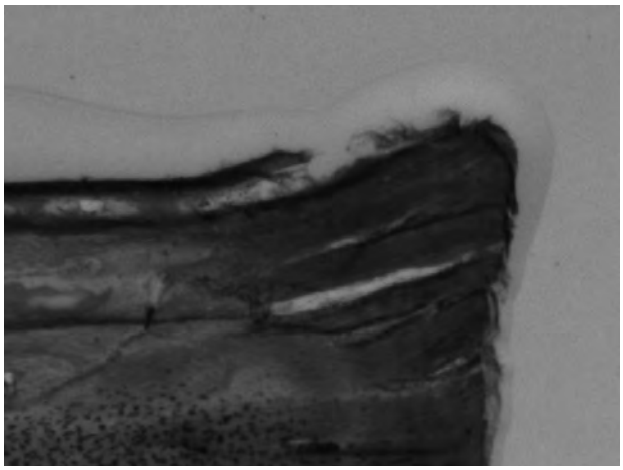

Fig. 25. *Piezoelectric osteotome ES007 T-Black, LM perpendicular section.*

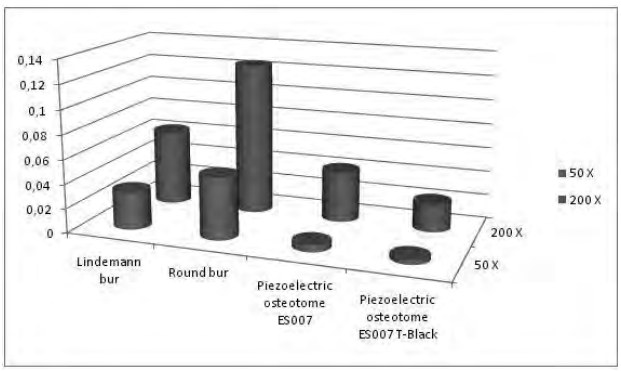

Fig. 26. *Graph of the percentage of debris.*

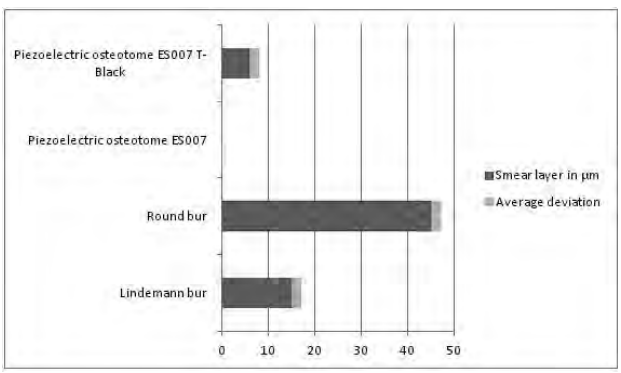

Fig. 27. *Graph about smear layer thickness in parallel LM sections.*

bone chips. Therefore it can be concluded that the greater the number of bone chips producted, the greater the magnitude of the inflammatory process induced (due to the stimulation of macrophage cells by such small fragments), as well as the possibility of a greater bone loss and delay in wound healing bone near the osteotomized surfaces.

Preti ‘s study has provided us with the concrete

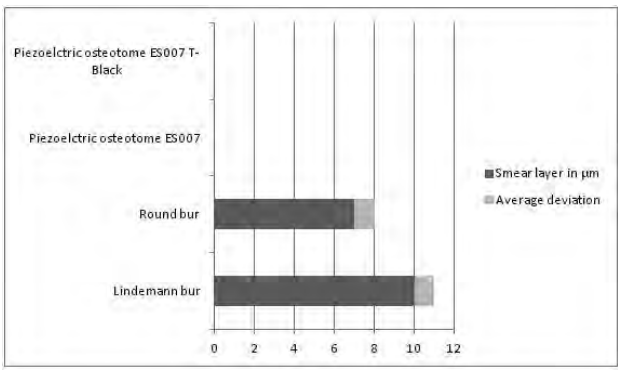

Fig. 28. *Graph about smear layer thickness in perpendicular LM sections.*

explanation at the best healing process that can be obtained with the instrument piezoelectric (10). Biomolecular analysis has shown that, in addition to the greater degree of bone morphogenetic proteins and the transforming growth factor (TGF)-BETA2 (components useful to repair bone in the samples treated with the piezosurgery), it was possible to obtain also a lower amount of pro inflammatory cytokines acting as TNF-alpha and interleukins -1 and -10, compared to samples treated with drills (10). These results lead us to conclude that the new method is more efficient in controlling inflammatory processes and in promoting bone healing in the early stages, because it stimulates tissue remodeling within the first 56 days of treatment (10). The improved process of healing around the surgical site prepared with the Ultrasonic Surgery Device is due to the extreme regularity of cutting edges, so as to respect the bony architectural (13, 14). In fact, even the histological sections of this study demonstrate the integrity of the osteocytes, perfectly cut by the instrument, without damage or lacerations.

In the present study, according to literature, ultrasonic surgery‘s validity is confirmed and it was possible to highlight the many benefits of using the Ultrasonic Device in bone surgery procedures. These consist essentially of a better quality of the cut made by the instrument in terms of precision and regularity, as it has allowed the creation of sharp edges, precise, smooth and free of bone debris. These characteristics allow less traumatic cut of tissues, faster healing and less bone remodeling near the cutting edges. In particular there were statistical differences between the two burs taken into consideration: the cutter of Lindemann appears to be more precise and effective in giving a clean cut. There were significant differences even between the two piezoelectric inserts and both were significantly superior compared to the drills: these are able

to ensure a more precise and clear cut and, in particular, the T-Black allowed greater accuracy of all the tools taken into consideration.

REFERENCES

1. Eggers*G, Klein J, Blank J, Hassfeld S. Piezosurgery®: an ultrasound device for cutting bone and its use and limitations in maxillofacial surgery. British Journal of Oral and Maxillofacial Surgery (2004) **42**, 451—453.
2. Pavlı´kova´ G, Folta´n R, Horka´ M, Hanzelka T, Borunska´ H, S˘edy´: J. Piezosurgery in oral and maxillofacial surgery. Int. J. Oral Maxillofac. Surg. 2011; 40: 451–457.
3. Heinemanna F, Hasanc I, Kunert-Keila C, Götzd W, Gedrangea T, Spassova A, Schweppea J, Gredesa T. Experimental and histological investigations of the bone using two different Oscillating Osteotomy techniques compared with conventional rotary osteotomy. Ann. Anatomy (2011), doi:10.1016/j.aanat.2011.10.005.
4. Romeo U, Del Vecchio A, Palaia G, Tenore G, Visca P, Maggiore C. Bone damage induced by different cutting instruments-an in vitro study. Braz Dent J. 2009;20(2):162-8.
5. Hollstein S, Hoffmann E, Vogel J, Heyroth F, Prochnow N, Maurer P. Micromorphometrical analyses of five different ultrasonic osteotomy devices at the rabbit skull. Clin. Oral Impl. Res xx, 2011; 000–000 doi: 10.1111/j.1600-0501.2011.02185.x
6. Trubiani O, Fulle S, Traini T, Paludi M, La Rovere R, Orciani M, Caputi S, Piattelli A. Functional assay, expression of growth factors and proteins modulating bone-arrangement in human osteoblasts seeded on an anorganic bovine bone biomaterial. Eur Cell Mater 2010; 20:72-83.
7. Siervo S, Ruggli-Milic S, Radici M, Siervo P, Jager K. Piezoelectric surgery. An alternative method of minimally invasive surgery. Schweizer Monatsschrift fu¨r Zahnmedizin 2004; 114:365–377.
8. Stübinger S, Kuttenberger J, Filippi A, Sader R, Zeilhofer HF. Intraoral piezosurgery: preliminary results of a new technique. J Oral Maxillofac Surg 2005; 63(9):1283-7.
9. Doan N, Reher P, Meghji S, Harris M et al. In vitro effects of therapeutic ultrasound on cell proliferation, protein synthesis, and cytokine production by human fibroblasts, osteoblasts, and monocytes. J Oral Maxillofac Surg 1999; 57(4):409-19; discussion 420.
10. Preti G, Martinasso G, Peirone B, Navone R, Manzella C, Muzio G, Russo C, Canuto RA, Schierano G. Cytokines and growth factors involved in the osseointegration of oral titanium implants positioned using piezoelectric bone surgery versus a drill technique: a pilot study in minipigs. J Periodontol 2007; 78(4):716-22.
11. Vercellotti T, Nevins ML, Kim DM, Nevins M, Wada K, Schenk RK, Fiorellini JP. Osseous response following resective therapy with piezosurgery. Int J Periodontics Restorative Dent 2005: 25: 543–549.
12. Trisi P, Carlesi T, Colagiovanni M, Perfetti G. Implant Stability Quotient (ISQ) vs direct in vitro measurement of primary stability (micromotion): effect of bone density and insertion torque" J Osteol Biomat 2010; 1:141-151.
13. Horton JE., Tarpley TM. Jr, Wood LD. The Healing of Surgical defects in Alveolar Bone with Ultrasonic Instrumentation, Chisel and Rotaryn Bur. Oral Surg Oral Med Oral Pathol 1979; 39:536-546.
14. Di Alberti L, Donnini F, Di Alberti C, Camerino M. A comparative study of bone densitometry during osseointegration: piezoelectric surgery versus rotary protocols. Quintessence Int 2010; 41(8):639-44.

SUBJECTIVE PAIN RESPONSE TO TWO ANESTHETIC SYSTEMS IN DENTAL SURGERY: TRADITIONAL SYRINGE VS. A COMPUTER CONTROLLED DELIVERY SYSTEM

R. PATINI[1], V. COVIELLO[2], L. RAFFAELLI[1], P.F. MANICONE[1], S. Z. DEHKHARGANI[1], F. VERDUGO[3], G. PERFETTI[4], A. D'ADDONA[1]

[1]Department of Oral Sciences, Catholic University, Rome, Italy.
[2]Department of Oral and Maxillofacial Sciences, "Sapienza" University of Rome,Rome, Italy.
[3]VA Hospital, Greater Los Angeles. Private Practice Altadena, Los Angeles, CA, USA.
[4]Department of Oral Sciences, University of Chieti, Italy.

The present study was conducted to evaluate human pain perception at different phases of dental surgery using a computer controlled device, the Single Tooth Anesthesia System (STA System®), versus the traditional syringe technique. One hundred healthy patients participated in this single-blind split-mouth design study. Individuals provided pain ratings at needle insertion, delivery of anesthetic solution and tooth extraction via a numeric visual rating scale or NVRS. The anterior middle superior alveolar, or AMSA, injection was compared with traditional syringe injections in maxillary quadrants. NVRS scores for AMSA were significantly lower for the STA System® when compared to traditional syringe technique at needle insertion, delivery of anesthetic solution ($p<0.0001$) and also during tooth extractions ($p=0.0002$). A higher percentage of patients (23%) required a second injection after the traditional syringe technique. Subjects reported having less clinical pain with AMSA injection at every step of the dental surgery. The STA System® combines an anesthetic pathway and controlled flow rate resulting in virtually imperceptible needle insertion and injection, and a rapid onset of profound anesthesia. NVRS scoring system facilitated patient comprehension in assessing pain value and intensity experienced. The two anesthetic delivery techniques were therapeutically equivalent for maxillary injections but AMSA/computer controlled protocol significantly minimizes subjective pain perception at needle insertion, anesthetic delivery and during tooth extraction.

Local anesthesia and pain control is one of the most important elements of dentistry, and particularly dental surgery. Fear of dental injections is a common event reported by patients (1-3). This fear can be a significant impediment to dental care because it frequently causes patients to delay or even avoid treatment (4). Pain arises from mechanical trauma of needle insertion into the site of injection, or from sudden tissue distension that follows a rapid anesthetic discharge. Pain can also be caused by the stimulation of the first few drops of the local anesthetic (5,6). Contrary to conventional ideas, needle tissue penetration is not the primary reason for pain. The anesthetic volume injected and tissue pressure is the main cause of distress and pain (7). Nevertheless, the administration of local infiltrations by conventional syringe injection is still the most common method used in dentistry to deliver the anesthetic. Recently, a precision-metered dental injection system called the STA System® (Milestone Scientific, Livingston, NJ) has become available. This system is the latest computer-controlled local anesthetic delivery system that provides a precise injection flow-rate regardless of tissue resistance. The delivery process starts from a conventional 1.8 ml anesthetic cartridge through a plastic micro-tubing into a plastic handle where a luer-lok connecting needle is attached. The anesthetic flow is computer-controlled and initiated by exerting pressure on a foot pedale. The pump allows administration of local anesthetic at three slow but constant rates, and the computer compensates for variation in resistance to flow (5,7). During needle insertion, continuous positive pressure yields a constant anesthetic drip that precedes the needle. The combination

Key words: tooth extraction; syringes; anesthesia; analogue pain scale; pain measurement.

Mailing address:
Dr L. Raffaelli
Catholic University of the Sacred Heart
Department of Oral Sciences
Largo A.Gemelli, 8
00168 Rome, Italy – Fax +39 06 30154079
E-mail: lraffaelli@rm.unicatt.it

0393-974X (2012)

of an anesthetic pathway and a controlled flow rate results in virtually imperceptible injections, rapid anesthesia onset (7) and decreased patient anxiety levels (4,8). The theory behind it is that when administered slowly, the drops of solution anesthetize the tissue ahead of the needle, thereby yielding a virtually painless process (4,7,8). All techniques of local intraoral anesthesia, such as maxillary and mandibular infiltrations, mandibular block (9), intraligamentary (10), anterior middle superior alveolar (AMSA) injection (11), and anterior superior alveolar (ASA) injection (12) can be performed with the STA System®. Maxillary teeth extending from the central incisor to mesiobuccal side of the first molar, and the associated palatal tissue, can be anesthetized with AMSA injection (13).

The aim of this single-blinded split-mouth design study is to compare traditional syringe technique versus computer-controlled STA® anesthetic System to evaluate pain perception at needle insertion, delivery of local anesthetic solution and during tooth extraction, in patients requiring at least two tooth extractions on opposite sides of the maxilla.

MATERIALS AND METHOD

One hundred adult patients (52 men and 48 female) who needed at least two dental extractions on both left and right maxillary arches participated in this single-blind study at the Department of Oral Sciences, Catholic University of Sacred Heart, Rome, Italy, from March 2010 through October 2011. They were systemically healthy and had no contraindications to local anesthetics. Patients were not taking any medications that would alter pain perception, as determined by a written medical health form and oral questionnaire. Pregnant females were not included in the present study. All study subjects volunteered to participate and verbal informed consents were obtained prior to inception. This study was conducted in accordance with the Helsinki Declaration of 1975, as revised in 2000. Patients were informed that a computer controlled and traditional syringe techniques would be used for their dental procedures. All patients had previously experienced a conventional syringe technique and none had received the STA® injection.

Pain ratings were explained to patients before injections. NRS, VRS and Visual Analogue Scale (VAS) systems are the most common pain rating scales used to evaluate patients' painful sensation and behaviors in research studies (15,16,26-29). Pain differences at needle insertion, delivery of local anesthetic solution and during tooth extractions were analyzed using a pain scale (30-32) based on Numeric Rating Scale (NRS) and Verbal Rating Scale (VRS) named Numeric Verbal Rating Scale (NVRS). Pain level descriptions were as follows: 0= no pain; 1-3= minimal pain; 4-6= mild pain; 7-9= severe pain; 10= worst pain possible. Every verbal expression is graphically linked to a range of three numeric values (Figure 1).

One half of the maxilla was anesthetized using the STA® system and the contralateral half by a traditional infiltration approach following the AMSA technique. Anesthesia was administered by the same experienced operator. The order of techniques was randomly selected. The AMSA palatal injection site is located at a point that bisects the maxillary first and second premolars, and midway between the crest of gingival margin and mid-palatine suture. The needle is orientated at a 45 degree angle with the bevel facing the palatal tissue, while rotating the STA® needle. The AMSA is easily administered and profound anesthesia is achieved within approximately 5-7 minutes of injection. Buccal infiltrations and contralateral palatal injections were administered for the traditional technique. A distraction technique in the form of a check wiggle was employed for the buccal infiltration upon insertion of the syringe. For the traditional palatal injection, pressure was applied using a cotton tip applicator, similar to that used with the STA System® injection, before insertion of the syringe. Once anesthesia was achieved, tooth extractions were performed. Patients were blindfolded with a commonly used sleeping mask so they would not distinguish which anesthetic delivery system was being used. Anesthesia procedures and tooth extractions were completed in the same session according to a split-mouth design. The STA System® produces audible beeps as the injection is administered. Beeping tones cannot be turned off with a switch. Therefore, the beeping sound was produced during both injection methods so that subjects would be unable to distinguish between techniques. Immediately after needle insertion, delivery of local anesthetic and tooth extractions, patients were asked to remove their mask and rate the pain for both conventional and STA System® techniques.

All patients received mepivacaine 3% with a vasoconstrictor (Carboplyina 20 mg/ml with epinephrine 1:100.000 Dentsply Italia srl) at a temperature of 25° C. A 1.8 mL anesthetic cartridge was used for both procedures (STA® vs. traditional) following the AMSA technique. The local anesthetic was injected with a 30 gauge dental needle for both STA® (30 G handpiece and needle, Milestone Scientific) and traditional (Trend Ject 0.30x21mm) injections. The products used in this study are presented in Figure 2.

Groups were labeled as follows: Group ($T^{ins/del}$) pain perception scores at needle insertion and delivery of anesthetic solution for the traditional technique; Group (T^{ext}) pain perception scores at tooth extraction for the traditional technique; Group ($S^{ins/del}$) pain perception scores at needle insertion and delivery of anesthetic solution for the STA® technique; Group (S^{ext}) pain perception scores at tooth extraction for the STA® technique.

Descriptive analysis of data was expressed as mean ± standard deviation (SD). Differences in pain ratings at needle insertion, delivery of local anesthetic and during tooth extraction were analyzed using a commercially available software program (SPSS®, version 20.0, SPSS Inc., Chicago, IL, USA).

RESULTS

One hundred adult patients 18 to 65 years old (mean: 54.39 ± 21,14 years) participated in this study. The NVRS data are shown in Table 1. Median scores, mean values, minimum and maximum pain rating values

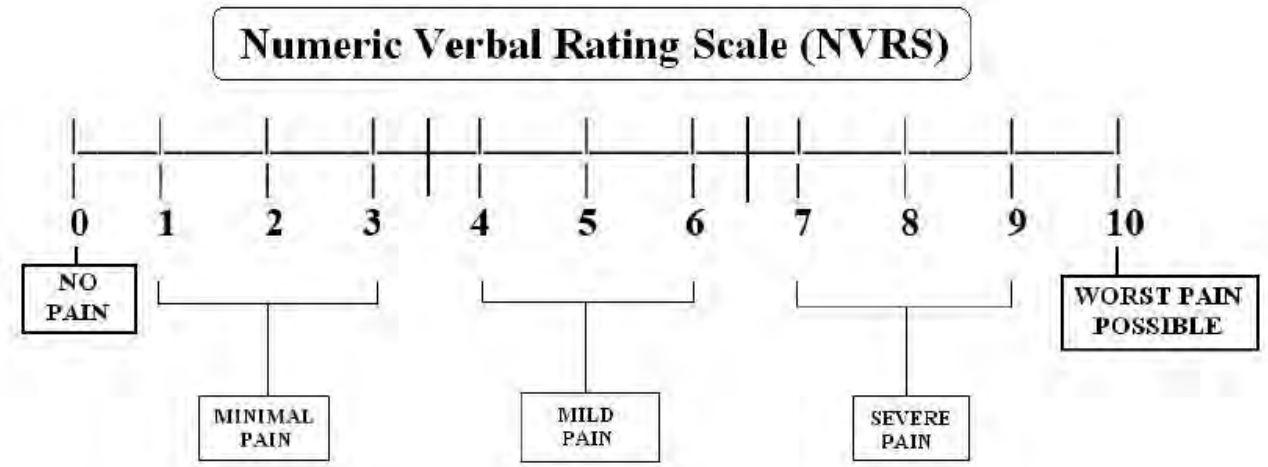

Fig. 1. *Numeric Verbal Rating Scale (NVRS).*

Materials	Product/Composition	Manufacturer
Computer controlled anesthesia device	The STA System	Milestone Scientific, Livingston, NJ
Handpiece with luer needle	The Sta System Handpiece with 30 gauge needle	Milestone Scientific
Conventional dental syringe	Carpule 2ml conventional dental syringe	ASA Dental spa
Luer needle	30 gauge needle (0, 30x21mm)	Trend Ject
Cartridge anesthetic solution	1.8 ml Carboplyina cartridge (20 mg/ml mepivacaine hydrochloride and 0.018 mg epinephrine hydrochloride)	Dentsply Italia srl

Fig. 2. *Materials used in the present study.*

Table I. *Pain scores for traditional vs. computer-controlled (STA) anesthesia delivery groups.*

				Traditional Pain scores		The STA System Pain scores	
Tooth number*	Traditional	Tooth number*	The STA System	$T^{ins/del}$	T^{ext}	$S^{ins/del}$	S^{ext}
1.6, 1.5		2.3, 2.4		3	3	1	5
2.2, 2.5		1.4, 1.5		2	6	0	3
1.1, 1.2, 1.3		2.2, 2.3, 2.4		2	3	2	3
1.4, 1.3		2.1, 2.6		2	5	1	3
2.5, 2.4		1.1, 1.2		3	4	0	5
1.4, 1.6		2.3, 2.5		2	4	1	4
1.4, 1.6		2.2, 2.4		0	6	2	1
2.1, 1.4		1.3, 1.4		4	5	2	2
1.6, 1.5		2.2, 2.5		3	3	3	3
1.1, 1.4, 1.5		2.3, 2.4		3	4	3	3
2.1, 2.2		1.4, 1.5		5	4	2	5
1.4, 1.5, 1.6		1.3, 1.1		2	6	2	2
1.3, 1.4		2.3, 2.5		3	5	2	1
2.2, 2.4		1.1, 1.5		3	4	1	5
1.4, 1.5		2.3, 2.4		4	5	2	3
1.1, 1.2		2.4, 2.5		0	4	0	4
1.4, 1.2		2.1, 2.2		2	3	2	2
2.4, 2.6		1.5, 1.2		3	4	1	5
2.1, 2.2		1.3, 1.5		4	4	1	5
1.5, 1.6		2.1, 2.3		2	3	3	3
2.2, 2.3, 2.4		1.5, 1.1		2	4	3	1
1.6, 1.1		2.4, 2.5		4	6	1	2
1.5, 1.6		2.5, 2.6		3	5	0	1
2.3, 2.4		1.1, 1.4		4	6	2	3
1.3, 1.6		2.2, 2.3		2	2	2	4
2.2, 2.4		1.1, 1.2		3	5	1	2
2.3, 2.5		1.3, 1.4		2	6	1	1
2.4, 2.5		1.5, 1.4		3	6	0	3
1.1, 1.2		2.6, 2.4		3	3	1	2
1.4, 1.5		2.1, 2.6		3	4	1	3
1.5, 1.6		2.6, 2.5		2	6	0	1
2.3, 2.5		1.6, 1.4		5	6	0	5
2.5, 2.6		1.3, 1.5		3	3	0	3
2.1, 2.6		1.5, 1.6		3	5	1	5
1.2, 1.3		2.2, 2.3, 2.4		3	6	0	1
1.4, 1.6		2.4, 2.5, 2.6		3	3	0	4
1.6, 1.2		2.5, 2.6		2	3	3	4
2.3, 2.5		1.3, 1.4, 1.5		5	6	2	3
1.5, 1.3		2.3, 2.4		2	4	3	3
2.5, 2.6		1.2, 1.3		2	4	0	5
1.1, 1.2		2.4, 2.6		3	5	1	0
1.4, 1.6		2.4, 2.5, 2.6		2	3	1	0

2.3, 2.5	1.2, 1.3	2	5	0	2
2.3, 2.4	1.1, 1.4, 1.5	3	4	2	1
2.1, 2.6	1.4, 1.6	3	2	2	4
1.3, 1.5	2.5, 2.6	2	4	0	5
1.5, 1.4	2.1, 2.6	3	6	2	5
2.4, 2.6	1.4, 1.6	0	2	0	0
2.6, 2.5	1.1, 1.2	2	2	2	1
1.4, 1.6	2.5, 2.4	3	2	1	2
2.6, 2.4	1.1, 1.2, 1.3	1	4	1	4
1.1, 1.4, 1.5	2.3, 2.4	3	5	1	3
2.5, 2.6	1.3, 1.5	3	6	1	0
2.3, 2.5	1.1, 1.4	4	6	1	1
2.3, 2.5	1.2, 1.3	3	5	1	5
1.3, 1.5	2.5, 2.6	3	4	1	5
1.1, 1.2	2.5, 2.6	3	2	1	4
2.2, 2.5	1.6, 1.1	2	2	1	4
1.3, 1.5	2.2, 2.1	1	5	3	4
2.4, 2.5	1.4, 1.5	3	5	1	1
2.5, 2.6	1.1, 1.4	2	5	3	4
1.4, 1.6	2.2, 2.4	1	3	1	4
2.2, 2.4	1.2, 1.4	1	6	0	4
1.3, 1.4	2.1, 2.6	2	3	0	1
1.1, 1.2	2.5, 2.6	4	2	0	5
2.3, 2.5	1.1, 1.2, 1.4	3	6	0	4
2.2, 2.3, 2.4	1.1, 1.2	3	5	3	3
1.3, 1.4	2.5, 2.6	1	6	0	3
2.1, 2.6	1.3, 1.6	2	3	2	3
2.3, 2.4	1.4, 1.3	1	4	0	3
1.1, 1.2	2.3, 2.5	5	2	1	4
1.3, 1.5	2.5, 2.6	5	2	1	2
2.4, 2.5	1.1, 1.6	5	4	2	5
2.3, 2.4	1.1, 1.2	5	4	2	5
1.4, 1.6	2.2, 2.5	4	4	2	4
1.4, 1.6	2.2, 2.1	0	5	1	5
1.6, 1.5	2.1, 2.2	1	5	2	2
2.4, 2.5	1.4, 1.6	0	4	0	1
1.1, 1.5, 1.4	2.3, 2.4, 2.5	0	4	0	5
1.4, 1.3	2.4, 2.5	1	4	0	2
2.3, 2.5	1.3, 1.5	3	4	2	3
2.3, 2.5	1.2, 1.3	3	4	0	5
1.1, 1.2	2.3, 2.4	1	3	0	5
2.3, 2.5	1.2, 1.3	2	3	2	5
1.6, 1.4	2.5, 2.6	4	2	1	4
1.1, 1.2, 1.3, 1.4, 1.5	2.1, 2.2, 2.3, 2.4, 2.5	4	5	2	3
1.4, 1.6	2.2, 2.3, 2.4	4	4	2	4

2.5, 2.1	1.6, 1.4	2	4	1	5
2.3, 2.5	1.4, 1.5	2	2	1	4
2.3, 2.5	1.2, 1.4	3	0	0	4
1.4, 1.5, 1.6	2.3, 2.4	3	2	2	5
2.3, 2.4	1.1, 1.2	0	4	3	4
1.4, 1.5	2.6, 2.5	3	6	0	5
2.3, 2.5	1.1, 1.5	4	4	1	4
1.3, 1.6	2.3, 2.5	5	3	2	3
1.1, 1.2	2.2, 2.3	5	3	2	4
2.5, 2.6	1.4, 1.6	2	4	2	5
2.3, 2.4	1.1, 1.2	0	3	1	5

**FDI (Federation of Dental International) notation system*

Table II. *Descriptive statistics for the two anesthesia techniques during 2 phases.*

Anesthesia techniques	Groups	Median scores	Minimum	Maximum
Traditional	$T^{ins/del}$	3	0	5
	T^{ext}	4	2	6
The STA System	$S^{ins/del}$	1	0	3
	S^{ext}	3.5	0	5

$T^{ins/del}$, needle insertion and delivery of anesthetic for traditional group

T^{ext}, tooth extraction for traditional group

$S^{ins/del}$, needle insertion and delivery of anesthetic for STA® technique

S^{ext}, tooth extraction for STA® technique

Table III. *Pain perception differences between the two anesthesia techniques.*

Insertion of needle and delivery of anesthetic solution					
	Mean	SD	SEM	N	P VALUE
Traditional	2.62	1.301	0.130	100	< 0.0001
STA System	1.22	0.980	0.098	100	
Tooth extraction					
	Mean	SD	SEM	N	P VALUE
Traditional	4.05	1.35	0.14	100	0.0002
STA System	3.27	1.50	0.15	100	

SD, Standard Deviation

SEM, Standard Error of the Mean

N, Number of patients

after needle insertion, delivery of local anesthetic and tooth extraction for both traditional and STA System® techniques, are shown in Table 2 and Table 3. STA System® registered significantly lower pain levels at needle insertion and delivery of anesthetic as compared to conventional injection technique ($p<0.0001$). Moreover, the STA® technique registered lower pain levels than the conventional injection during tooth extractions ($p=0.0002$). Statistical results are presented in Table 3. A higher percentage of patients (23%) required a second injection after the traditional syringe technique ($p=0.002$). Only two patients (2%) required a supplementary injection when it was administered with the STA System®. The above difference was statistically significant ($p=0.005$).

DISCUSSION

The results of this study demonstrate a statistically significant reduction in pain perception, with the STA System® as compared to traditional injections, at different phases. Pain perception was significantly higher when using the traditional injection technique at needle insertion, anesthetic delivery and tooth extraction.

The majority of literature on computer-controlled injection systems deals with pain perception at injection using a computer-assisted injection device, and compares it to the conventional syringe injection technique (4,11,14-20). For the most part, results have been favorable (14,17,19-21) to the computer-assisted injection system, with only two studies showing no difference in pain perception (15,20) and one study showing higher pain ratings (4).

Computer-controlled anesthetic devices are largely attributable to procedures performed in pediatric dentistry, restorative dentistry, endodontics, periodontology, and maxillofacial surgery (7) but there are limited research data on the efficacy of the STA System® in dental surgery (17, 22).

Traditionally, maxillary teeth have been anesthetized administering an infiltration injection on the buccal or labial aspects of the target tooth. Palatal injections, used to anesthetized the palatal mucosa, are generally considered the most painful injections (6,7,23). Wahl et al. showed that palatal injections caused significantly more pain than most intraoral injections (24). The traditional buccal intraoral infiltration approach routinely anesthetizes the surrounding tissues (lips, surface of the face) and can also affect muscle activity. Patient's natural response, as well as active facial expressions are temporarily affected, including a distortion of the smile and the annoying sensation of facial numbness (7,13). The palatal approach AMSA nerve block can be attempted with a traditional manual syringe, but the precise pressure and volume ratios of the STA® are virtually impossible to reproduce (13). The clinician can anesthetize several teeth in the maxillary arch, extending from the mesiobuccal root of the first molar to the central incisor, by means of a single palatal infiltration without numbing the lips, face or interfering with the muscles of facial expression (7,12,17). The traditional syringe technique, on the contrary, requires several injections on the vestibular and mucobuccal side of the target teeth.

The present study showed highly significant ($p<0.0001$) differences for pain ratings at needle insertion and anesthetic solution delivery when the conventional buccal and AMSA technique versus the STA System® injection were compared. The STA system registered lower pain levels than those registered with the conventional technique during tooth extractions ($p=0.0002$).

The STA System® offers several advantages over conventional syringes, including excellent tactile sensation due to a lightweight plastic handle and the ability to rotate the needle as it is introduced into tissues, producing a coring penetration that minimizes needle deflection (7,25). The slow rate of anesthetic flow reduces patient discomfort compared with palatal injections administered with a traditional syringe (25). Friedman and Hochman stated that careful needle insertion and slow anesthetic delivery could reduce painful sensation at needle insertion. Nevertheless, anesthetic flow rate is independent of applied pressure with the STA System® (13,23,26).

NRS, VRS and VAS systems are the most common pain rating scales used to evaluate patients' painful sensation and behaviors in research studies (15,16,23-32). These scales are not always easily understandable or intuitive for patients. The VAS system seems to be particularly cumbersome for them to comprehend in our experience. The NRVS scale system was created to facilitate clear comprehension of pain perception levels and intensity. The NRVS rating system gives patients the possibility to better express pain intensity by choosing a numeric value for each verbal expression.

CONCLUSIONS

The AMSA technique administered using the STA System® in a dental surgery treatment reduced pain significantly more than the conventional syringe technique at needle insertion, delivery of local anesthetic and tooth extraction. The NRVS scale has proven to be a very effective and intuitive system to evaluate pain perception at different clinical phases of anesthetic delivery. Computer-controlled anesthesia using the STA System® seems to be less painful and more clinically effective for dental surgery procedures due to the greater extent of anesthetic effect.

REFERENCES

1. Kleinknecht RA, Klepac RK, Alexander LD. Origins and characteristics of fear of dentistry. J Am Dent Assoc. 1973; 86:842-8.
2. Milgrom P, Weinstein P, Getz T. Treating fearful dental patients. A patient management handbook. 2nd Ed. Seattle:University of Washington; 1995. p.14-20.
3. Kroeger R. Managing the apprehensive dental patient. Cincinnati: Heritage Commnunication; 1987. P.23-30.
4. Goodell GG, Gallagher FJ, Nicoll BK. Comparison of a controlled injection pressure system with a conventional technique. Oral Surg Oral Med Oral Pathol Oral Radiol Endod. 2000; 90:88-94.
5. Ballard BE. Biopharmaceutical considerations in subcutaneous and intramuscular drug administration. J Pharm Sci. 1968; 57:357-78.
6. Hutchins HS, Young FA, Lackland DT, Fishburne CP. The effectiveness of topical anesthesia and vibration in alleviating the pain of oral injections. Anesth Prog. 1997; 44:87-9.
7. Yenisey M. Comparison of the pain levels of computer-controlled and conventional anesthesia techniques in prosthodontic treatment. J Appl Oral Sci. 2009; 17:414-20.
8. Krochak M, Friedman N. Using a precision metered injection system to minimize dental injection anxiety. Compendium of Continuing Education in Dentistry 1998; 19:137-50.
9. Oztaş N, Ulusu T, Bodur H, Doğan C. The wand in pulp therapy: an alternative to inferior alveolar nerve block. Quintessence Int. 2005; 36:559-64.
10. Ram D, Peretz B. Assessing the pain reaction of children receiving periodontal ligament anesthesia using a computerized device (Wand). J Clin Pediatr Dent. 2003; 27:247-50.
11. Fukayama H, Yoshikawa F, Kohase H, Umino M, Suzuki N. Efficacy of anterior and middle superior alveolar (AMSA) anesthesia using a new injection system: the Wand. Quintessence Int. 2003; 34:537-41.
12. Ram D, Kassirer J. Assessment of a palatal approach-anterior superior alveolar (P-ASA) nerve block with the Wand in pediatric dental patients. Int J Paediatr Dent. 2006; 16:348-51.
13. Friedman MJ, Hochman MN. The AMSA injection: a new concept for local anesthesia of maxillary teeth using a computer-controlled injection system. Quintessence Int. 1998; 29:297-303.
14. Allen KD, Kotil D, Larzelere RE, Hutfless S, Beiraghi S. Comparison of a computerized anesthesia device with a traditional syringe in preschool children. Pediatr Dent. 2002; 24:315-20.
15. Asarch T, Allen K, Petersen B, Beiraghi S. Efficacy of a computerized local anesthesia device in pediatric dentistry. Pediatr Dent. 1999; 21:421-4.
16. Gibson RS, Allen K, Hutfless S, Beiraghi S. The Wand vs. traditional injection: a comparison of pain related behaviors. Pediatr Dent. 2000; 22:458-62.
17. Lee S, Reader A, Nusstein J, Beck M, Weaver J. Anesthetic efficacy of the anterior middle superior alveolar (AMSA) injection. Anesth Prog. 2004; 51:80-9.
18. Nicholson JW, Berry TG, Summitt JB, Yuan CH, Witten TM. Pain perception and utility: a comparison of the syringe and computerized local injection techniques. Gen Dent. 2001; 49:167-73.
19. Rosenberg ES. A computer-controlled anesthetic delivery system in a periodontal practice: patient satisfaction and acceptance. J Esthet Restor Dent. 2002; 14:39-46.
20. Saloum FS, Baumgartner JC, Marshall G, Tinkle J. A clinical comparison of pain perception to the Wand and a traditional syringe. Oral Surg Oral Med Oral Pathol Oral Radiol Endod. 2000; 89:691-5.
21. Primosch RE, Brooks R. Influence of anesthetic flow rate delivered by the Wand Local Anesthetic System on pain response to palatal injections. Am J Dent. 2002; 15:15-20.
22. Ashkenazi M, Blumer S, Eli I. Effectiveness of various modes of computerized delivery of local anesthesia in primary maxillary molars. Pediatr Dent. 2006; 28:29-38.
23. Friedman MJ, Hochman MN. Using AMSA and P-ASA nerve blocks for esthetic restorative dentistry. Gen Dent. 2001; 49:506-11.
24. Wahl MJ, Schmitt MM, Overton DA, Gordon MK. Injection pain of bupivacaine with epinephrine vs. prilocaine plain. J Am Dent Assoc. 2002; 13:1652-6.Blanton PL, Jeske AH, Dental local anesthetics: alternative delivery methods. J Am Dent Assoc. 2003; 134:228-34.
25. Hochman M, Chiarello D, Hochman CB, Lopatkin R, Pergola S. Computerized local anesthetic delivery vs. traditional syringe technique. Subjective pain response. N Y State Dent J. 1997; 63:24-9.
26. Nusstein J, Berlin J, Reader A, Beck M, Weaver JM. Comparison of injection pain, heart rate increase, and postinjection pain of articaine and lidocaine in a primary intraligamentary injection administered with a computer-controlled local anesthetic delivery system. Anesth Prog. 2004; 51:126-33.
27. Versloot J, Veerkamp JS, Hoogstraten J. Computerized anesthesia delivery system vs. traditional syringe:

comparing pain and pain-related behavior in children. Eur J Oral Sci. 2005; 113:488-93.

28. Loomer PM, Perry DA. Computer-controlled delivery versus syringe delivery of local anesthetic injections for therapeutic scaling and root planing. J Am Dent Assoc. 2004; 135:358-65.
29. Nusstein J, Claffey E, Reader A, Beck M, Weaver J. Anesthetic effectiveness of the supplemental intraligamentary injection, administered with a computer-controlled local anesthetic delivery system, in patients with irreversible pulpitis. J Endod. 2005; 31:354-8.
30. Nusstein J, Lee S, Reader A, Beck M, Weaver J. Injection pain and postinjection pain of the anterior middle superior alveolar injection administered with the Wand or conventional syringe. Oral Surg Oral Med Oral Pathol Oral Radiol Endod. 2004; 98:124-31.
31. Nusstein J, Burns Y, Reader A, Beck M, Weaver J. Injection pain and postinjection pain of the palatal-anterior superior alveolar injection, administered with the Wand Plus system, comparing 2% lidocaine with 1:100,000 epinephrine to 3% mepivacaine. Oral Surg Oral Med Oral Pathol Oral Radiol Endod. 2004; 97:164-72.